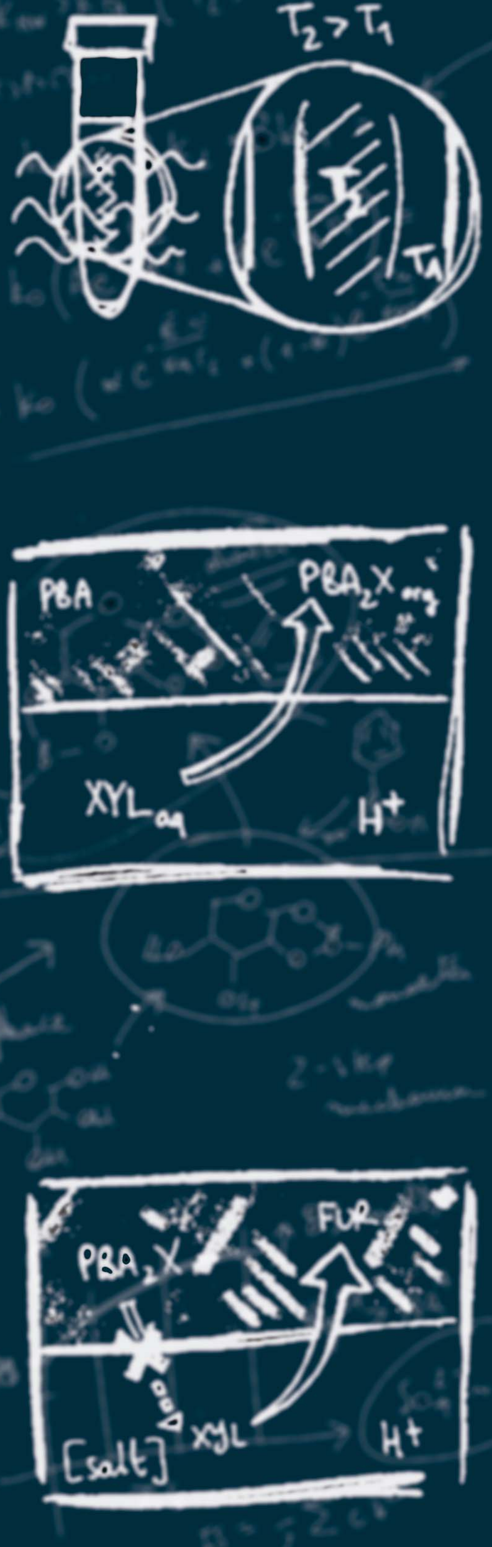

Furfural Manufacture from Xylose: Routes towards High Selectivity and Novel Processes Luca Ricciardi 2021

Furfural Manufacture from Xylose: Routes towards High Selectivity and Novel Processes

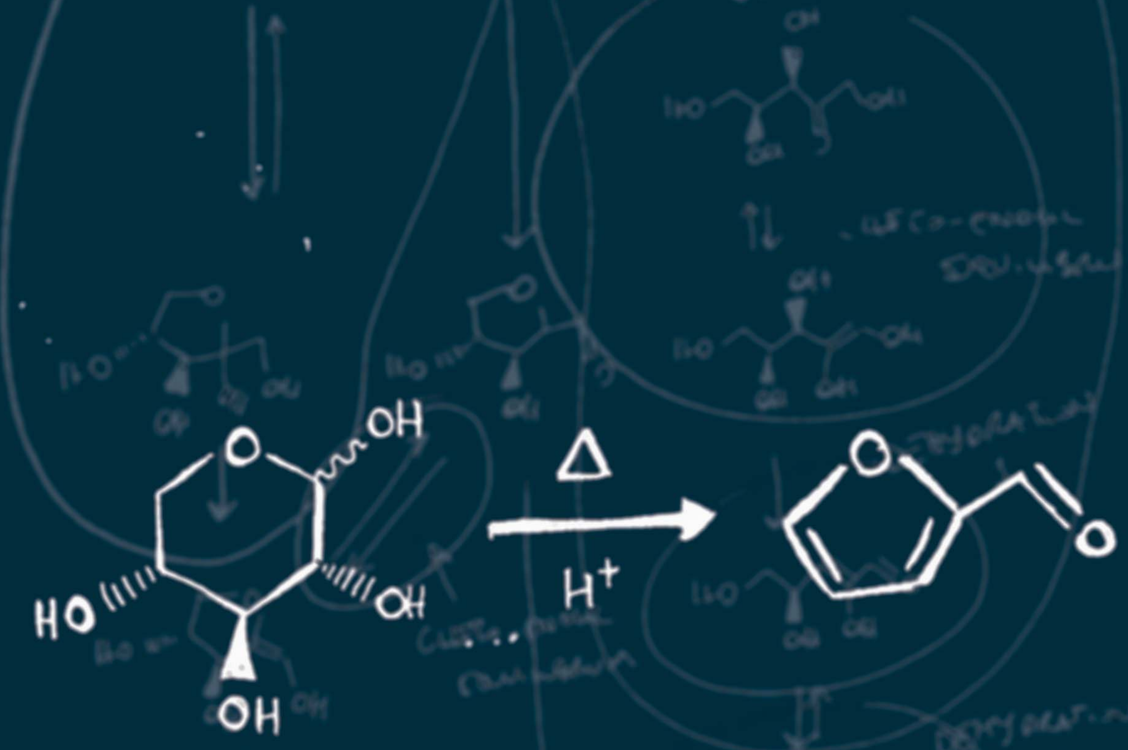

Luca Ricciardi

Furfural Manufacture from Xylose: Routes towards High Selectivity and Novel Processes

Luca Ricciardi

Members of the committee:

Chairman:	prof. dr. J. L. Herek
Promotors:	prof. dr. ir. J. Huskens (UT)
	prof. dr. J.-P. Lange (UT)
Co-promotor:	dr. W. Verboom (UT)
Members:	prof. dr. B. Sels (KU Leuven)
	prof. dr. S. Harutyunyan (RUG)
	prof. dr. J. J. L. M. Cornelissen (UT)
	prof. dr. ir. S. R. A. Kersten (UT)
	dr. J. A. Faria Albanese (UT)

The research described in this thesis was performed within the laboratories of the Molecular NanoFabrication (MnF) group, part of the Department of Molecules and Materials (MolMat), at the MESA+ Institute for Nanotechnology and the Faculty of Science and Technology (TNW) of the University of Twente. Financial support from Shell Global Solutions International B.V. is gratefully acknowledged.

UNIVERSITY OF TWENTE. MESA+ INSTITUTE FOR NANOTECHNOLOGY

Furfural Manufacture from Xylose: Routes towards High Selectivity and Novel Processes

DISSERTATION

to obtain
the degree of doctor at the University of Twente
on the authority of the rector magnificus
prof. dr. ir. A. Veldkamp,
on the account of the decision of the doctoral board,
to be publicly defended on
Friday October 29th, 2021 at 12.45 h.

by

Luca Ricciardi

born on December 30th, 1993,

in Naples, Italy.

This dissertation has been approved by the promotors:

prof. dr. ir. J. Huskens

prof. dr. J.-P. Lange

dr. W. Verboom

Furfural Manufacture from Xylose: Routes towards High Selectivity and Novel Processes

ISBN : 978-90-365-5259-2

DOI : 10.3990/1.9789036552592

Cover art : Luca Ricciardi

Printed by : Gildeprint, Enschede, The Netherlands

“The one important thing I have learned over the years is the difference between taking one's work seriously and taking one's self seriously. The first is imperative and the second is disastrous.”

Margot Fonteyn

Table of Contents

Chapter 1

General Introduction

Planet Earth is facing a human-induced climate crisis.[1] Scientists from numerous nations have raised concern about this issue at various instances in the past, with one of the latest public warning having arrived in January 2020.[1] The alarming trends observed in the parameters that we use to describe climate and environment (*e.g.*, desertification, availability of fresh water, air pollution) show that drastic, politically driven changes are urgently necessary.[1] With greenhouse gas (GHG) emissions still rapidly rising, and most public discussions focused on global surface temperature only, it is of fundamental importance to understand that this environmental crisis is related to social and economic factors embedded in our society.[1,2]

In parallel, and strongly related, to the climate crisis, our society is facing an energy crisis, which is directly connected to the steep rise in energy demand.[3,4] These two crises are intertwined, since the combustion of crude oil, natural gas and coal still is the primary energy sources worldwide, both for transportation of people and goods, fueling industry and infrastructures, and for ensuring the stability of the energy grid.[4] The product of combustion of these fossil fuels is CO_2, which is an important contributor to the greenhouse effect. The increased energy demand is due to worldwide industrial development, coupled with an average increase of wealth.[3-5] This scenario, in combination with the increasing costs of extraction and manufacture of fossil fuels, is becoming a troubling bottleneck for economic development.[3-5] Currently, the addition of green and/or renewable sources of energy (*e.g.*, hydroelectric, solar, wind and nuclear energy) is rapidly growing.[5] Yet, we must realize that just compensating the growing energy demand with these 'clean' energy sources is not sufficient. Reducing the (absolute) contributions of fossil fuels to the energy palette is absolutely necessary to act on the climate crisis and reduce, for example the CO_2 levels in the atmosphere.[5]

Making humanity fully independent from fossil fuels is an incredibly complex task.[1,2] To do so, the chain of production and consumption of energy, at all levels, needs to be redesigned with drastic, both politically and economically driven international choices.[1,2] Next to these necessary societal changes, research is needed to explore possible alternatives for fossil fuels, which would ease this transition with the aim to avoid, or minimize, an economic crisis.[1-5] Particularly, some sectors of industry and transportation, *e.g.*, heavy industry and aviation, are extremely challenging to decarbonize and cannot solely rely on solar and wind energy, requiring the development of renewable fuels and chemicals.[6]

Reducing, and finally eliminating, fossil resources such as oil is exceptionally complex, as these resources are also the basis for the current petrochemical industry.[6,7] The petrochemical industry, one of the largest during the last century, continues to grow to this day, with the awareness of the fact that Earth's resources are limited.[7] Many chemicals commonly used in industry and research, as well as every-day-use bulk

polymers (*e.g.*, polypropylene, acrylonitrile-butadiene-styrene, polyurethanes), are produced from the chemical processing of oil (*e.g.*, olefins and aromatics).[6,7] In fact, it is reported that, with gasoline use predicted to wane, oil-to-chemicals plants could dominate the petrochemical industry in the next future.[6,7]

Biomass, which is waste from agriculture, forestry, livestock, industries and urban areas, is a very promising renewable resource, both for energy and chemical applications, which would come with the plus of waste repurposing and valorization.[8,9] More specifically, lignocellulosic biomass, a complex biological resource composed of various biopolymers (*i.e.*, lignin, cellulose and hemicellulose), is the most abundant biomass, and it can serve as a feedstock for the production of valuable chemicals, such as sugars, furans, aromatics, alcohols and commercially relevant carboxylic acids.[10-15] The number of different chemicals that can be obtained from lignocellulosic biomass opens the possibility not only for the production of biofuels (*e.g.*, bioethanol and bio-based diesel), but also for the redesigning of chemical industry, reducing the amount of fossil feedstock needed for the manufacture of plastics, solvents, detergent and others.[9,10]

Among the chemicals that can be produced from lignocellulosic biomass, furfural is recognized as a top value-added chemical, as it offers a large number of highly commercially valuable derivatives and promising performances as blending component for gasoline and diesel.[16-18] Furfural is obtained from the acid-catalyzed dehydration of D-xylose, a monomeric subunit of hemicellulose, which is a component of lignocellulosic feedstock.[15-19] The industrial approach for furfural production employs the direct digestion of lignocellulose in aqueous medium and mineral acid catalysis.[16-20] Emerging technologies aim to fractionate biomass for better valorization, but are yet to be applied in industrial processes.[20] The acid-catalyzed dehydration of xylose in aqueous medium gives rise to a maximum xylose-to-furfural selectivity of approx. 45-50 mol% on xylose base.[17,21] This non-ideal selectivity is due to several reactions that occur in parallel and subsequent to the xylose dehydration.[17,18,22] Of particular importance are the xylose degradation to carboxylic acids (*e.g.*, formic acid, acetic acid and levulinic acid) and the formation of insoluble by-products (humins) by xylose-furfural condensation reactions and furfural-furfural resinification.[18-22]

Consistent xylose-to-furfural selectivity improvements have been obtained using different solvent systems, from aqueous-organic biphasic, to fully organic monophasic systems.[18,23-25] The selectivity enhancements are assigned to: (i) stabilization of furfural, either through continuous extraction (under biphasic conditions) or with the inhibition of furfural degradation, and (ii) the effect on the sugar conformation and the reaction mechanism, due to different solvent-solute interactions.[10,23,26,27]

Microwave heating, which is widely applied in organic synthesis, has been used for the dehydration of sugars to furans as well.[28,29] Generally, microwave heating results in a consistent rate enhancement, in comparison with traditional heating, which has been ascribed to purely thermal effects.[30-32] However, the microwave responsiveness of the solvent used in such reaction remains a crucial parameter to be taken into account, as heat transfer under microwave conditions is related to the dielectric properties of the medium.[30-33]

The aim of the work described in this thesis is to explore novel approaches for furfural manufacture and, based on them, develop, and conceptually validate feasible industrial processes. Part of this work focuses on the effect of microwave heating on the reaction of xylose dehydration, both under monophasic and biphasic conditions (Chapters 3 and 4). In the second part (Chapters 5 to 7), a process of liquid-liquid extraction of xylose as its boronate diester (PBA_2X) and its subsequent dehydration to furfural is presented as well as control of the nature of the solvent system and its effect on the selectivity and rate of the reaction. Based on the results of Chapters 5, 6 and 7, preliminary process concepts for xylose isolation and dehydration to furfural are provided in the respective chapters. Chapter 8 provides a wider outlook onto the further exploration of the results achieved in this thesis.

Chapter 2 provides a literature overview on the acid-catalyzed dehydration of sugars into furans, focusing specifically on the cases in which this reaction is performed in the presence of polar organic solvents. Insights into the mechanistic aspects and effects on sugar-to-furan selectivity are discussed as well.

Chapter 3 explores the combination of microwave heating and reactive extraction. The asymmetric response of the two phases in an aqueous-organic biphasic system to microwave heating is studied in the xylose dehydration to furfural. The reaction parameters (*i.e.,* xylose conversion and xylose-to-furfural selectivity) have been analyzed, with the aim to determine the beneficial effect of the combined microwave–biphasic operation.

Chapter 4 deepens the examination of the effect of microwave heating on the aqueous monophasic dehydration of xylose into furfural. In this chapter, traditional and microwave heating are compared in the case study of xylose dehydration, aiming to model the solvent response to microwave heating. The widely reported rate enhancement of chemical reactions in microwave heating is shown to be connected to localized overheating, which is built in the model and validated through experimental evidence.

Chapter 5 describes the extraction of xylose from acidic hydrolysate as a neutral boronate diester. The extraction conditions and its mechanism are rationalized and discussed. The recovery of xylose from PBA_2X, by back-extraction, is also investigated.

Chapter 6 studies the use of a three-solvent mixture, composed of water, an apolar, aromatic organic solvent, and a polar aprotic solvent, conversion of xylose to furfural, in the presence of phenylboronic acid (PBA). The aim is to integrate this reaction with the pre-extraction step of xylose described in Chapter 5. The temperature-dependent phase behavior of the system is analyzed, combined with its effect on the xylose dehydration reaction parameters.

Chapter 7 explores the combination of the extraction process described in Chapter 5 and biphasic operation, with a highly salted aqueous phase. The aim is to boost the xylose-to-furfural selectivity and get insight into the mechanism of the dehydration of PBA_2X to furfural in such a reaction medium.

Chapter 8 offers future perspectives related to the overarching aim of this thesis, beyond the research described in the previous chapters. Potential applications of the concepts explored in this thesis, their extensions to other systems, and their socio-economic impacts will be discussed without attempting to be exhaustive.

1.1 References

1. W. J. Ripple, C. Wolf, T. M. Newsome, P. Barnard, W. R. Moomaw, *BioScience* **2020**, *70*, 8–12.
2. Stephen Briggs, Charles F. Kennel, David G. Victor, *Nat. Clim. Chang.* **2015**, *5*, 969–970.
3. B. H. Kreps, *Am. J. Econ. Sociol.* **2020**, *79*, 695-717.
4. R. York, S. E. Bell, *Energy Res. Soc. Sci.* **2019**, *51*, 40-43.
5. A. Lewandowska-Bernat, U. Desideri, *Appl. Energ.* **2018**, *228*, 57-67.
6. J.-P. Lange, *Energy Environ. Sci.* **2021**, *14*, 1-19.
7. H. Hassani, E. Sirimal Silva, A. M. Al Kaabic, *Technol. Forecast. Soc. Change* **2017**, *119*, 1-17.
8. P. Morseletto, *Resour. Conserv. Recy.* **2020**, *153*, 1-12.
9. Z. Wang, Q. Bui, B. Zhang, T. L. H. Pham, *Sci. Total Environ.* **2020**, *743*, 1-11.
10. I. K. M. Yu, D. C. W. Tsang, *Bioresour. Technol.* **2017**, *238*, 716-732.
11. P. L. Arias, J. A. Cecilia, I. Gandarias, J. Iglesias, M. López Granados, R. Mariscal, G. Morales, R. Moreno-Tost, P. Maireles-Torres, *Catal. Sci. Technol.* **2020**, *10*, 2721-2757.
12. Y. Luo, Z. Li, X. Li, X. Liu, J. Fan, J. H. Clark, C. Hu, *Catal. Today* **2019**, *319*, 14-24.

13. H. Wang, C. Zhu, D. Li, Q. Liu, J. Tan, C. Wang, C. Cai, L. Ma, *Renew. Sust. Energ. Rev.* **2019**, *103*, 227–247.
14. A. A. Rosatella, S. P. Simeonov, R. F. M. Frade, C. A. M. Afonso, *Green Chem.* **2011**, *13*, 754-793.
15. K. Gupta , R. K. Rai, S. K. Singh, *ChemCatChem* **2018**, *10*, 2326-2349.
16. R. Mariscal, P. Maireles-Torres, M. Ojeda, I. Sádaba, M. López Granados, *Energy Environ. Sci.* **2016**, *9*, 1144–1189.
17. P. Gallezot, *Chem. Soc. Rev.* **2012**, *41*, 1538−1558.
18. J.-P. Lange, E. van der Heide, J. van Buijtenen, R. Price, *ChemSusChem* **2012**, *5*, 150–166.
19. J.-P. Lange, I. Lewandowski, P. Ayoub, in *Sustainable Development in the Process Industry—cases and impacts*, John Wiley & Sons, Hoboken (New Jersey) **2010**, pp. 171–208.
20. J.-P. Lange, *Biofuels, Bioprod. Bioref.* **2007**, *1*, 39-48.
21. P. Priecel, J. E. Perez Mejia, P. D. Carà, J. A. Lopez-Sanchez, in *Sustainable Catalysis for Biorefineries*, Royal Society of Chemistry, London, **2018**, pp. 243–299.
22. J. E. Romo, N. Bollar, C. J. Zimmermann, S. G. Wettstein, *ChemCatChem* **2018**, *10*, 4805–4816.
23. L. Shuai, J. Luterbacher, *ChemSusChem* **2016**, *9*, 133– 155.
24. C. Sener, A. H. Motagamwala, D. M. Alonso, J. A. Dumesic, *ChemSusChem* **2018**, *11*, 2321– 2331.
25. Y. Román-Leshkov, J. N. Chheda, J. A. Dumesic, *Science* **2006**, *312*, 1933– 1937.
26. M. Peters, M. F. Eckstein, G. Hartjen, A. C. Spiess, W. Leitner, L. Greiner, *Ind. Eng. Chem. Res.* **2007**, *46*, 7073– 7078.
27. F. Delbecq, Y. Takahashi, T. Kondo, C. C. Corbas, E. R. Ramos, C. Len, *Catal. Commun.* **2018**, *110*, 74-78.
28. M. B. Gawande, S. N. Shelke, R. Zboril, R. S. Varma, *Acc. Chem. Res.* **2014**, *47*, 1338– 1348.
29. Y. Wang, F. Delbecq, R. S. Varma, C. Len, *Mol. Catal.* **2018**, *445*, 73– 79.
30. Á. Díaz-Ortiz, P. Prieto, A. de la Hoz, *Chem. Rec.* **2019**, *19*, 85– 97.
31. C. O. Kappe, *Acc. Chem. Res.* **2013**, *46*, 1579– 1587.
32. M. A. Herrero, J. M. Kremsner, C. O. Kappe, *J. Org. Chem.* **2008**, *73*, 36– 47.
33. C. Gabriel, S. Gabriel, E. H. Grant, B. S. J. Halstead, D. M. P. Mingos, *Chem. Soc. Rev.* **1998**, *27*, 213– 224.

Chapter 2

Production of Furans from C_5 and C_6 Sugars in Presence of Polar Organic Solvents

Furfural and hydroxymethylfurfural are top added-value chemicals, provide a rich source of derivatives and have promising performances as additives for fuels. These furanic compounds are the product of the acid-catalyzed dehydration of sugars (e.g., xylose and glucose), components obtained from lignocellulosic biomass. The conventional industrial approach for manufacturing furans employs the use of mineral acid catalysts (e.g., H_2SO_4) in an aqueous medium. This approach limits the selectivity towards furans to approx. 45-50 mol%, mainly by the formation of solid by-products (humins), which are generated by acid-catalyzed condensation and degradation reactions. The use of aqueous-organic biphasic conditions mitigates this limitation, raising the selectivity to approx. 75 mol%. However, numerous experimental examples have shown that high-yield furan production (>80 mol%) can be achieved by switching to mainly (or fully) organic solvent systems. Specifically, aprotic polar organic solvents (e.g., DMSO) can improve both the conversion and the selectivity from sugars to platform molecules. The presence of aprotic polar organic solvents has an influence on the solvent shell of the sugar and on the activity of the catalyst. Studying these two major effects on the system is crucially important to characterize and understand improvements of the selectivity. The aim of this review is to explore and contextualize the use of polar organic solvents in the process of the manufacture of furans, while addressing the challenges of its industrial application.

2.1 Introduction

Research of the last decades has been devoted to the exploration and development of new, non-fossil sources, to produce fuels and chemicals.[1-5] This is achieved by a series of chemical processes referred to as biorefinery, which is an alternative to the fossil-based oil refinery and the related chemical complexes.[3-7] Biorefinery does not include processes of chemical recycling or CO_2-to-chemical processes.[3-7] The application of biorefinery technology is key to upgrade complex biological resources, such as non-edible biomass (*e.g.*, forestry and agricultural waste), into valuable chemicals, which can also be used as bio-based alternatives to fossil fuels.[3-18] In this scenario, lignocellulosic biomass serves as an important renewable starting material for biorefinery.[8-11] It is, in fact, the most abundant plant dry matter and can be obtained from a wide range of sources, *e.g.*, sugarcane bagasse, maple wood, corncob, corn stover, pinewood, eucalyptus, wheat straw, and barley husk, as well as food waste, such as waste cooked rice, bread waste, vegetable waste, and fruit waste.[8-11]

Lignocellulosic biomass is composed mainly of three biopolymers: lignin, cellulose and hemicellulose (Figure 1.1).[1,12-14] Cellulose is a source of glucose, which can be isomerized to fructose and other C_6 sugars.[1] In lignocellulosic biomass, C_5 sugars, *e.g.*, xylose and arabinose, are present mainly as glucuronoxylan, and minor quantities of xyloglucan, in hardwoods and as glucoronoarabinoxylan in grasses and, in minor quantities, in softwood.[1] The average xylan contents is up to 5 w% in softwoods, 15 w% in hardwoods, and 20 w% in grasses.[1,12]

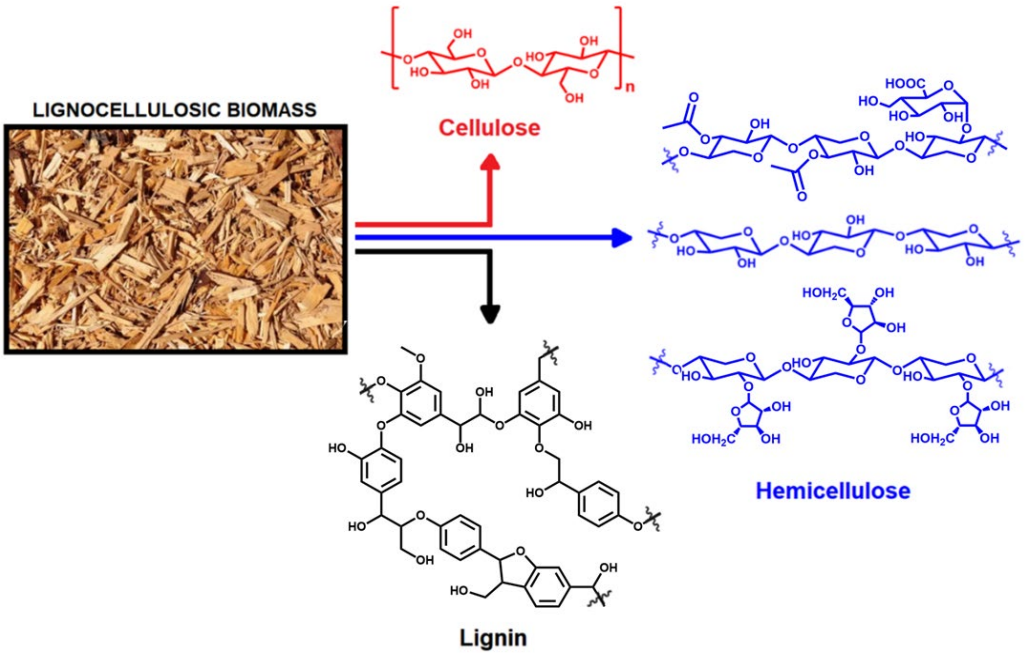

Figure 1.1 Composition of lignocellulosic biomass in various biopolymers. Specifically, hemicellulose (in blue) is represented, from top to bottom, by glucuronoxylan, xylan and arabinoxylan.

The conversion of biomass is much more challenging than that of model carbohydrates, as the decomposition behavior of the feedstock depends also on the interactions between its components (*i.e.*, cellulose, hemicellulose, and lignin).[8-14] Various methodologies of fractionaction are used to separate the different components of biomass.[3,5,15,16] Typically, the aim is to extract the hemicellulose and/or the lignin to deliver a cellulose-rich pulp.[8-16]

The fractionation of biomass into its building blocks is followed by the synthesis of a variety of high-value products.[17,18] Amongst the products that can be obtained through biorefinery, furfural and 5-hydroxymethylfurfural (HMF) stand out as top added-value platform molecules for chemicals and fuels.[1-3] In particular, these two furanic compounds and their rich tree of derivatives offer many opportunities for fuel and chemical manufacture.[1,2,4-7] HMF can be upgraded to several added-value intermediates like 2,5-furandicarboxylic acid (FDCA), 2,5-dimethylfuran, several furan-derived other molecules, higher alkanes and aromatic gasoline.[1,3-7,17,19] Furfural can be upgraded to THF, furan, butane and pentane diols, esters (*e.g.*, furfuryl acetate, esters of levulinic acid and dimethyl pentanoate), and diesel alkanes.[1-3,6,7,17,19-21]

Furfural and HMF are generally produced by an acid-catalyzed dehydration of C_5 and C_6 sugars, respectively.[1-3,22] The most common substrates for the production of HMF are fructose and glucose.[3,4] While the production of HMF from fructose is efficient and direct, using glucose as a starting material requires the use of an isomerization catalyst.[3.4] In the production of furfural from xylose, this additional isomerization step is not implemented, as no specific preferential isomer has been detected yet.[1,2] Today, the industrial production of furans still largely relies on the batch dehydration of biomass using sulfuric acid, with yields of furfural and HMF of typically around 45-50%.[1,2,22]

There are several inherent differences between HMF and furfural in terms of stability and water solubility.[1] HMF easily suffers from a rehydration reaction to form levulinic acid.[23] Its hydroxymethyl group easily undergoes alkylation and triggers the production of humins.[24] Furfural is much more stable intrinsically, as its degradation arises from a subsequent condensation reaction with sugar molecules and acid-catalyzed resinification reactions, both of which lead to the formation of solid humic by-products.[1,2] Additionally, due to its hydroxymethyl group, HMF is highly water soluble, while furfural has a solubility limit of 8 w% in water.[1,25]

Several strategies have been employed to improve the sugar-to-furan selectivity.[1-3,26-32] The parameters used for optimizing this reaction are the choice of the catalyst and possible additives, such as halide salts or metal ions, but also changing the characteristics of the solvent system.[26-32] Most of the strategies applied to optimize this selectivity have been recently reviewed.[26-33] Shuai and Luterbacher reviewed the effect of solvents on general biomass processing, focusing on the solvent effect on the behavior of the biopolymers lignin and cellulose.[29] Lee and Wu reviewed all the solvent systems used in furfural production, including ionic liquids and deep eutectic solvents.[32] Zhao *et al.* offered a comprehensive review for the production of furfural and HMF through the hydrothermal conversion of biomass, focusing on homogeneous catalysis in different solvent environments.[33]

This review focuses on the use of polar organic solvents (*e.g.*, DMSO and ethanol) as a promising reaction environment or as additives to the solvent system, with the aim to boost reactivity and selectivity. Recent developments in the understanding of their beneficial effects on the sugar-to-furan selectivity and their effect on catalyst activity are discussed, both in homogeneous and heterogeneous catalysis. Moreover, the feasibility of the possible application of such systems in industrial processes will be discussed.

2.2 Reaction Mechanisms of Dehydration of Sugars

The key step in the conversion of a sugar to a furanic compound is an acid-catalyzed dehydration reaction.[1] Several mechanisms have been proposed in different studies under various reaction conditions.[22] Various aspects seem to influence the pathway of the reaction, such as catalyst type, salt concentration, presence of specific metal ions and the solvent system.[22,33-36]

The reaction can be performed both in monophasic and biphasic environments, using both homogeneous and heterogeneous catalysis.[1,30] In industrial setups, homogeneous catalysis from mineral acids, such as H_2SO_4 and HCl, is the preferred choice for such reactions.[1] There are, however, other examples in literature in which supercritical CO_2 and carboxylic acids have been used to catalyze the production of both furfural and HMF.[36] Various heterogeneous catalysts, such as zeolites, sulfonated resins, heteropolyacids and other acidic solids, have been successfully applied to produce furanic compounds from sugars.[1,30,32,33] Moreover, due to the formation of acidic by-products, the dehydration of a sugar shows autocatalytic behavior.[1,37] Heterogeneous catalysis potentially offers the benefit of ease of separation of solvent and catalyst, aiding the recyclability of the latter.[38] Heterogeneous catalysts are not reported to be beneficial over homogeneous catalysts in terms of sugar-to-furan selectivity, which still strongly depends on the reaction conditions and the solvent system.[1,30,37,38] More importantly, however, the heterogeneous catalysts are prone to fouling and deactivation by humins , which remains a problem in its industrial application.[38,39]

Rationalizing the mechanism of these reactions is a key aspect for their further optimization.[22,33] From a mechanistic point of view, several intermediate steps, such as isomerization, ring opening and closing, have been hypothesized in the dehydration process of both C_5 and C_6 sugars (see Schemes 2.1 and 2.2, respectively).[22,33-41] As previously mentioned, an intermediate isomerization step to fructose occurs in the production of HMF from glucose (Scheme 2.2).[1,3,4,26] In the case of furfural manufacture from xylose, several groups have studied the importance of a molecule analogous to fructose, *i.e.*, xylulose.[22,40-42] However, even though xylulose can be detected in various concentrations depending on the reaction conditions, its key relevance as an intermediate in the process of furfural formation has been ruled out by Ershova *et al.*, who showed, using both experiments and kinetic modeling, the role of xylulose to be along a parallel reaction pathway.[40]

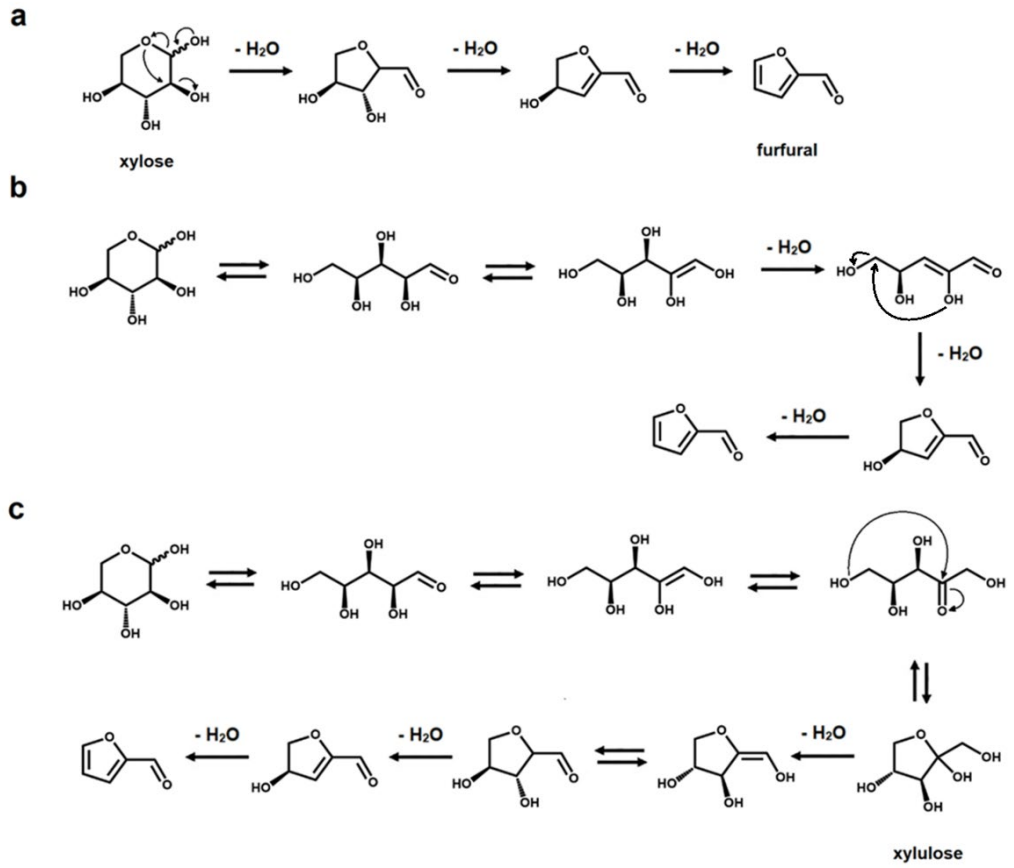

Scheme 2.1 Mechanistic pathways from xylose to furfural. (a) Closed-ring pathway, dehydration in three steps with no isomerization. (b) Open-ring pathway, including a keto-enol equilibrium. (c) Closed-ring mechanistic pathway inclusive of xylose-to-xylulose isomerization.

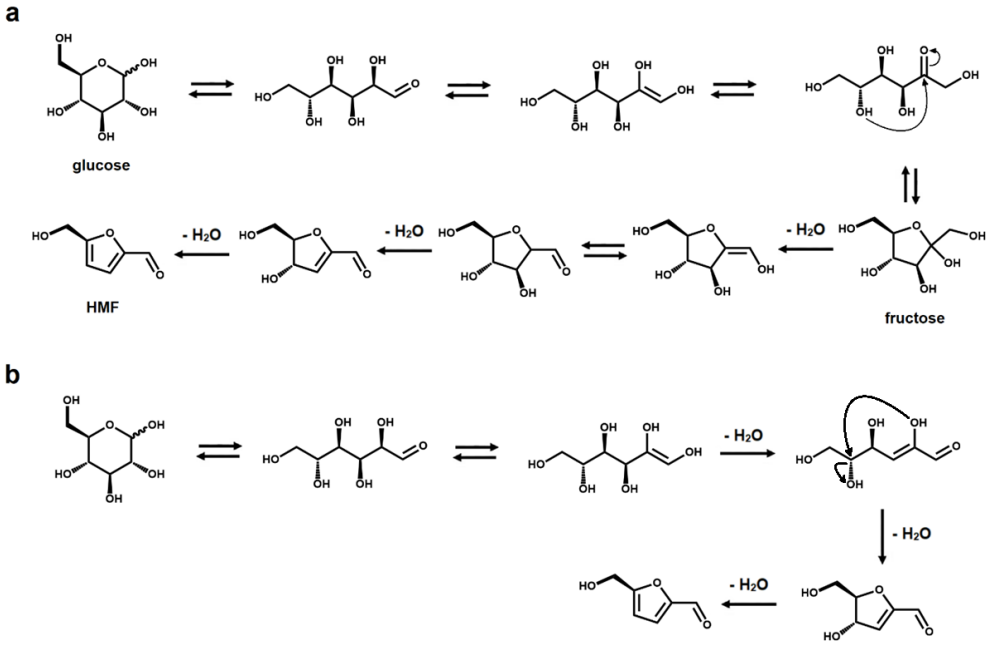

Scheme 2.2 Mechanistic pathways from glucose and fructose to HMF. (a) Closed-ring pathway, including glucose-to-fructose isomerization. (b) Open-ring pathway, including a keto-enol equilibrium.

Some of the side-products, such as carboxylic acids (*e.g.*, levulinic acid, acetic acid and formic acid), lactones (*e.g.*, ɣ-valerolactone and angelica lactone) and cyclohexanones, can be reutilized and valorized.[1-3,30,37,43-50] Humic by-products can also be processed and applied as platform meterials such as graphene oxide, even if their high heterogeneity limits their possible applications.[51-53]

2.3 Aqueous-Organic Solvent Systems

A common, and widely applied, strategy to improve the selectivity toward furfural and HMF is the use of water-*immiscible* organic solvents, such as toluene, methylisobutylketone, diethyl ether, ɣ-valerolactone (GVL) or *p*-xylene, to form an aqueous-organic biphasic system.[1,30,37,54-58] Such aqueous-organic biphasic systems can be low-cost, relatively non-toxic and environmentally friendly. The concept of biphasic operation, based on the process of reactive extraction, exploits the continuous liquid-liquid extraction of the newly formed HMF or furfural into the organic phase.[59-63] The characteristics of these biphasic systems are variable in terms of catalysis and composition.[30,37,54-56] While homogeneous catalysis from mineral acids remains the

preferred source, in several studies heterogeneous catalysis has also been successfully applied at biphasic conditions.[30,37] The effect of adding a water-immiscible layer affects the sugar-to-furan selectivity by continuous extraction of the newly formed HMF or furfural into the organic phase.[1-3,30,37] In both cases the sugar-to-furan selectivity increases, on average, to 60-70 mol% because of the suppression of the furan-sugar condensation reaction towards solid by-products.[1,30,37,44,45]

Biphasic operation has been applied to sugar dehydration at several aqueous-organic volume ratios, with mostly organic biphasic systems being reported to be the most beneficial in terms of sugar-to-furan selectivity.[1,20,37,54-56] Large fractions of organic solvent, however, can be a limit for the efficiency of the process, as the feed for such a reaction comes as an aqueous solution and limiting the volume of the aqueous phase limits the final furan production.[1,57,58]

The so-called 'solvent effect' resulting from adding such a co-solvent refers to changes in reaction rate, reaction pathway, product distribution, and yield.[29,32,33] Contrary to biphasic operation, the use of this type of co-solvents will affect the interaction between the solute (*i.e.*, the C_5 and C_6 sugars) and the solvent (*i.e.*, water).[29,32,33] These changes occur because of the influence of the co-solvent on hydrogen bonding and the overall thermodynamic behavior of the solvent system.[29,32,33] Below, the effects of such miscible co-solvents on the production of HMF and furfural will be reviewed.

2.3.1 Protic Organic Solvents

In the realm of water-miscible organic solvents, there is a distinction between protic solvents, such as ethanol, and aprotic polar solvents, such as DMSO.[29] Protic solvents can both accept and donate hydrogen bonds, whereas the aprotic ones can only accept hydrogen bonding.[29] Protic solvents, like isopropanol and ethanol, have been successfully used both in HMF and furfural synthesis.[64-67] The use of a protic solvent is justified because of the beneficial suppressing effect on the formation of humic by-products by sugar-furan condensation.[64,67] In fact, the *in-situ* formation of an alkyl-glucoside has been hypothesized to protect the sugar, suppressing parallel condensation reactions that result in the formation of humic by-products (Scheme 2.3).[64] This approach was also successfully applied using heterogeneous and metal-free catalysis conditions, but the most promising results in terms of sugar-to-furan selectivity have been observed under homogeneous catalysis conditions.[64-67] Specifically, about 75 mol% xylose-to-furfural selectivity was obtained using a water-ethanol (1:1 v-v) mixture, using H_2SO_4 as acid catalyst.[64] Among the alcohols, *n*-butanol has the specific characteristic of forming a biphasic system with water at $T < 80\ ^oC$, transitioning into a monophasic system at $T > 80\ ^oC$.[68]

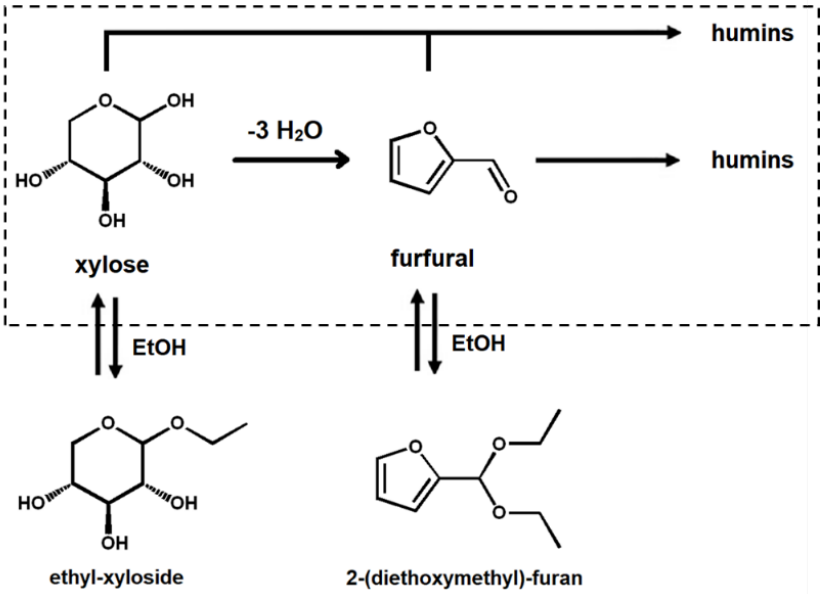

Scheme 2.3 Possible reaction pathway for the formation of the ethyl-xyloside and 2-(diethoxymethyl)-furan in a water-ethanol solvent system. The dashed box indicates the species present in a water-only system.

The use of different organic solvents, like formic acid, as additives to the aqueous phase, has also been reported.[69] Specifically, the addition of increasing non-catalytic amounts of formic acid (> 0.5 M), resulted in a consistent increase in the selectivity of the fructose dehydration to HMF, with an ultimate selectivity of about 80 mol% in a water/*n*-butanol 1:3 v-v system.[69]

Using formic acid as a co-catalyst allows the production of furfural combined in tandem with that of other derivatives, *e.g.*, furfuryl alcohol (with an overall yield of approx. 70 mol%).[70] The same effect was obtained using other carboxylic acids (*e.g.*, oxalic acid), which are also routinely used for the formation of deep eutectic solvents (DES).[71,72] A related combined approach has also been reported for isopropanol.[73,74] In this case furfural is reduced to furfuryl alcohol through catalytic hydrogen transfer (CHT) over metal-organic frameworks (MOFs).[73] CHT in alcohol media has also been reported in a tandem process for the production of furfural, and minor percentages of furfuryl alcohol and levulinic acid, from a xylose feed.[74] A similar facilitative effect has been observed for *tert*-butanol.[75] In this context, it is worth mentioning that formic acid decomposes to CO_2/H_2.[75]

2.3.2 Aprotic Polar Solvents

As previously discussed, aprotic solvents behave in a fundamentally different way than protic ones.[29,32,33] This results in differences in the solvent-solute interaction, which also reflects on the reaction parameters, mechanism, and kinetics, with no possibility of forming glucosides.[76-79] Specifically, the presence of aprotic solvents in the mixture has been reported to promote the glucose-to-fructose isomerization (Scheme 2.2) and the formation of furanose-aldehyde intermediates (Schemes 2.1a and 2.2a).[76] The product/by-product distribution is also affected, largely increasing the selectivity of the dehydration towards HMF.[76] This specific behavior of aprotic solvents can be generalized to all dehydration reactions, with a direct effect on its mechanism, owing to competition between water and the polar organic solvent in the interaction with the hydroxyl groups, analyzed through DFT simulations of the spatial distribution of the solvents.[77]

Aprotic solvents alter the relative stability of initial and transition states in the dehydration reactions.[78,79] This opens the possibility of predicting and rationalizing the effect of a specific solvent in this type of acid-catalyzed processes[78] through computational work.[79,80] Several aprotic solvents have been used for the dehydration of sugars both in water and in water-free environments, providing a wide variety of sugar-to-furan selectivities depending on the reaction conditions.[34,81-115] The presence of an aprotic organic solvent in a solvent system has a direct effect on the mutarotation of sugars.[86] Specifically, in a mainly aqueous environment at room temperature, the β-pyranose form of a sugar is dominant, whereas in mainly organic environments, the α-pyranose form is favored (Figure 2.2).[86] In presence of organic solvents, such as DMSO, THF, ɣ-butyrolactone (GBL) and DMF, this influence is maximized.[86] Moreover, the xylose-solvent hydrogen bond formation affects the overall sugar reactivity, as the reactivity of the functional group depends strongly on the conformation of the sugar (*e.g.*, in reaction of dehydration and hydrogenation).[86]

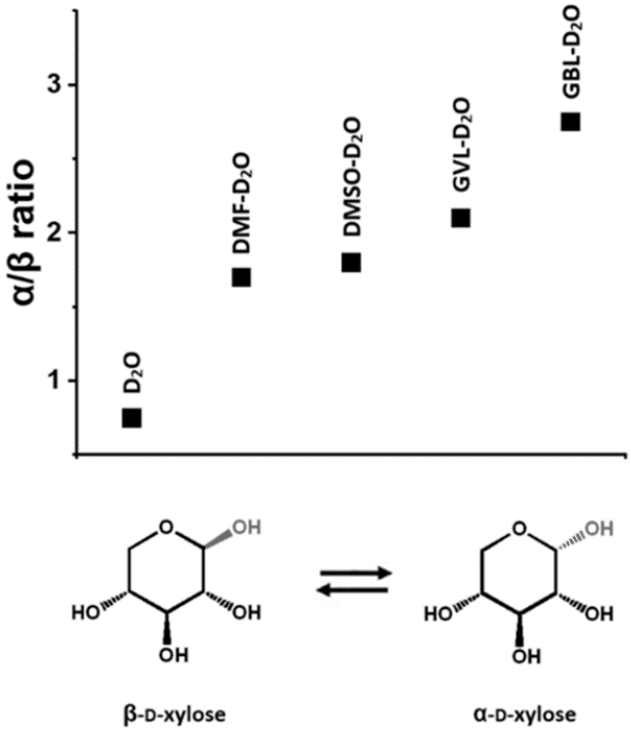

Figure 2.2 α/β-Anomer ratios in different solvent systems, determined by ^{1}H-NMR spectroscopy. Data from ref. 86.

2.3.2.1 Dimethylsulfoxide

The most common solvent for these studies, both in the production of furfural and HMF, is dimethylsulfoxide (DMSO), and it is used from highly aqueous to water-free systems (Table 2.1).[81-95] Highly aqueous conditions (7:3 v-v water-DMSO monophasic systems), paired with microwave heating and a metal catalyst (*i.e.*, $CrCl_3$ or $Al(NO_3)_3$), resulted in a relatively high fructose-to-HMF selectivity (approx. 65 mol%) when compared with fully aqueous monophasic conditions.[81] However, the reaction from glucose and xylose is highly ineffective (with yields <15 mol%), possibly because of shortcomings in the isomerization reactions needed for the sugar-to-furan conversion (see above), which were hypothesized to be a result of poor solubility of the Lewis acid catalyst in the solvent system.[22,33-40,81] The use of DMSO enables the effective solubilization of rather recalcitrant starting materials (*e.g.*, coffee grounds, bread waste or cellulose formate).[81-83] Moving from a fully aqueous monophasic system to a 1:1 water-DMSO mixture, with HCl and $AlCl_3$ as cocatalysts, has resulted into a 35 mol%

selectivity improvement in the conversion of cellulose formate to HMF, with a concomitant reduction of the production of levulinic acid.[83] This selectivity improvement is explained by specific interactions between the reactant (*i.e.*, formylated sugars) and the aprotic solvent (see above).[83] However, it has to be noted that some of the mentioned side reactions (*e.g.*, HMF to levulinic acid) are the result of rehydration, so operating in a water-lean environment will also have a non-negligible effect.[1,2]

Table 2.1 Selection of sugar-to-furan selectivities obtained under various reaction conditions for both furfural and HMF in partially or fully organic DMSO-containing solvent systems. Sugar conversion is quantitative, if not otherwise specified.

DMSO:H_2O (v-v)	Starting material	Product	Catalyst	Sel.[a]	ref.
1:1	Fructose	HMF	Maleic acid – $SnCl_4$	54	83
1:1	Xylose	Furfural	$Sn_{0.625}Cs_{0.5}PW$	61	87
3:1	Cellulose formate	HMF	$HCl/AlCl_3$	52	83
1:0	Fructose	HMF	H_2SO_4	81	84
1:0	Xylose	Furfural	$H_3PW_{12}O_{40}$	67	88
1:0	Fructose	HMF	SiO_2-SO_3H	91	90
1:0	Fructose	HMF	HPC-P2Y–S[b]	98	92
1:0	Fructose	HMF	Nb_2O_5	86	93
1:0	Fructose	HMF	EKLSC[c]	85[d]	94

[a] Expressed in mol%.

[b] Hierarchically porous carbon-based catalyst.

[c] Sulfonated carbon catalyst based on Eucalyptus Kraft lignin.

[d] Maximum sugar conversion 90 mol%

Experimental evidence supports that the effect of DMSO on the sugar-to-furan selectivity is mainly the result of solvation of the sugar, and not of catalysis by acidic species generated by the degradation of DMSO.[84-86] Moreover, solvation of the product can also be a contributor, as adding aprotic organic solvents will result in a stabilization of HMF and furfural.[84] Molecular dynamics simulations on the interaction of glucose in progressively more organic solvent mixtures of water with DMSO, THF and DMF, exhibited that these solvents compete with water in forming the first solvation shell around the sugar, even upon the addition of relatively low amounts (< 40-50 vol%).[85]

A 20-25 mol% xylose-to-furfural selectivity improvement is observed when moving from monophasic aqueous systems to 1:1 v-v water-DMSO conditions, using bi-metallic salts of heteropolyacids as catalysts.[87] It was demonstrated that the presence of DMSO improved the catalytic activity and stability, with the catalyst retaining >90% of its activity after six reaction cycles.[87] Similar results have been obtained using Preyssler

heteropolyacids as catalysts in a water-free DMSO monophasic system, with xylose-to-furfural selectivities as high as 80 mol%, which value can compete with biphasic operations.[88] In this study, DMSO was also combined with other organic solvents (namely, dichloromethane and methylisobuthylketone), with the aim of further stabilizing the produced furfural and limiting the subsequent resinification reactions.[88] This effect was also supported by the analysis of the Gibbs free energy of different tautomers of fructose in different solvent systems, performed by Fu *et al.*, who state that the presence of DMSO has a direct effect on the mechanism of the reaction.[89] Specifically, the presence of DMSO (as well as dioxane and NMP) stabilizes the α-furanose form of fructose, favoring, as also previously mentioned, the closed-ring dehydration mechanism (Scheme 2.2a).[89] Moreover, the presence of aprotic solvents suppresses the formation of fructose-HMF oligomers, thereby improving the fructose-to-HMF selectivity.[89]

Using DMSO as the sole component of a monophasic system is rather common in the heterogeneously catalyzed production of furans both from xylose, glucose and fructose.[88,90-94] Among heterogeneous catalysts, sulfonated solids (*e.g.*, silica, carbon and palygorskite) are specifically used, always with sugar-to-furan selectivities >85 mol%.[90-94] Metal catalysts (*e.g.*, Nb_2O_5) have also been successfully applied, specifically for the dehydration of fructose, with HMF production of approx. 85-90 mol% selectivity.[93]

2.3.2.2 Tetrahydrofuran

Another polar organic solvent commonly used in sugar dehydration is tetrahydrofuran (THF; Table 2.2).[82,91,95-99] In this solvent, additional analyses have been performed on the effect of polar aprotic solvents on the dehydration mechanism.[95] Specifically, experimental evidence and molecular dynamics simulations suggest that a mainly organic solvent environment (*e.g.*, 9:1 v-v THF-water or dioxane-water), combined with catalytic amounts of Cl^- anions, results in the stabilization of protonated transition states of the acid-catalyzed process, leading to significant increases in reactivity and selectivity (approx. 80 mol% fructose-to-HMF selectivity).[95] Increasing the THF content of the solvent system resulted in an increased xylose-to-furfural selectivity, catalyzed by pressurized CO_2, leading to a selectivity improvement of approx. 30-40 mol% when moving from mainly aqueous to mainly organic systems.[96] A similar pattern has been observed when producing furfural from alginic acid, in a reaction catalyzed by heteropolyacids in a 95:5 THF-water system.[97]

Table 2.2 Selection of sugar-to-furan selectivities obtained under various reaction conditions for both furfural and HMF in partially or fully organic THF-containing solvent systems. Sugar conversion is quantitative in all cases.

THF:H_2O (v-v)	Starting material	Product	Catalyst	Sel.[a]	ref.
1:1	Xylose	Furfural	CO_2 (pressurized)	84	96
1:1	Xylose	Furfural	---	51	99
9:1	Fructose	HMF	HCl	78	95
1:0	Fructose	HMF	PSS-30IL-SO_3H[b]	98	98

[a] Expressed in mol%.

[b]Poly(styrene sulfonate) with ionic liquid moieties.

Extremely high fructose-to-HMF selectivities (> 95 mol%) were obtained when performing fructose dehydration in water-free THF.[98] As in the case of DMSO, the absence of water is generally combined with a heterogeneous catalyst. In this case, the best performing catalyst is a functionalized poly(styrene sulfonate) (PSS), which bears ionic liquid moieties (PSS-30IL-SO_3H), yielding an almost quantitative HMF production from fructose.[98]

2.3.2.3 Sulfolane

The effect of polar organic solvents is also observed in the absence of a catalyst, in a 1:1 v-v organic-aqueous system.[99] Among different solvents, the best performing one is sulfolane, which is structurally similar to DMSO, yielding a xylose-to-furfural selectivity up to approx. 70 mol%, with an enhancement from 10 to 25 mol% compared with other organic solvents, *e.g.*, THF, GVL, and GBL (Table 2.3).[99-103] However, the high boiling point of sulfolane (285 °C), compared with that of other aprotic organic solvents (*e.g.*, DMSO 189 °C and THF 66 °C), allows for more complex reaction setups, such as reactive distillation.[100] Continuous furfural removal by means of distillation would allow to avoid subsequent side-reactions that limit the selectivity.[100] However, this stays a challenge in such systems, and the balance between the various system components is yet to be found.[100]

Table 2.3 Selection of sugar-to-furan selectivities obtained under various reaction conditions for both furfural and HMF in partially or fully organic sulfolane-containing solvent systems. Sugar conversion is quantitative, if not otherwise specified.

Sulfolane:H_2O (v-v)	Starting material	Product	Catalyst	Sel.[a]	ref.
1:1	Xylose	Furfural	---	68	99
4:1	Xylose	Furfural	H-β zeolite	70	100
9:1	Bamboo biomass	Furfural[b]	$AlCl_3$	25	101[c]
9:1	Bamboo biomass	HMF[b]	$AlCl_3$	39	101[c]
1:0	Fructose	HMF	LiCl	67	102
1:0	Fructose	HMF	HBr	91	102

[a] Expressed in mol%.

[b]In this specific case, furfural and HMF are produced concomitantly.

[c] Maximum sugar conversion 88 mol%

In reaction systems which don't exploit reactive distillation, the use of highly organic sulfolane-water mixtures (9:1 v-v) in combination with metal chlorides (*e.g.,* $SnCl_4$ and $FeCl_3$) resulted in 25-30 mol% fructose-to-HMF selectivity improvements, when compared with fully aqueous systems.[101] This is rationalized by the fact that the solvent system is homogeneous in the presence of sulfolane, whereas in a fully aqueous system the catalyst (*i.e.*, $SnCl_4$) is present also as a solid, impairing its activity.[101] $SnCl_4$ has been reported to hydrolyze, and Liu *et al.* have hypothesized, based on ESI-MS spectrometry, about a possible synergic effect of the presence of tin hydroxides in catalyzing a glucose-to-fructose isomerization.[101] The effect of the solvent system on the activity of metal halides has been confirmed by Caes and Raines, who studied several metal halides to catalyze the dehydration of fructose to HMF in a water-free sulfolane environment.[102] Compared to catalyst-free conditions, they showed fructose-to-HMF improvements up to 60-70 mol%.[102]

Polar aprotic solvents are not interchangeable, in fact, switching from sulfolane to DMSO in 9:1 v-v organic-aqueous system in the H_2SO_4-catalyzed degradation of cellulose resulted in a 45 mol% selectivity increase towards HMF (from approx. 25 to 70 mol%).[103] Moreover, moving from DMSO to dioxane in the dehydration of fructose, catalyzed by phosphate-functionalized porous organic polymers and performed in fully organic environment, resulted in a 20 mol% fructose-to-HMF selectivity increase, up to 97 mol%.[104] This, as in the case of DMSO, can be rationalized by specific interactions between solvent and sugars, and solvent and catalysts.[84-86] It is proven, in fact, that no acidic species are formed due to solvent degradation.[84]

2.3.2.4 Dioxane

Dioxane is another rather commonly used polar organic solvent (Table 2.4).[91,104-109] Dioxane has an effect on the glucose-fructose isomerization, mediated by a Sn-β metal catalyst, with progressively more aqueous dioxane-water solvent systems being less and less effective in the sugar conversion.[105] Specifically, the fructose conversion after 2 h of reaction drops from >90 mol% to approx. 50 mol% when moving from exclusively dioxane to a 9:1 v-v dioxane-water mixture.[105] Jeong *et al.* reported the use of thick corn syrup with high fructose content (water content less than 25 w%) as a starting material.[106] Using Amberlyst-15 as the acid catalyst and dioxane as the solvent an ultimate fructose-to-HMF selectivity of approx. 80 mol% was reached.[106]

Table 2.4 Selection of sugar-to-furan selectivities obtained under various reaction conditions for both furfural and HMF in partially or fully organic dioxane-containing solvent systems. Sugar conversion is quantitative in all cases.

Dioxane:H_2O (v-v)	Starting material	Product	Catalyst	Sel.[a]	ref.
9:1	Fructose	HMF	HCl	73	95
9:1	Glucose/fructose	HMF	Amberlyst-131	75	105
9:1	Fructose syrup	HMF	Amberlyst-15	72	106
1:0	Fructose	HMF	B-POP[b]	78	104
1:0	Xylose	Furfural	SC-GCa-800[c]	76	107
1:0	Bamboo biomass	Furfural	HCl	83	108

[a] Expressed in mol%.
[b] Phosphate-functionalized polymer catalyst.
[c] Calcium gluconate-derived sulfonated carbon catalyst.

Water-free dioxane was also used to produce furfural from xylose with approx. 75-80 mol% selectivity in the presence of a solid carbon-based acid catalyst, derived from calcium gluconate.[107] Like DMSO, dioxane has also been employed in the treatment of more recalcitrant starting materials (*e.g.*, corncob and bamboo lignocellulosic biomass), with very promising outcomes.[108,109] Specifically, a fully organic dioxane environment gave rise to >90 mol% yield of furfural starting from bamboo biomass, in an HCl-catalyzed process.[108] A more complex solvent system, composed of a mixture of ethanol, dioxane and formic acid, was successfully used for lignocellulosic biomass liquefaction, which yielded furans such as furfural and HMF.[109]

2.3.2.5 Acetone, GBL and others

Several other polar organic solvents have been used in the production of furans from sugars, *e.g.*, acetone, butanone, GBL, and acetonitrile (Table 2.5).[82,86,99,104,107,110-115]

Acetone in combination with a choline chloride-ethylene glycol deep eutectic solvent (2:5 v-v DES-acetone mixture) gave furfural starting from xylose with approx. 70 mol% selectivity, using H_2SO_4 as a catalyst.[110] Wang *et al.* reported that using a 7:3 v-v acetone-water mixture and pressurized phosphoric acid as a catalyst resulted in a xylose-to-furfural selectivity improvement of approx. 20 mol%, in comparison with pure water.[111] Motagamwala *et al.* demonstrated that a 4:1 v-v acetone-water system, using HCl as catalyst, gave rise to an almost quantitative HMF production from fructose (>95 mol% selectivity).[113] GBL has been successfully used, in combination with water, to produce both furfural and HMF using zeolites or Amberlyst-15 as solid acid catalysts, giving sugar-to-furan selectivities up to 70 mol%.[113-114] Butanone, although it is only partially miscible with water, has been used in highly organic aqueous-organic mixtures with xylose-to-furfural selectivity improvements up to 40 mol% when compared with pure water.[115]

Table 2.5 Selection of sugar-to-furan selectivities obtained under various reaction conditions for both furfural and HMF in partially or fully organic solvent systems. Sugar conversion is quantitative, if not otherwise specified.

Solvent	Solvent:H_2O (v-v)	Starting material	Product	Catalyst	Sel.[a]	ref.
Acetone	5:3[b]	Xylose	Furfural	H_2SO_4	70	110[c]
Acetone	7:3	Sugarcane	Furfural	PPA[d]	45	111
Acetone	4:1	Fructose	HMF	HCl	98	112
Acetone	4:1	Fructose	HMF	H_2SO_4	97	112
Acetone	4:1	Fructose	HMF	Amberlyst-15	95	112
Butanone	2:1	Xylose	Furfural	[bmim]Cl/$FeCl_3$[e]	53	115[f]
GBL	1:1	Xylose	Furfural	---	57	99
GBL	9:1	Fructose	HMF	HY zeolite	67	113
GBL	1:0	Xylose	Furfural	SC-GCa-800[g]	82	107

[a] Expressed in mol%.
[b] This solvent system also includes a DES.
[c] Sugar conversion < 30 mol%.
[d] Pressurize phosphoric acid.
[e] 1-butyl-3-methylimidazolium chloroferrate
[f] Maximum sugar conversion 65 mol%
[g] Calcium gluconate-derived sulfonated carbon catalyst.

2.3.2.6 Aprotic solvents in mostly or fully organic operations

When the water content of the system is limited or even absent, the characterization of the behavior of the acid catalyst is more complex.[84-86,88,90-94,98,102,106-109] The acid-

catalyzed process of sugar dehydration involves a proton transfer from the catalyst onto the sugar, which affects the β-elimination of the hydroxyl groups.[1,22,33-40] In mainly aqueous media, such proton transfer is mediated by water molecules, but with the decrease of the water content the catalyst activity increases.[88,90-94,98,102,105-109] In some instances, this increase of the catalytic activity can be explained by a complete solubilization of the catalyst in the solvent system, or by a stabilization of the catalyst, which reduces its progressive deactivation.[86,101] However, this increased activity can also be approached from a more fundamental point of view, which includes the inherent process of proton transfer, involved in the acid catalysis of the dehydration reaction.[116-123]

Proton transfer can happen even in the complete absence of water.[116-123] In fact, the equilibria of the dissociation of acids and bases are strongly influenced by the properties of the solvent.[116,117] It is assumed that proton transfer reactions generally take place along hydrogen bonds, with the proton forming a full bond to a base as it breaks its full bond to another.[116] The dissociation constants of several acids vary quite significantly even when moving from one aprotic solvent to another, mirroring well the behavior observed in literature on sugar dehydration (see above).[103,104,117]

Several mechanistic aspects may influence the rate of proton transfer, hence affecting the catalyst activity: steric factors, polarity of the solvent, possible delocalization of the charges and stabilization of transition states.[118] Formation of ion pairs in solution (*e.g.*, in the case of DMSO) is also an important factor to take into account, both in mainly organic and water-free environments,[118] since it affects the formation of hydrogen bonds and hence proton transfer.[119] Furthermore, molecular dynamics simulations confirm that solvent-water interactions influence the stability of H_3O^+ cations in mixed water-organic solvent environments, while only some organic solvents (*e.g.*, DMSO) successfully stabilize H^+ in purely organic solution.[120] The nature of the solvent system influences strongly the activity of solid catalysts (*i.e.*, supported sulfonic acid catalysts) as well.[121] Direct interactions between the catalyst and the solvent are reported to affect the strength of solid acid catalysts, with higher acid strengths in organic solvents compared to aqueous conditions.[121] All this information is used to rationalize and design solvent environments beneficial to biomass processing.[122,123]

2.4 Application Perspectives

Highly organic and fully organic polar monophasic solvent systems result in high sugar-to-furan selectivities, both for the processing of xylose and of glucose and fructose.[88,90-98,100-109,111,112] In this scenario, Walker *et al.* rationalized the choice of a suitable solvent system for biomass conversion processes based on molecular dynamics and machine learning tools, combined with a specific experimental workflow based on two case

studies (*i.e.*, the dehydration of cyclohexanol to cyclohexene and that of fructose to HMF).[123] Predictive tools were developed for the selection of top candidate mixed solvent systems, depending on their desired properties.[123] Walker *et al.* show that a computational screening method efficiently allows to select the best-performing candidates among a library of solvent systems, with the aim of minimizing experimental screening.[123] The efficiency of the specific reaction, however, is not the only important factor to be considered in the choice of the solvent system.[124]

Biphasic organic-aqueous operations are the state of the art for the production of furans at industrial scale, despite their limitations in sugar-to-furan selectivity.[1,30,37,54-58] The application of polar organic solvents can cause logistic problems in industrial set-ups in which the starting material is wet biomass (Figure 2.3). Specifically, the major shortcoming of the application of polar organic solvents is the loss of solvent in the waste disposal step.[1] When sugars are separated from the other products of biomass processing, all the leftovers need to be processed to remove the polar organic solvents, to limit the dispersal in the environment, which is a problem from both environmental and economical points of view.[1,125,126,127] Most of the common polar organic solvents (*e.g.*, DMSO, DMF, THF) have detrimental effects both on the environment and on human health, hence green and more safe alternatives are needed.[127] Specifically, green alternatives for conventional dipolar aprotic solvents mainly include more task-specific replacements, formulated by rational design.[127] Biobased solvents (*e.g.,* GVL and GBL) can be seen as possible alternatives because of their renewability, biodegradability, and also their commercial availability.[127] However, applications are limited due to their instability toward strong acids and the already mentioned challenge of solvent-product separation.[127]

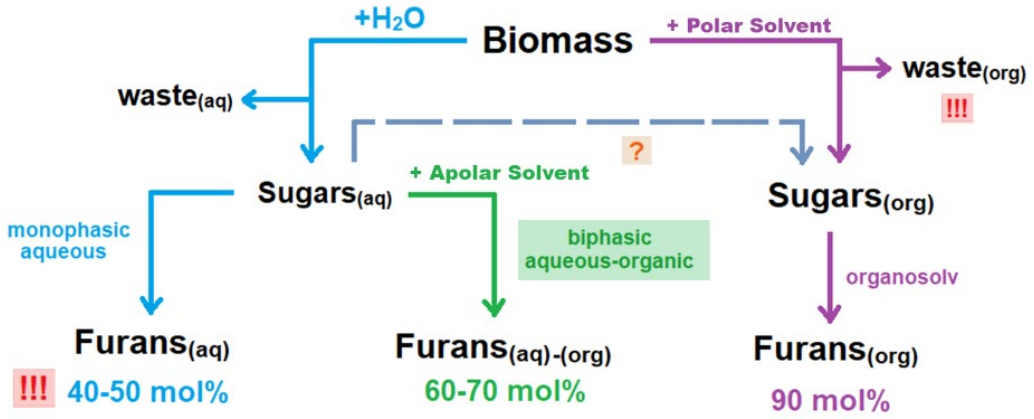

Figure 2.3 Comparison between the different operations currently available for the production of furans. Fully aqueous monophasic operation suffers from low sugar-to-furan selectivity (approx. 40-50 mol%). Fully organic operation (starting from biomass) is open to possible solvent losses through the waste stream, with negative environmental and economic impact. Isolating the sugar in water and only then switching to organic operation is a potentially viable compromise.

Product recovery is generally operated by means of distillation and, therefore, requires the solvent and solute to have suitable boiling points and chemical/thermal stabilities.[126,128,129] To minimize the energy demand, the product is preferably recovered from the product stream by distillation.[1,126] Therefore, the boiling point of the solvents, either at atmospheric pressure or at reduced pressure, needs to be sufficiently high with respect to that of HMF or furfural to minimize the distillation resistance.[128,129] For this reason, sulfolane (bp 285 °C) can be more suitable for industrial application in the case of furfural (bp 162 °C) than DMSO (bp 189 °C), which also suffers thermal degradation.[126,128]

An interesting alternative for non-green polar organic solvents could be cyrene (*i.e.*, dihydrolevoglucosenone), which is a water-miscible, high-boiling (bp 226 °C), biobased and fully biodegradable aprotic polar organic solvent (Scheme 2.4a).[130-134] Its properties are comparable with the most common non-biobased polar organic solvents and, for this reason, it has been used as a replacement of its 'less green' counterparts in several chemical processes.[130-132] Cyrene has been successfully used as a solvent for fluorination reactions, the synthesis of ureas and S_N2 substitution reactions, which are usually performed in DMF or NMP.[130-132] Recently, cyrene was employed in the pretreatment of biomass, in combination with water and other aprotic solvents (*e.g.*, dioxane), to obtain free carbohydrates through enzymatic hydrolysis.[133] However, to the best of our knowledge, applications of this solvent for sugar dehydration reactions

have not been reported so far. However, the application for sugar dehydration reactions requires every component of the solvent system to be stable at low pH and high temperature, hence, the analysis stability of cyrene at the reaction conditions is of top importance.

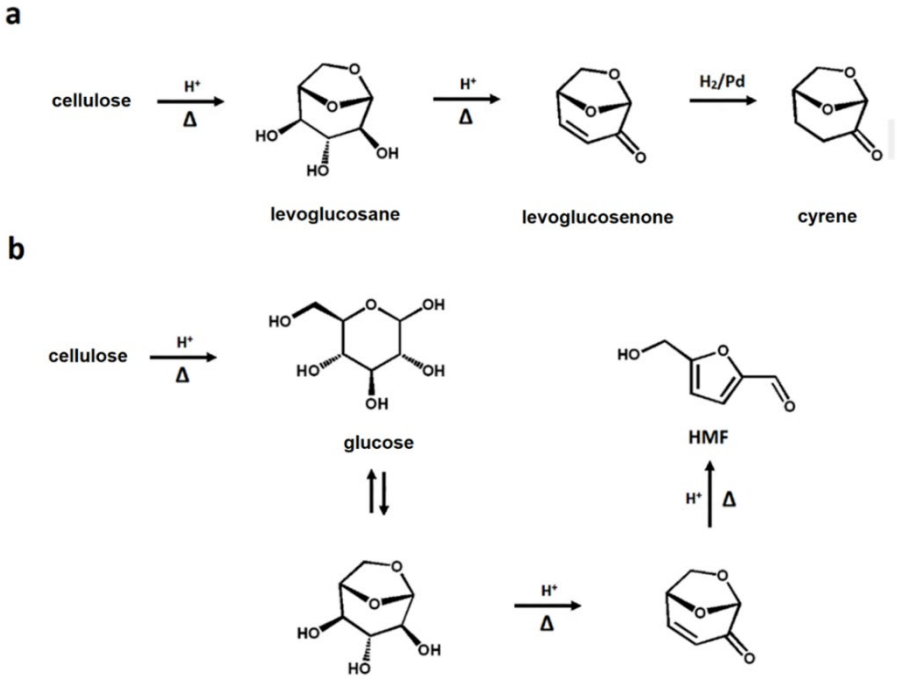

Scheme 2.4 (a) Cyrene production from cellulose. (b) Levoglucosenone as an intermediate of fructose dehydration to HMF.

Isolating the sugar from a sugar-rich feed in water and taking it into and reacting it an organic solvent (Figure 2.3) is another viable option for implementing polar organic solvents in an industrial setup. Typically, the industrial feed for the production of furans is an acidic aqueous stream containing a few percent (*e.g.*, 5 w%) of sugar, which is derived by pretreatment of biomass.[1,2,124] Removal of water from this stream is highly costly and ineffective, because water distillation is characterized by a prohibitive distillation resistance.[128,129] There are alternative approaches to remove the desired sugars from this aqueous stream, *e.g.*, by membrane enrichment, sugar crystallization, and liquid-liquid extraction.[135-137] The latter employs the formation of an organic-soluble boronate ester, and this method has already been used successfully to produce sugar alcohols selectively and to isolate solid sugars from a sugar-rich hydrolysate (Scheme 2.5).[135-137] This promising approach is challenging due to the high solubility of sugar in water and the operation parameters (mainly the high pH, ≥ 6), which are not

compatible with those of an industrial application as the aqueous stream has a pH around 3.[136,137] When performed at alkaline pH, the extraction relies on the phase transfer of a negatively charged monoester, formed by condensation of the sugar and the negatively charged tetragonal boronate anion (Scheme 2.5a), operated by a phase transfer agent (PTA), *e.g.*, halide salts of organic-soluble quaternary ammonium salts like Aliquat 366.[136] When performed at pH < pK_a of the boronic acid, the extraction relies on the formation of a diester between the sugar and the neutral trigonal form of the boronic acid (Scheme 2.5b). The latter method is the best candidate for implementation in an industrial setup, as it does not require additional components like PTAs. Extracting the sugar into an organic phase opens the way for a change of solvent for performing the dehydration of sugars.[137] However, prior to dehydration, the sugar boronate ester needs to be hydrolyzed to release the sugar. [137]

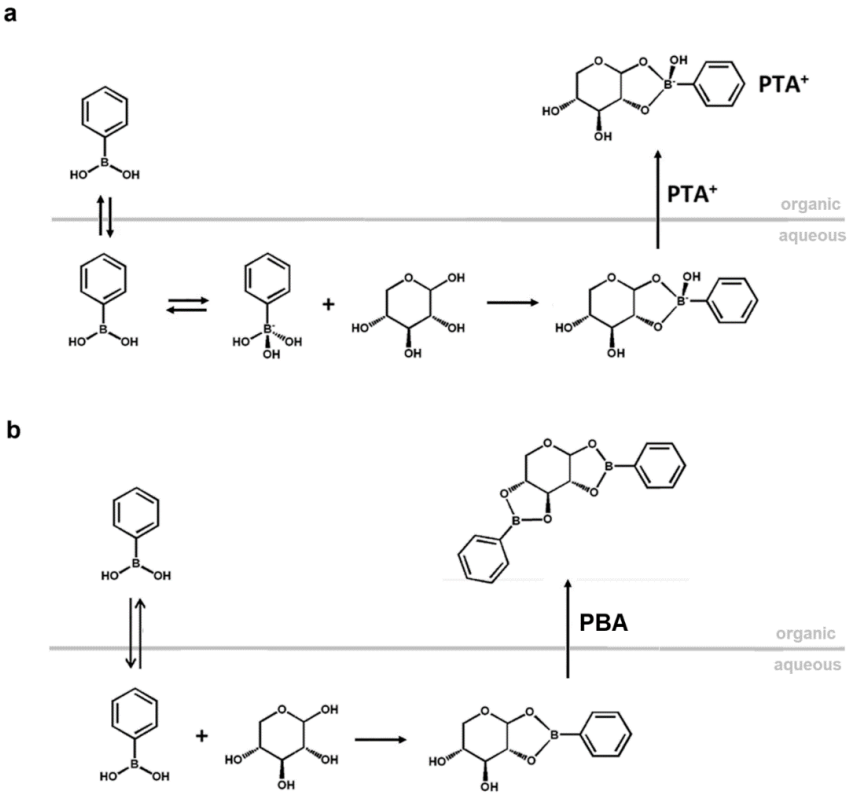

Scheme 2.5 Liquid-liquid xylose extraction via formation of (a) a negatively charged PBA monoester, mediated by a phase transfer agent (PTA), (b) an uncharged PBA diester, without any phase transfer agent.

2.5 Conclusions and Outlook

The application of polar organic solvents in the production of HMF and furfural from C_5 and C_6 sugars leads to sugar-to-furan selectivities up to 90-95 mol%, depending on the reaction conditions. This is an improvement compared to fully aqueous conditions, for which the sugar-to-furan selectivity is limited to approx. 45-50 mol%. This improvement can be rationalized by solvent effects involving the interaction with both the starting material and the catalyst, leading to: (i) specific conformational changes in the sugars, (ii) a change in the catalyst activity, and (iii) faster and more selective dehydration reactions. Each aprotic organic solvent shows a specific behavior, depending on the specific solvent-sugar and solvent-catalyst interactions, leading to different outcomes for each solvent at different reaction conditions.

The beneficial effect of polar solvents on the reaction parameters of sugar dehydration is a promising factor for the implementation of such solvent systems in the production of furfural and HMF on an industrial scale. However, the implementation of polar organic solvents in industrial setups is a challenging task, due to its effect on the nature of the feed, product separation and environmental impact. Candidates (*e.g.*, GBL and cyrene), favorable in terms of physicochemical properties and environmental friendliness, are available for such implementation, and are currently under evaluation. Moreover, additional techniques for ensuring the full compatibility with highly organic operations and the industrial feed, *e.g.*, liquid-liquid sugar extraction, are to be taken into consideration. All these additional steps will inevitably increase the process costs and complexity, requiring the sugar-to-furfural yield to be sufficiently high to justify such a trade-off. Although additional research and investigation of the upscaling of viable process concepts are needed, organic-aqueous monophasic conditions remain promising to improve the selectivity in the production of furans from biomass.

2.6 References

1. J.-P. Lange, E. van der Heide, J. van Buijtenen, R. Price, *ChemSusChem* **2012**, *5*, 150–166.
2. R. Mariscal, P. Maireles-Torres, M. Ojeda, I. Sádaba, M. López Granadosa, *Energy Environ. Sci.* **2016**, *9*, 1144–1189.
3. P. L. Arias, J. A. Cecilia, I. Gandarias, J. Iglesias, M. López Granados, R. Mariscal, G. Morales, R. Moreno-Tost, P. Maireles-Torres, *Catal. Sci. Technol.* **2020**, *10*, 2721-2757.
4. Y. Luo, Z. Li, X. Li, X. Liu, J. Fan, J. H. Clark, C. Hu, *Catal. Today* **2019**, *319*, 14-24.

5. H. Wang, C. Zhu, D. Li, Q. Liu, J. Tan, C. Wang, C. Cai, L. Ma, *Renew. Sust. Energ. Rev.* **2019**, *103*, 227–247.
6. A. A. Rosatella, S. P. Simeonov, R. F. M. Frade, C. A. M. Afonso, *Green Chem.* **2011**, *13*, 754-793.
7. K. Gupta, R. K. Rai, S. K. Singh, *ChemCatChem* **2018**, *10*, 2326-2349.
8. I. K. M. Yu, D. C. W. Tsang *Bioresour. Technol.* **2017**, *238*, 716-732.
9. B. Ward, *Bacterial Energy Metabolism in Molecular Medical Microbiology*, 2nd Edition, Academic Press, Cambridge (Massachusetts) **2014**, pp. 201-233.
10. J. Cai, Y. He, X. Yu, S. W. Banks, Y. Yang, X. Zhang, Y. Yu, R. Liu, A. V. Bridgwater, *Renew. Sust. Energ. Rev.* **2017**, *76*, 309-322.
11. A. Zoghlami, G. Paës, *Front. Chem.* **2019**, *7*, 1-11.
12. X. Li, Y. Chen, J. Nielsen, *Curr. Opin. Biotechnol.* **2019**, *57*, 56–65.
13. S. K. Bhatia, S. S. Jagtap, A. A. Bedekar, R. K. Bhatia, A. K. Patel, D. Pant, J. R. Banu, C. V. Rao, Y.-G. Kim, Y.-H. Yang, *Bioresour. Technol.* **2020**, *300*, 1-13.
14. J. Baruah, B. K. Nath, R. Sharma, S. Kumar, R C. Deka, D. C. Baruah, E. Kalita, *Front. Energy Res.* **2018**, *6*, 1-19.
15. Y. Kawamata, T. Yoshikawa, Y. Koyama, H. Ishimaru, S. Ohtsuki, E. Fumoto, S. Sato, Y. Nakasaka, T. Masuda, *Ind. Crops Prod.* **2021**, *159*, 113078.
16. B. Song, R. Lin, C. H. Lam, H. Wu, T.-H. Tsui, Y. Yu, *Renew. Sust. Energ. Rev.* **2021**, *135*, 110370.
17. Y. Jing, Y. Guo, Q. Xi, X. Liu, Y. Wang, *Chem* **2019**, *5*, 2520–2546.
18. R. Calvo-Serrano, M. Guo, C. Pozo, Á. Galán-Martín, G Guillén-Gosálbez, *ACS Sus. Chem. Eng.* **2019**, *7*, 10570–10582.
19. J. M. J. M. Ravasco, C. M. Monteiro, F. Siopa, A. F. Trindade, J. Oble, G. Poli, S. P. Simeonov, C. A. M. Afonso, *ChemSusChem* **2019**, *12*, 4629-4635.
20. S. Jiang, W. Ramdani, E. Muller, C. Ma, M. Pera-Titus, F. Jerôme, K. De Oliveira Vigiera, *ChemCatChem* **2020**, *13*, 1699-1704.
21. J. Xu, N. Li, X. Yang, G. Li, A. Wang, Y. Cong, X. Wang, T. Zhang, *ACS Catal.* **2017**, *7*, 5880–5886.
22. B. Danon, G. Marcotullio, W. de Jong, *Green Chem.* **2014**, *16*, 39-54.
23. B. Girisuta, L. P. B. M. Janssena, H. J. Heeres, *Green Chem.* **2006**, *8*, 701-709.
24. G. Tsilomelekis, M. J. Orella, Z. Lin, Z. Cheng, W. Zheng, V. Nikolakis, D. G. Vlachos, *Green Chem.* **2016**, *18*, 1983-1993.
25. I. Agirrezabal-Telleria, I. Gandarias, P.L. Arias, *Bioresour. Technol.* **2013**, *143*, 258–264.
26. A. Mukherjee, M.-J. Dumont, V. Raghavan, *Biomass Bioenerg.* **2015**, *72*, 143-183.
27. S. Peleteiro, S. Rivas, J. L. A. V. Santos, J. C. Parajó, *Bioresour. Technol.* **2016**, *202*, 181-191.

28. Z. Xue, M.-G. Ma, Z. Li, T. Mu, *RSC Adv.* **2016**, *6*, 98874-98892.
29. L. Shuai, J. Luterbacher, *ChemSusChem* **2016**, *9*, 133-155.
30. J. E. Romo, N. V. Bollar, C. J. Zimmermann, S. G. Wettstein, *ChemCatChem* **2018**, *10*, 4805–4816.
31. U. Tyagi, N. Anand, D. Kumar, *Bioresour. Technol.* **2019**, *289*, 1-9.
32. C. B. T. L. Lee, T. Y. Wu, *Renew. Sust. Energ. Rev.* **2021**, *137*, 1-19.
33. Y. Zhao, K. Lu, H. Xu, L. Zhu, S. Wang, *Renew. Sust. Energ. Rev.* **2021***, 139*, 1-27.
34. O. Ershova, K. Nieminen, H. Sixta, *ChemCatChem* **2017**, *9*, 3031–3040.
35. Y. Kim, A. Mittal, D. J. Robichaud, H. M. Pilath, B. D. Etz, P. C. St. John, D. K. Johnson, S. Kim, *ACS Catal.* **2020**, *10*, 14707−14721.
36. M. Sajid, M. R. Dilshad, M. S. U. Rehman, D. Liu, X. Zhao, *Molecules* **2021**, *26*, 1-17.
37. M. Peters, M. F. Eckstein, G. Hartjen, A. C. Spiess, W. Leitner, L. Greiner, *Ind. Eng. Chem. Res.* **2007**, *46*, 7073–7078.
38. I. Agirrezabal-Telleria, I. Gandarias, P. L. Arias, *Catal. Today* **2014**, *234*, 42–58.
39. S. Shrestha, X. Fonoll, S. K. Khanal, L. Raskin, *Bioresour. Technol.* **2017**, *245*, 1245–1257.
40. O. Ershova, J. Kanervo, S. Hellsten, H. Sixta, *RSC Adv.* **2015**, *5*, 66727-66737.
41. L. Zhu, X. Fu, Y. Hu, C. Hu, *ChemSusChem* **2020**, *18*, 4812-4832.
42. E. Nikolla, Y. Román-Leshkov, M. Moliner, M. E. Davis, *ACS Catal.* **2011***, 1,* 1724–1728.
43. J. M. R. Gallo, D. M. Alonso, M. A. Mellmera, J. A. Dumesic, *Green Chem.* **2013**, *15*, 85-90.
44. H. Shen, H. Shan, Li Liu, *ChemSusChem* **2020**, *13*, 513-519.
45. N. Shi, Q. Liu, H. Cen, R. Ju, X. He, L. Ma, *Biomass Convers. Bior.* **2020**, *10*, 277–287.
46. A. Toftgaard Pedersen, R. Hoffmeyer Ringborg, T. Grotkjær, S. Pedersen, J. M. Woodley, *Chem. Eng. Technol.* **2015**, *273*, 455–464.
47. Y. Zhao, H. Xu, K. Lu, Y. Qu, L. Zhu, S. Wang, *Energy Sci. Eng.* **2019**, *7*, 2237–2246.
48. Z. Chen, X. Bai, A. Lusi, W. A. Jacoby, C. Wan, *Bioresour. Technol.* **2019**, *289*, 1-8.
49. R. Xing, W. Qi, G. W. Huber, *Energy Environ. Sci.* **2011**, *4*, 2193-2205.
50. A. Mitta, S. K. Black, T. B. Vinzant, M. O'Brien, M. P. Tucker, D. K. Johnson, *ACS Sus. Chem. Eng.* **2017**, *5*, 5694–5701.
51. T. M. C. Hoang, L. Lefferts, K. Seshan, *ChemSusChem* **2013**, *6*, 1651–1658.
52. J.-M. Pin, N. Guigo, A. Mija, L. Vincent, N. Sbirrazzuoli, J. C. van der Waal, E. de Jong, *ACS Sus. Chem. Eng.* **2014**, *2*, 2182–2190.

53. R. M. Abdilla-Santes, S. Agarwal, X. Xi, H. Heeres, P. J. Deuss, H. J. Heeres, *J. Anal. App. Pyrolysis* **2020**, *152*, 1-10.
54. B. Saha, M. M. Abu-Omar, *Green Chem.* **2014**, *16*, 24-38.
55. R. Weingarten, J. Cho, W. C. Conner Jr., G. W. Huber, *Green Chem.* **2010**, *12*, 1423-1429.
56. Z. Wang, S. Bhattacharyya, D. G. Vlachos, *Green Chem.* **2020**, *22*, 8699-8712.
57. J. Esteban, A. J. Vorholt, W. Leitner, *Green Chem*. **2020**, *22*, 2097-2128.
58. F. Delbecq, Y. Takahashi, T, Kondo, C. Cara Corbas, E. Ruiz Ramos, C. Len, *Catal. Commun.* **2018**, *110*, 74–78.
59. M. Papaioannou, R. J. T. Kleijwegt, J. van der Schaaf, M. F. N. d'Angelo, *Ind. Eng. Chem. Res.* **2019**, *58*, 16106–16115
60. G.-T. Jeong, S.-K. Kim, D.-H. Park, Biotechnol. Bioprocess Eng. **2013**, *18*, 88-93.
61. A. A. Kiss, J.-P. Lange, B. Schuur, D. W. F. Brilman, A. G. J. van der Ham, S. R. A. Kersten, *Biomass Bioenerg.* **2016**, *95*, 296-309.
62. S. Kumar, S. Pandey, K. L. Wasewar, N. Ak, H. Uslu, *J. Chem. Eng. Data* **2021**, *66*, 1557–1573
63. T.-Y. Chen, P. Desir, M. Bracconi, B. Saha, M. Maestri, D. G. Vlachos, *Ind. Eng. Chem. Res.* **2021**, *60*, 3723–3735.
64. J. Köchermann, J. Schreiber, M. Klemm, *ACS Sus. Chem. Eng.* **2019**, *7*, 12323−12330.
65. X. Zhang, H. Lu, K. Wu, Y. Liu, C. Liu, Y. Zhu, B. Liang, *Chin. J. Chem. Eng.* **2020**, *28*, 136–142.
66. J. K. C. N. Agutaya, R. Inoue, S. Siew Vin Tsie, A. T. Quitain, J. de la Peña-García, H. Perez-Sànchez, M. Sasaki, T. Kida, *Ind. Eng. Chem. Res.* **2020**, *59*, 16527−16538.
67. K. Sun, Q. Li, L. Zhang, Y. Shao, Z. Zhang, S. Zhang, Q. Liu, Y. Wang, X. Hu, *Bioresour. Technol.* **2020**, *10*, 1-10.
68. Y. Romàn-Leshkov, J. A. Dumesic, *Top Catal.* **2009**, *52*, 297-303.
69. N. Jiang, R. Huang, W. Qi, R. Su, Z. He, *Bioenergy Res*. **2012**, *5*, 380–386.
70. L. Xu, R. Nie, H. Xu, X. Chen, Y. Li, X. Lu, *Ind. Eng. Chem. Res.* **2020**, *59*, 2754−2760.
71. X.-X. Xue, C.-L. Ma, J.-H. Di, X.-Y. Huo, Y.-C. He, *Bioresour. Technol.* **2018**, *268*, 292-299.
72. M. Zdanowicz, K. Wilpiszewska, T. Spychaj, *Carbohydr. Polym.* **2018**, *200*, 361-380.
73. J. Sittiwong, S. Boonmark, W. Nunthakitgoson, T. Maihom, C. Wattanakit, J. Limtrakul, *Inorg. Chem.* **2021**, *60*, 7, 4860–4868.
74. A. Gupta, S. U. Nandanwar, P. Niphadkar, I. Simakova, V. Bokade, *Biomass Bioenerg.* **2020**, *139*, 1-8.

75. L. Peng, M. Wang, H. Li, J. Wang, J. Zhang, L. He, *Green Chem.* **2020**, *22*, 5656-5665.
76. B Song, Z. Wu, Y. Yu, H. Wu, *Ind. Eng. Chem. Res.* **2020**, *59*, 7336−7345.
77. A. K. Chew, T. W. Walker, Z. Shen, B. Demir, L. Witteman, J. Euclide, G. W. Huber, J. A. Dumesic, R. C. Van Lehn, *ACS Catal.* **2020**, *10*, 1679–1691.
78. M. A. Mellmer, C. Sanpitakseree, B. Demir, P. Bai, K. Ma, M. Neurock, J. A. Dumesic, *Nat. Catal.* **2018**, *1*, 199–207.
79. J. J. Varghese, S. H. Mushrif, *React. Chem. Eng.* **2019**, *4*, 165-206.
80. J. Chen, B. Chan, Y. Shao, J. Ho, *Phys. Chem. Chem. Phys.* **2020**, *22*, 3855-3866.
81. R. J. J. Ganado, D. E. C. Yu DEC, F. C. Franco, *Ind. Eng. Chem. Res.* **2019**, *58*, 14621–14631.
82. I. K. M. Yu, D. C. W. Tsang, S. S. Chen, L. Wang, A. J. Hunt, J. Sherwood, K. De Oliveira Vigier, F. Jérôme, Y. Sik Ok, C. Sun Poon, *Bioresour. Technol.* **2017**, *245*, 456-462.
83. C. Jin, N. Xiang, X. Zhu, S. E, K. Sheng, X. Zhang, *Appl. Catal. B* **2021**, *285*, 1-11.
84. M. R. Whitaker, A. Parulkar, P. Ranadive, R. Joshi, N. A. Brunelli, *ChemSusChem* **2019**, *12*, 2211-2219.
85. V. Vasudevana, S. H. Mushrif, *RSC Adv.* **2015**, *5*, 20756-20763.
86. Q. Lin, S. Liao, L. Li, W. Li, F. Yue, F. Peng, J. Ren, *Green Chem*. **2020**, *22*, 532-539.
87. X. Guo, F. Guo, Y. Li, Z. Zheng, Z. Xing, Z. Zhu, T. Liu, X. Zhang, Y. Jin, *Appl. Catal. A* **2018**, *558*, 18-25.
88. O. H. Pardo Cuervo, G. P. Romanelli, J. A. Cubillos, H. A. Rojas, J. J. Martínez, *ChemistrySelect* **2020**, *5*, 4186-4193.
89. X. Fu, Y. Hu, Y. Zhang, Y. Zhang, D. Tang, L. Zhu, C. Hu, *ChemSusChem* **2020**, *13*, 501-512.
90. S. L. Barbosa, M. de S. Freitas, W. T. P. dos Santos, D. Lee Nelson, S. I. Klein, G. Cesar Clososki, F. J. Caires, A. C. M. Baroni, A. P. Wentz, *Sci. Rep*. **2021**, *11*, 1-5.
91. R. Wang , X. Liang, F. Shen, M. Qiu, J. Yang, X. Qi, *ACS Sus. Chem. Eng.* **2020**, *8*, 1163–1170.
92. S. Luan, W. Li, Z. Guo, W. Li, X. Hou, Y. Song, R. Wang, Q. Wang, *Green Energy Environ.* **2021**, *in press*.
93. F. Wang, H. Z. Wu, C. L. Liu, R. Z. Yang, W. S. Dong, *Carbohydr. Res.* **2013**, *368*, 78–83.
94. R. S. Nunes, G. M. Reis, L. M. Vieira, D. Mandelli, W. A. Carvalho, *Catal. Lett.* **2021**, *151*, 398–408.

95. M. A. Mellmer, C. Sanpitakseree, B. Demir, K. Ma, W. A. Elliott, P. Bai, R. L. Johnson, T. W. Walker, B. H. Shanks, R. M. Rioux, M. Neurock, J. A. Dumesic, *Nat. Commun.* **2019**, *10*, 1-10.
96. A. R. C. Morais, R. Bogel-Lukasik, *Green Chem.* **2016**, *18*, 2331-2334.
97. G. Park, W. Jeon, C. Ban, H. C. Woo, D. H. Kim, *Energy Convers. Manag.* **2016**, *118*, 135–141.
98. Q. Sun, S. Wang, B. Aguila, X. Meng, S. Ma, F.-S. Xiao, *Nat. Commun.* **2018**, *9*, 1-8.
99. J. E. Romo, K. C. Miller, T. L. Sundsted, A. L. Job, K. A. Hoo, S. G. Wettstein, *ChemCatChem* **2019**, *11*, 4715-4719.
100. P. S. Metkar, E. J. Till , D. R. Corbin , C. J. Pereira , K. W. Hutchenson, S. K. Sengupta, *Green Chem.* **2015**, *17*, 1453-1466.
101. C. Liu, M. Wei, F. Wang, L. Wei, X. Yin, J. Jiang, K. Wang, *J. Energy Inst.* **2020**, *93*, 1642-1650.
102. B. R. Caes, R. T. Raines, *ChemSusChem* **2011**, *4*, 353-356.
103. K. Wang, J. Ye, M. Zhou, P. Liu, X. Liang, J. Xu, J. Jiang, *Cellulose* **2017**, *24*, 1383–1394.
104. S. Ravi, Y. Choi, J. K. Choe, *Appl. Catal. B* **2020**, *271*, 1-12.
105. Q. Guo, L. Ren, S. M. Alhassan, M. Tsapatsis, *Chem. Commun.* **2019**, *55*, 14942-14945.
106. J. Jeong, C. A. Antonyraj, S. Shin, S. Kim, B. Kim, K.-Y. Lee, J. K. Cho, *J. Ind. Eng. Chem.* **2013**, *19*, 1106-1111.
107. T. Yang, W. Li, M. Su, Y. Liu, M. Liu, *New J. Chem.* **2020**, *44*, 7968-7975.
108. L. Ji, P. Li, F. Lei, X. Song, J. Jiang, K. Wang, *Energies* **2020**, *13*, 1-17.
109. Z. Wu, F. Wang, L. Hu, Y. Jiang, X. Wang, J. Xu, *J. Chem. Technol. Biotechnol.* **2021**, *96*, 971–979.
110. Z. Chen, W. A. Jacoby, C. Wan, *Bioresour. Technol. Rep.* **2019**, *8*, 1-4.
111. Q. Wang, X. Zhuang, W. Wang, X. Tan, Q. Yu, W. Qi, Z. Yuan, *Chem. Eng. J.* **2018**, *334*, 698-706.
112. A. H. Motagamwala, K. Huang, C. T. Maravelias, J. A. Dumesic, *Energy Environ. Sci.* **2019**, *12*, 2212-2222.
113. L. Wang, H. Guo, Q. Xie, J. Wang, B. Hou, L. Jia, J. Cui, D. Li, *Appl. Catal. A* **2019**, *572*, 51-60.
114. H. Kim, S. Yang, D. H. Kim, *Environ. Res.* **2020**, *187*, 1-7.
115. Y. Zhao, H. Xu, K. Wang, K. Lu, Y. Qu, L. Zhu, S. Wang, *Sustain. Energy Fuels* **2019**, *3*, 3208-3218.
116. I. M. Kolthoff, *Anal. Chem.* **1974**, *46*, 1992-2003.
117. W. C. Barrette Jr., H. W. Johnson Jr., D. T. Sawyer, *Anal. Chem.* **1984**, *56*, 1898-1902.

118. A. Jarczewski, C. D. Hubbard, J. Mol. Struct. **2003**, *649*, 287–307.
119. S. Kong, I. G. Shenderovich, M. V. Vener, *J. Phys. Chem. A* **2010**, *114*, 2393-2399.
120. A. K. Chew, R. C. van Lehn, *Front. Chem.* **2019**, *7*, 1-14.
121. S. Koujout, D. R. Brown, *Catal. Lett.* **2004**, *98*, 195-202.
122. A. K. Chew, T. W. Walker, Z. Shen, B. Demir, L. Witteman, J. Euclide, G. W. Huber, J. A. Dumesic, R. C. Van Lehn, *ACS Catal.* **2020**, *10*, 1679−1691.
123. T. W. Walker, A. K. Chew, R. C. Van Lehn, J. A. Dumesic, G. W. Huber, *Top. Catal.* **2020**, *63*, 649–663.
124. X. Li, Y. Chen, J. Nielsen, *Curr. Opin. Biotechnol.* **2019**, *57*, 56−65.
125. S. Ramaswamy, H.J. Huang, B. V. Ramarao, Separation and Purification Technologies in Biorefineries, *John Wiley & Sons*, Hoboken (New Jersey) **2013**, pp. 233−258.
126. J.-P. Lange, *ChemSusChem* **2017**, *10*, 245–252.
127. F. Gao, R. Bai, F. Ferlin, L. Vaccaro, M. Li, Y. Gu, *Green Chem.* **2020**, *22*, 6240-6257.
128. D. L. Head, C. G. McCarty, *Tetrahedron* **1973**, *16*, 1405-1408.
129. B. F. M. Kuster, *Starch* **1900***, 42,* 314–321.
130. J. Sherwood, M. De bruyn, A. Constantinou, L. Moity, C. R. McElroy, T. J. Farmer, T. Duncan, W. Raverty, A. J. Hunt, J. H. Clark, *Chem. Commun.* **2014**, *50*, 9650-9652.
131. J. E. Camp, *ChemSusChem* **2018**, *11*, 3048-3055.
132. L. Mistry , K. Mapesa , T. W. Bousfield, J. E. Camp, *Green Chem.* **2017**, *19*, 2123-2128.
133. X. Meng, Y. Pu, M. Li, A. J. Ragauskas, *Green Chem*. **2020**, *22*, 2862-2872.
134. F. Cao, T. J. Schwartz, D. J. McClelland, S. H. Krishna, J. A. Dumesic, G. W. Huber, *Energy Environ. Sci.* **2015**, *8*, 1808-1815.
135. G. J. Griffin, L. Shu, *J. Chem. Technol. Biotechnol.* **2004**, *79*, 505−511.
136. N. Sánchez-Bastardo, I. Delidovich, E. Alonso, *ACS Sus. Chem. Eng.* **2018**, *6*, 11930–11938.
137. S. S. Gori, M. V. Ramakrishnam Raju, D. A. Fonseca, J. Satyavolu, C. T. Burns, M. H. Nantz, *ACS Sus. Chem. Eng.* **2015**, *3*, 2452–2457.

Chapter 3

Reactive Extraction Enhanced by Microwave Heating: Furfural Yield Boost in Biphasic Systems

Reactive extraction is an emerging operation in the industry, particularly in biorefining. Here, reactive extraction was demonstrated, enhanced by microwave irradiation to selectively heat the reactive phase (for efficient reaction) without unduly heating the extractive phase (for efficient extraction). These conditions aimed at maximizing the asymmetries in dielectric constants and volumes of the reaction as well as extraction phases, which resulted in an asymmetric thermal response of the two phases. The efficiency improvement was demonstrated by dehydrating xylose (5 w% in water) to furfural with an optimal yield of approximately 80 mol% compared with 60–65 mol% under conventional biphasic conditions, which corresponds to approximately 50% reduction of byproducts.

Part of this chapter has been published in: L. Ricciardi, W. Verboom, J.-P. Lange, J. Huskens, *ChemSusChem* **2020**, *13*, 3589 – 3593.

3.1 Introduction

Reactive extraction has emerged recently as a promising technology for the conversion of biobased feedstock.[1-3] This technique is a cost-effective way to circumvent problems in biorefinery, such as recovering and recycling catalysts, separating products, and suppressing side reactions.[1-3] Reactive extraction shows a wide scope of applications and can be also used in the conversion of sugars into furans (*e.g.*, furfural).[3] Furfural has a rich source of derivatives and can be used as an additive for fuels with promising performance.[4,5] Furfural can be obtained from the acid-catalyzed dehydration of D-xylose, a monomeric subunit of hemicellulose, which is a component of lignocellulosic feedstock.[4–7] Furfural production in aqueous medium and mineral acid catalysis (H_2SO_4) does not deliver furfural yields beyond approximately 45 mol% on xylose base.[4,5,7,8] This shortcoming is mainly caused by the formation of insoluble byproducts called humins, resulting from furfural–xylose condensation and direct resinification of furfural at high conversion.[4,5,8] Several examples of high-yield (> 80 mol%) furfural production have been reported using polar aprotic organic solvents.[9,10] However, such approaches suffer from the need to extract the xylose from the aqueous phase to resolubilize it in the polar organic solvent. An alternative approach, based on reactive extraction in biphasic operation, reached furfural yields of approximately 65 mol%.[10–12] This selectivity enhancement is generally assigned to continuous extraction of furfural into the organic phase, with the consequent inhibition of furfural degradation.[8,11,13–16]

Microwave heating has been widely applied to organic synthesis in general and has been abundantly used for the dehydration of sugars to furans, for example, of xylose to furfural.[14,17–19] When applied to monophasic aqueous xylose solution, microwave heating does not result in improvement of the selectivity but only in a rate enhancement.[20-22] This has been explained through purely thermal effects such as inhomogeneous heating.[20–22] Incidentally, biphasic operation has been combined with microwave heating, but no specific effects have been recognized.[23,24] Nevertheless, the combination of microwave heating and biphasic operation could have a synergic effect on the selectivity of the furfural production (Figure 3.1).

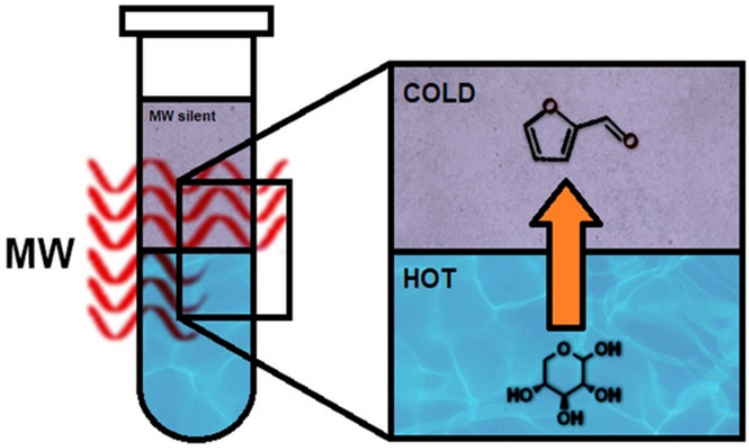

Figure 3.1 Visualization of the effect of having an asymmetric response in the biphasic system on reactive extraction of furfural. Furfural is formed in the microwave-active 'hot' aqueous phase and extracted and stored in the MW-silent 'cold' toluene phase.

Microwave heating could heat up the aqueous phase to accelerate the dehydration of xylose while leaving the organic phase colder to favor the extraction of furfural. This chapter shows that the combination of microwave heating and biphasic operation can indeed create a synergic effect that permits operation at higher xylose conversions than normally applied and pushes reaction parameters (*i.e.*, furfural yield, xylose conversion and xylose-to-furfural selectivity) to values that cannot be attained by one of the conditions alone (Figure 3.2). Application to the combined microwave–biphasic operation may thus yield a further enhancement owing to the synergic effect, moving the optimal operation point to high xylose conversion, with an effect that is related to the microwave responsiveness of the two phases (Figure 3.2). By unravelling the basis of this effect, we pave the way to improving a wide range of reactive extraction processes.

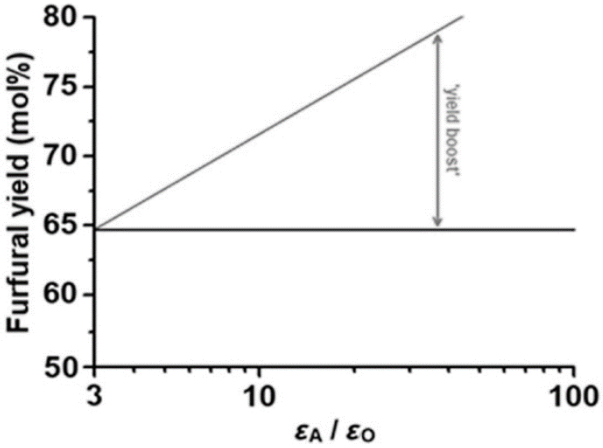

Figure 3.2 Visualization of the 'yield boost' at biphasic conditions in relation with the difference in polarity between the two phases of the system, in which ε_A is the dielectric constant of the aqueous phase and ε_O is that of the organic phase. The yield boost at microwave conditions will arise at a higher ratio (oblique line), as the microwave responsiveness changes accordingly, whereas at traditional heating conditions the difference in dielectric properties does not have any influence on the heating profile, resulting in an unvaried final yield (horizontal line).

3.2 Results and Discussion

In biphasic systems, the microwave responsiveness of each phase is strongly dependent on its dielectric properties: a higher polarity corresponds to a higher dielectric loss at microwave conditions, which results in a more efficient heating.[25,26] The combination of a non-polar organic solvent (*e.g.*, toluene or methylcyclohexane) and a highly polar aqueous phase (*e.g.*, water with a high ionic strength) might lead to an inhomogeneous temperature distribution between the two phases because the aqueous phase gets selectively heated by the microwave irradiation.[11,15]

It is crucially important to accurately monitor the reaction temperature under microwave conditions.[20–22] Fiber-optic sensors are commonly used to internally monitor the temperature, but if the homogeneity of the mixing cannot be ensured such sensors show surprisingly large temperature gradients throughout the reaction medium.[20] Owing to the high operation temperatures applied in this Chapter and the necessity to seal the pressurized reaction vessels, the temperature was monitored by using an IR temperature control system. Under microwave heating, more information about the global temperature of the medium is obtained by comparing the operating pressure (≈ 18–20 bar) to the equivalent saturated pressure (Figure 3.3). The operating pressure measured in the presence of the biphasic water/toluene mixture

of 1:1 volume ratio suggests a bulk liquid temperature that deviates less than ± 10 °C from that measured by the IR sensor.[27] Nevertheless, these calibration data do not give any quantitative information on local temperature differences between the two liquid phases.

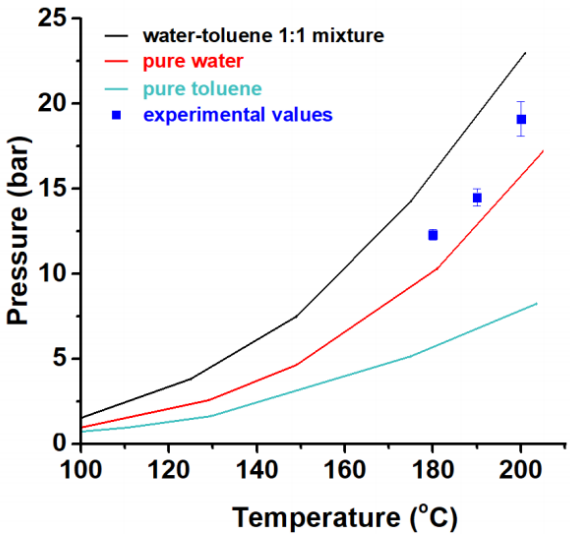

Figure 3.3 Pressure (bar) *versus* temperature (°C) plot, as an indication for the experimental temperature at microwave conditions, comparison between the observed experimental pressure (blue dots) with literature values for pure water (red line), pure toluene (cyan line) and a water-toluene 1:1 mixture (black line). The experimental values fall in the expected interval and is closest to the water line, which is the hottest phase in our system and, thereby, dictates the pyrometer reading.

For this study a biphasic system of an aqueous solution of xylose (350 mm, pH = 1 from H_2SO_4) and an organic solvent of choice was heated to 200 °C both at traditional batch and microwave heating conditions. To tune the microwave responsiveness of the biphasic system, the volume ratio of the two phases and their chemical composition were varied. Toluene, commonly used as organic phase under biphasic conditions, was chosen as a benchmark hydrophobic solvent for its low dielectric constant (ε_r = 2.4), which results in negligible microwave activity, and for its aromaticity, which ensures high affinity for the extraction of furfural. The toluene phase is heated slightly upon contact with the aqueous phase, but this effect is minimized by operating at high toluene/water ratio. Our experimental setup did not allow us to gather information on the temperature of the two different phases. However, in the biphasic system the two phases remained immiscible even a thigh temperature.

Because the dehydration of xylose is acid catalyzed, the composition of the aqueous phase (pH = 1 from H_2SO_4) ensures both optimal catalytic conditions for furfural formation and high ionic strength for microwave responsiveness.[28,29] The concentrations of furfural and unreacted xylose in the crude reaction mixture were evaluated through ^{1}H-NMR spectroscopy to determine the rate and the selectivity of the xylose dehydration into furfural at biphasic conditions, which can also be compared with the monophasic system (Figures 3.4). At a 1:1 water/toluene ratio, both traditional heating and microwave heating could achieve full xylose conversion. Under traditional heating full xylose conversion was obtained after 360 min, at microwave conditions in 15 min (Figures 3.4a and 3.4b), illustrating the rate enhancement obtained under microwave conditions. The two heating methods can also be compared in terms of furfural selectivity and yield, as well as their optimal points of operation. At xylose conversions from 0 to 85–90 mol%, selectivity and yield run parallel for both heating methods (Figure 3.4c). In contrast, for xylose conversions > 90 mol% a higher furfural yield is recorded with microwave heating (Figure 3.4c), reaching a yield of approximately 75 mol% (at a conversion > 95 mol%), whereas traditional heating provides a maximum yield of approximately 65 mol%, reached at approximately 85 mol% conversion, as has also been observed in literature.[4,5,7,8] Correspondingly, at traditional heating conditions the maximum of selectivity is obtained at approximately 85 mol% xylose conversion (after 240 min of reaction; Figure 3.4d), whereas under microwave heating the maximum is reached at > 95 mol% xylose conversion (after approx. 13 min of reaction; Figure 3.4d). This observed rate enhancement cannot simply be assigned to a higher bulk temperature of the medium under microwave heating, as will be discussed in Chapter 4. Such differences in the reaction rate would correspond to effective bulk temperatures up to 50 ^{o}C higher than the measured ones. Not only do these values exceed the deviations shown by the calibration, but they would also result in an excessive saturated pressure that was not observed experimentally.

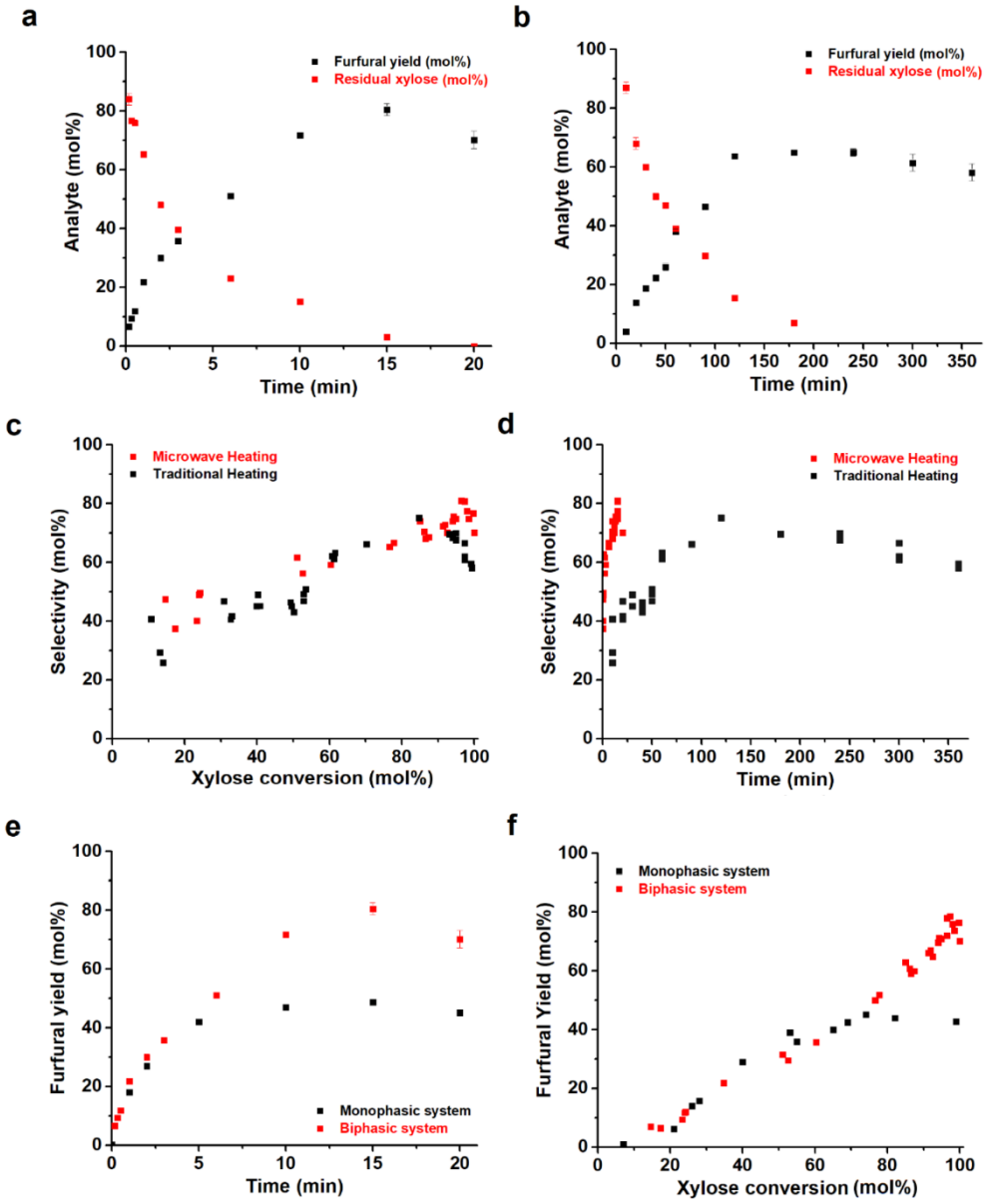

Figure 3.4 Rate of furfural production and xylose consumption, 1:1 water-toluene biphasic system, starting xylose concentration 350 mM, pH = 1 from H_2SO_4, target temperature 200 °C under (a) microwave heating and (b) traditional heating. Xylose-to-furfural selectivity (mol%) varying (c) over xylose conversion (mol%) or (d) time. It has to be noted that the selectivity profile of the two heating methods is the same in

the early stages of the reaction and diverges only at high xylose conversion, hinting to a similar selectivity in the beginning of the process. Comparison between monophasic and biphasic conditions (microwave heating, same pH, starting xylose concentration, target temperature) in terms of (e) rate of furfural production and (f) xylose-to-furfural selectivity (mol%) over xylose conversion (mol%). The reaction mixture reaches in all cases the target temperature within a small part of the reaction time. Therefore, any possible effect of the heating rate is ignored.

The observed yield boost is thus a result of a shift of the optimal operating point (maximum furfural yield) to higher xylose conversions. This can be rationalized by inhibition of furfural degradation pathways in the late stage of the reaction, provided by an improved furfural extraction from the highly reactive aqueous phase. The selectivity enhancement upon microwave-assisted biphasic operation appeared to depend on the toluene volume fraction. Varying the solvent volume ratio affected the overall dielectric properties of the system as well as the extraction capacity. As a result, the maximum yield at high xylose conversions slightly increased with the toluene volume fraction when operated under microwave irradiation, and these higher yields were again achieved at higher xylose conversions (Figure 3.5a). Thus, a maximum yield boost of approximately 30 mol% was achieved upon changing operation from monophasic to biphasic at 90 vol% toluene (Figure 3.5b). Control experiments showed that the toluene fraction did not affect the final furfural yield under traditional heating.

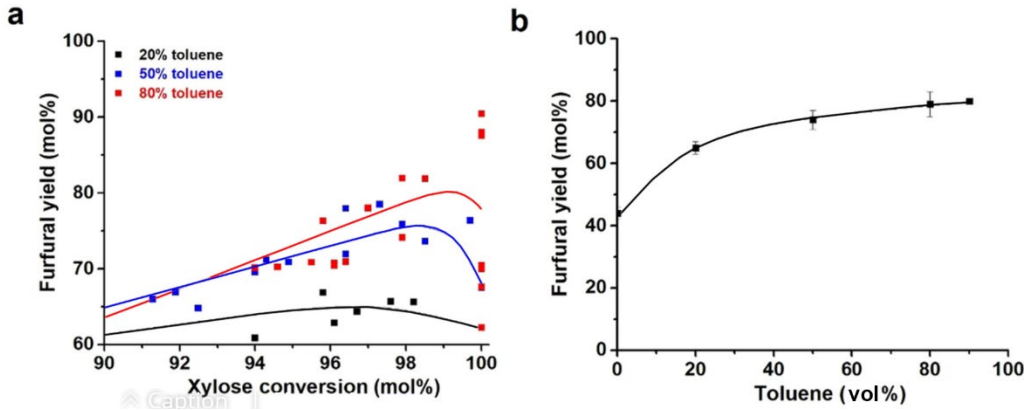

Figure 3.5 (a) Furfural yield (mol %) *versus* xylose conversion (mol%), at pH 1, at various water/toluene ratios, under microwave heating at 200 °C (section at conversions > 90 % shown). The multiple points at 100 mol% xylose conversion represent the progressive degradation of furfural with increasing reaction time. (b) Visualization of the yield boost obtained at the optimal operation points (at high

xylose conversion) varying the toluene percentage. The data point at 90 vol% toluene is the result of a single experiment and is therefore reported without an error bar.

The observed yield boost can be explained by the suppression of the acid-catalyzed degradation and condensation reactions of furfural, that is by a medium effect. The furfural is extracted and stored safely in the organic phase, which at microwave conditions has a lower temperature than the aqueous phase. This difference in temperature arises only at microwave conditions because the selective heating of the aqueous phase cannot be observed under traditional heating conditions, resulting in no selectivity enhancement under traditional heating. No significant yield enhancement was obtained by raising the toluene percentage over 80 vol% (Figure 3.5b). This upper limit for the yield can be rationalized by the fact that furfural partitions between the organic phase and the aqueous phase, in the latter of which acid-catalyzed degradation can occur.

As mentioned above, the relative polarity of the two phases is important (Figure 3.2b), and it can be influenced by independently varying the dielectric constants of the organic phase and of the aqueous phase. Various organic solvents with different polarities were employed to show the effect of varying the dielectric constant of the organic phase on this yield boost (Figure 3.6a). Based on the previous experiments, at microwave conditions the polarity of the solvent appeared to strongly affect the conversion of xylose to furfural (Figure 3.6a). At 1:1 biphasic conditions, a maximum furfural yield of approximately 75 mol% was obtained for low-polarity solvents such as toluene (ε_r = 2.4), methylcyclohexane (MCH, ε_r = 0.7), or perfluorotoluene ($\varepsilon_r \approx 0$). Upon moving to solvents with a higher polarity and significantly higher microwave absorption, the furfural yield decreased significantly to approximately 60 mol% with methylisobutylketone (MIBK, ε_r = 4.3) and octanol (ε_r = 10). In comparison, 45 mol% was achieved for the monophasic water system under microwave heating. Upon using toluene/water at traditional heating, only 65 mol% yield was achieved.

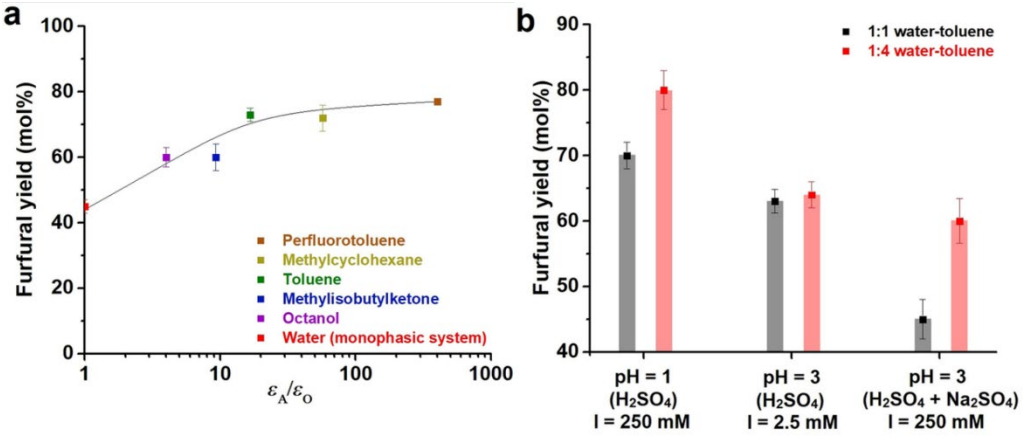

Figure 3.6 Maximum furfural yield (mol%) at xylose conversions > 90 mol% as a function of the ratio of the dielectric constants of the aqueous and organic phases (15–20 min, 200 °C, 1:1 solvent ratio, pH = 1). The line is a guide to the eye. (b) Visualization of the xylose-to-furfural yield boost in the reaction of xylose dehydration observed when varying the water/toluene ratio from 1:1 to 1:4 (200 °C, microwave heating), in relation with the ionic strength of the aqueous phase (dependent on acid and salt concentrations); data obtained at the optimal operation point (*i.e.*, at maximum yield).

The microwave responsiveness of the aqueous phase can also be tuned by varying the pH and/or salt concentration of the aqueous solution.[28] Two new sets of experiments were performed, one at pH = 3 from H_2SO_4 (at a significantly lower ionic strength) and one additional control in which a passive, non-reactive ion source (Na_2SO_4) was added to achieve the high ionic strength of the solution at pH = 1 used above while keeping the pH 3. Both sets were performed at 1:1 and 1:4 water/toluene ratios (Figure 3.6b). As described above, at pH 1 under microwave heating, the toluene percentage clearly influenced the process (Figure 3.5b). In contrast, at pH 3 no yield enhancement was observed (Figure 3.6b) upon varying the solvent ratio. However, upon adding an inert salt to the solution at pH 3 to reach the same ionic strength of the experiment performed at pH 1, a similar yield boost was observed when varying the solvent ratio (Figure 3.6b). However, this enhancement was always limited (as in the previous cases) at high xylose conversions. This shows that the microwave responsiveness of the aqueous phase, which is directly related to the ionic strength, is crucial to achieve the conditions that lead to a selectivity enhancement.[28,29] However, the best results in terms of furfural yield (mol%) were obtained in the system at pH 1, indicating that a fast reaction is mandatory to prevent degradation and humins formation. This is arguably owing to the reaction rate outcompeting the rate of heating the toluene phase upon contacting the aqueous phase.

3.3 Conclusions

There is a consistent yield improvement of approximately 10–15 mol% in the dehydration of xylose by synergistically combining two different factors: microwave heating and reactive extraction using two phases with asymmetric polarity and volumes. Generally, the improvement of the yield of a chemical process is obtained by the development and optimization of a catalyst, possibly assisted by plasmonics or ultrasound, or by varying the solvent system and using membranes or other components for the in situ separation of the various products.[30–36] This Chapter shows how a more optimal section of the reaction parameter space can be reached by the combination of microwave heating and specific biphasic conditions and by varying the dielectric properties of both phases. Such forms of synergism can become an important tool for organic synthesis and chemical processes. By unravelling the critical parameters of this process optimization, this approach can be applied to improve other reactive extraction processes.

3.4 Experimental Section

3.4.1 Chemicals

D-(+)-xylose (> 99%), D_2O (99.9% atom D), toluene-d_8 (99% atom D), dioxane (99.8%), 3- (trimethylsilyl)propionic-2,2,3,3-d_4 acid sodium salt (TMSP, 98% atom D), perfluorotoluene (98%), methylisobutylketone (> 99%), octanol (> 99%), methylcyclohexane (> 99%) and sodium sulphate decahydrate (> 99%) were purchased from Sigma-Aldrich.

3.4.2 Methods and Equipment

All chemicals are commercially available and were used without further purification. ^{1}H-NMR spectra were recorded at a 400 MHz Bruker spectrometer in a 1:1 H_2O/D_2O mixture with TMSP as the internal standard or in a 1:1 organic solvent/toluene-d_8 with dioxane as the internal standard. A microwave reactor (CEM Discover SP) equipped with a pressure sensor device (IntelliVent Pressure Sensor Assembly) was used to perform the reactions under microwave heating. The IR temperature sensor was calibrated following the cooling of ethylene glycol from the boiling point to room temperature in three different cycles. All of the data analysis and the fitting were performed using Origin 2016 (64 bit).

3.4.3 Xylose Dehydration under Traditional Heating

A solution of D-xylose (350 mM) in water (pH = 1 from H_2SO_4) was contacted with various volumes of toluene (for a total volume of 4 mL) to reach different aqueous-

organic ratios and heated with a Wood's metal bath at 200 °C, in a high pressure-proof hard glass vessel (ACE Glass Incorporated). The reaction mixing was performed with a magnetic stirrer (approx. 1000 rpm). The reactions were stopped and subsequently cooled with an ice bath, prior to data collection. The crude reaction mixture was analyzed with ^{1}H-NMR spectroscopy via a standardized procedure.

3.4.4 Xylose Dehydration under Microwave Heating

A solution of D-xylose (350 mM) in water (pH = 1 from H_2SO_4) was contacted with various volumes of toluene (for a total volume of 4 mL) to reach different aqueous-organic ratios, or alternatively contacted with equal volumes of the organic solvent of choice and heated at 200 °C in the microwave reactor. The reaction mixing was performed with a magnetic stirrer (approx. 1000 rpm). The reactions were stopped and cooled by blowing cold air on the vessel, prior to data collection. The crude reaction mixture was analyzed with ^{1}H-NMR spectroscopy via a standardized procedure.

3.5 References

1. H.-J. Huang, S. Ramaswamy, U. W. Tschirner, B. V. Ramarao*, Sep. Purif. Technol.* **2008**, *62*, 1–21.
2. S. Ramaswamy, H.-J. Huang, B. V. Ramarao, *Separation and Purification Technologies in Biorefineries*, Wiley, Chichester (UK), **2013**.
3. A. A. Kiss, J.-P. Lange, B. Schuur, D. W. F. Brilman, A. G. J. van der Ham, S. R. A. Kersten, *Biomass. Bioenergy* **2016**, *95*, 296–309.
4. J.-P. Lange, E. van der Heide, J. van Buijtenen, R. Price, *ChemSusChem* **2012**, *5*, 150 –166.
5. R. Mariscal, P. Maireles-Torres, M. Ojeda, I. Sádaba, M. López Granados, *Energy Environ. Sci.* **2016**, *9*, 1144–1189.
6. J.-P. Lange, I. Lewandowski, P. Ayoub, *Sustainable Development in the Process Industry—cases and impacts*, Wiley, Chichester (UK) **2010**, pp. 171–208.
7. P. Priecel, J. E. Perez Mejia, P. D. Carà, J. A. Lopez-Sanchez, *Sustainable Catalysis for Biorefineries*, Royal Society of Chemistry, Burlington House (London), **2018**, pp. 243–299.
8. J. E. Romo, N. Bollar, C. J. Zimmermann, S. G. Wettstein, *ChemCatChem* **2018**, *10*, 4805 –4816.
9. L. Shuai, J. Luterbacher, *ChemSusChem* **2016**, *9*, 133–155.
10. C. Sener, A. H. Motagamwala, D. M. Alonso, J. A. Dumesic, *ChemSusChem* **2018**, *11*, 2321–2331.

11. Y. Román-Leshkov, J. N. Chheda, J. A. Dumesic, *Science* **2006**, *312*, 1933-1937.
12. B. F. M. Kuster, *Starch/Staerke* **1990**, *42*, 314–321.
13. M. Peters, M. F. Eckstein, G. Hartjen, A. C. Spiess, W. Leitner, L. Greiner, *Ind. Eng. Chem. Res.* **2007**, *46*, 7073–7078.
14. F. Delbecq, Y. Takahashi, T. Kondo, C. C. Corbas, E. R. Ramos, C. Len, *Catal. Commun.* **2018**, *110*, 74–78.
15. R. Weingarten, J. Cho, W. C. Conner, Jr., G. W. Huber, *Green Chem.* **2010**, *12*, 1423–1429.
16. G. Gómez-Millán, S. Hellsten, A. W. T. King, J.-P. Pokki, J. Llorca, H. Sixta, *J. Ind. Eng. Chem.* **2019**, *72*, 354–363.
17. A. K. Rathi, M. B. Gawande, R. Zboril, R. S. Varma, *Coord. Chem. Rev.* **2015**, *291*, 68–94.
18. M. B. Gawande, S. N. Shelke, R. Zboril, R. S. Varma, *Acc. Chem. Res.* **2014**, *47*, 1338–1348.
19. Y. Wang, F. Delbecq, R. S. Varma, C. Len, *Mol. Catal.* **2018**, *445*,73–79.
20. Á. Díaz-Ortiz, P. Prieto, A. De la Hoz, *Chem. Rec.* **2019**, *19*, 85–97.
21. C. O. Kappe, *Acc. Chem. Res.* **2013**, *46*, 1579–1587.
22. M. A. Herrero, J. M. Kremsner, C. O. Kappe, *J. Org. Chem.* **2008**, *73*, 36–47.
23. K. Hayashi, S. Kim, Y. Kono, M. Tamura, K. Chiba, *Tetrahedron Lett.* **2006**, *47*, 171–174.
24. D. Bogdal, S. Bednarz, M. Łukasiewicz, M. Kasprzyk, *Chem. Eng. Process.* **2018**, *132*, 208–217.
25. Y. Wang, M. N. Afsar, *Prog. Electromagn. Res.* **2003**, *42*, 131–142.
26. L. Gai, L. Guo, Q. An, Z. Xiao, S. Zhai, Z. Li, *Microporous Mesoporous Mater.* **2019**, *288*, 1-13.
27. F. E. Anderson, J. M. Prausnitz, *Fluid Phase Equilib.* **1986**, *32*, 63–76.
28. C. Gabriel, S. Gabriel, E. H. Grant, B. S. J. Halstead, D. M. P. Mingos, *Chem. Soc. Rev.* **1998**, *27*, 213–224.
29. C. O. Kappe, *Angew.Chem. Int. Ed.* **2004**, *43*, 6250–6584.
30. E. S. Isbrandt, R. J. Sullivan, S. G. Newman, *Angew. Chem. Int. Ed*. **2019**, *58*, 7180–7191.
31. N. Jiang, Y. Zhao, C. Qiu, K. Shang, N. Lu, J. Li, Y. Wu, Y. Zhang, *Appl. Catal. B* **2019**, *259*, 1-15.
32. C. Guerrero, C.Vera, F. Acevedo, A. Illanes, *J. Biotechnol.* **2015**, *209*, 31–40.
33. G. Zeng, Y. Wang, D. Gong, Y. Zhang, P. Wu, Y. Sun, *ACS Cent. Sci.* **2019**, *5*, 1834–1843.
34. R. Joncour, A. Ferreira, N. Duguet, M. Lemaire, *Org. Process Res. Dev.* **2018**, *22*, 312–320.

35. C. Zhan, X. J. Chen, Y. F. Huang, D. Y. Wu, Z. Q. Tian, *Acc. Chem. Res.* **2019**, *52*, 2784–2792.
36. R. S. Varma, K. P. Naicker, D. Kumar, *J. Mol. Catal. A* **1999**, *14*, 153–160.

Chapter 4

Overheating Explains the Rate Enhancement of Xylose Dehydration at Microwave Conditions

The NH_4Cl-assisted dehydration of xylose to furfural was studied using traditional and microwave heating. Significant differences in rate, pH profiles and selectivity profiles were observed between both heating systems. A comparative kinetic analysis showed 7-13 times higher first-order rate constants for the xylose dehydration reaction under microwave heating. Dedicated experiments with varying irradiation power and liquid mixing intensity suggested that the differences are due to the development of overheated areas under microwave heating. This hypothesis was supported by modeling the rate enhancement observed under microwave heating using a simple kinetic model that assumes a minor overheated fraction amid a bulk liquid at target temperature.

Part of this chapter has been published in: L. Ricciardi, W. Verboom, J.-P. Lange, J. Huskens, *ACS Sus. Chem. Eng.* **2019**, *7*, 14273–14279.

4.1 Introduction

Microwave-assisted heating is being applied widely and successfully in organic chemistry.[1,2] The main characteristic of microwave-assisted organic synthesis (MAOS) is rate acceleration, observed in almost all reactions. Other results that cannot be obtained using traditional heating have been also reported, *e.g.*, unconventionally high yields and different reaction mechanisms.[1,3-5] Today, it is generally agreed upon that the observed rate enhancements in microwave-heated reactions are the result of solely thermal effects.[6] Specifically, the use of reaction vials made of silicon carbide (SiC), a highly microwave-absorbing material, by Kappe *et al.* has proven to be extremely valuable in investigating the non-existence of specific, non-thermal microwave effects.[6,7] In other words, "heating is just heating, whether by microwave or conventional methods".[7-9] However, microwave heating is fundamentally different from conventional heating, since it is derived from the selective interaction of the electromagnetic radiation with matter that leads to an energetic coupling at the molecular level.[10] The presence of thermal effects as superheating of the solvent are often postulated to explain the rate enhancement.[1,2] Local overheating is a consequence of the inhomogeneous electromagnetic field distribution along the sample. Temperature gradients at microwave conditions have been modeled to result from field inhomogeneity and have been detected by fiber optic sensors and by IR thermography, and through specific photochemical reactions.[5,8,10-12] However, to the best of our knowledge, there is no kinetic model that directly relates the local overheating to the rate enhancement under microwave heating.

Microwave heating has also been explored for the conversion of bio-based feedstock to fuels and chemicals, *e.g.*, for manufacturing furfural and hydroxymethylfurfural.[13-20] The existence of a specific, non-thermal microwave effect in the manufacture of furans has already been excluded using Kappe's SiC vessels.[21] However, these claims were nuanced by Ashley *et al.*, who showed significant microwave leakage through SiC.[22] Even more recently, De Bruyn *et al.* studied a demethylation reaction under conventional and microwave heating and found differences in kinetic behavior only when the reaction conditions allowed gaseous products to form gas bubbles and escape the reaction vessels.[5] Through a comprehensive modeling study, they claimed that the formation of gas bubbles would deform the microwave field and would, thereby, result in local overheating in the vicinity of the gas bubbles.[5] However, even if any specific microwave effect can be ruled out, no alternative explanation has been offered to explain the widely observed rate enhancement under microwave heating.[13,18]

The aim of this Chapter is to examine the rate enhancement of the dehydration of xylose into furfural under microwave heating, considering the presence of local overheating. To do so, this reaction was performed under traditional and microwave heating, in a temperature range from 140 °C to 200 °C. Rates and selectivities for both heating methods were monitored and compared. Based on the acquired information a kinetic model was developed that incorporates local overheating.

4.2 Results and Discussion

For this study an aqueous solution of xylose and NH_4Cl (350 mM and 500 mM, respectively) was heated between 140 and 200 °C either in a Wood's metal batch (traditional heating) or using a CEM Discover SP reactor (microwave heating). To ensure maximum comparability, the same amount of solution (5 mL) and identical stirring conditions (approx. 1000 rpm) have been used in both heating methods. Halide salts have been reported to have a positive effect on the selectivity of the xylose dehydration reaction catalyzed by mineral acids.[16,17] Therefore, NH_4Cl was chosen due to its Brönsted acid characteristics and used without any initial pH adjustment.[16,17]

Accurate temperature monitoring under microwave conditions is of crucial importance.[6,7] Fiber optic sensors have been used, coupled with IR temperature sensing, for internal temperature measurements at microwave conditions.[8] However, such sensors showed surprisingly large temperature gradients when homogeneity through effective mixing cannot be ensured.[8] In the present case such a sensor was not used due to the necessity to seal the vials on account of the development of high pressure. Hence the temperature was monitored with an IR temperature control system that was accurate to +0.35 ^{o}C (±1°C), as determined with an independent thermocouple prior to use. Under microwave heating, however, the comparison of operating pressure to equivalent saturated steam pressure indicated a temperature deviation between +4 (±1) °C at 140 °C to +10 (±4) °C at 200 °C (Figure 4.1). These calibration data and their significance for the results will be discussed in more details below. Due to the impossibility to take aliquots during the experiments, all the reactions were stopped and cooled at the desired time and analyzed with ^{1}H-NMR spectroscopy. The concentrations of furfural and unreacted xylose in the crude reaction mixture were calculated in order to determine the rate and the selectivity of the xylose dehydration into furfural.

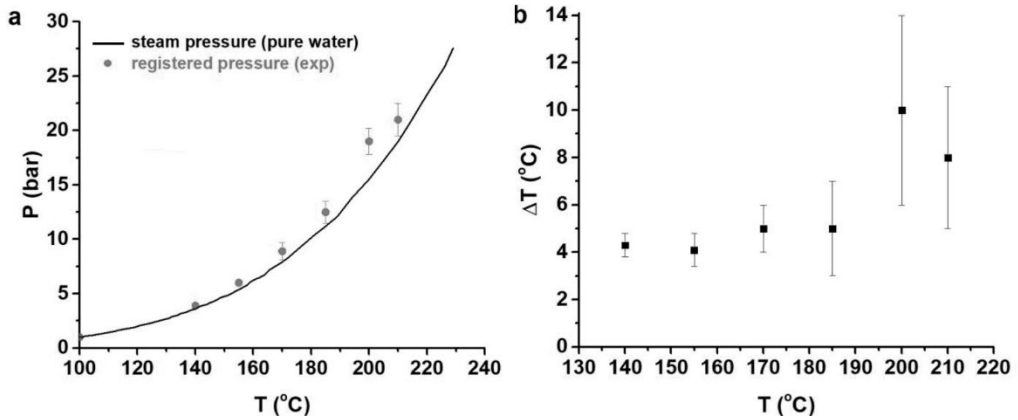

Figure 4.1 (a) Temperature versus pressure (independently monitored) profile for the reaction under microwave irradiation (points) and the theoretical values predicted by the Antoine equation for pure water (line). (b) Δ*T* versus *T* plot for the temperature uncertainty evaluated from analysis of the pressure fluctuations. Δ*T* is always > 0 and consistently raising with *T* (°C) from +4 (±1) °C at 140 °C to +10 (±4) °C at 200 °C. The average Δ*T* is 7 °C, with a standard deviation of 3 °C.

4.2.1 Conventional and Microwave Heating

The traditional heating at 140 °C gave rise to the formation of furfural with 35 mol% yield after 70 h (Figure 4.2a). However, the reaction was slow, and the conversion of xylose was still incomplete after 70 h. Performing the reaction at 200 °C resulted in a final yield of 45 mol% of furfural after 3 h and a conversion of 98 mol% (Figure 4.2a). The yield of furfural was strongly dependent on the concentration of NH_4Cl. However, the maximum yield typically did not exceed 45-48 mol% at a conversion > 90 mol% due to the occurrence of side reactions. The main side-reactions are xylose-furfural and furfural-furfural condensations, which lead to the formation of solid by-products. Over-oxidation and fragmentation of xylose and/or furfural into small molecules are also possible.[19,20] Changing the temperature from 140 °C to 200 °C resulted in a shift in selectivity path for the reaction (Figure 4.2b). At 140 °C, the reaction starts by converting xylose to an unidentified by-product and produces furfural only after 35 mol% conversion (Figure 4.2b). In contrast, at 200 °C, the yield of furfural increased from the onset of conversion. In both cases the maximum furfural selectivity was approx. 50 mol%. The formation of an intermediate, usually xylulose, has been postulated by several groups.[19,20,23]

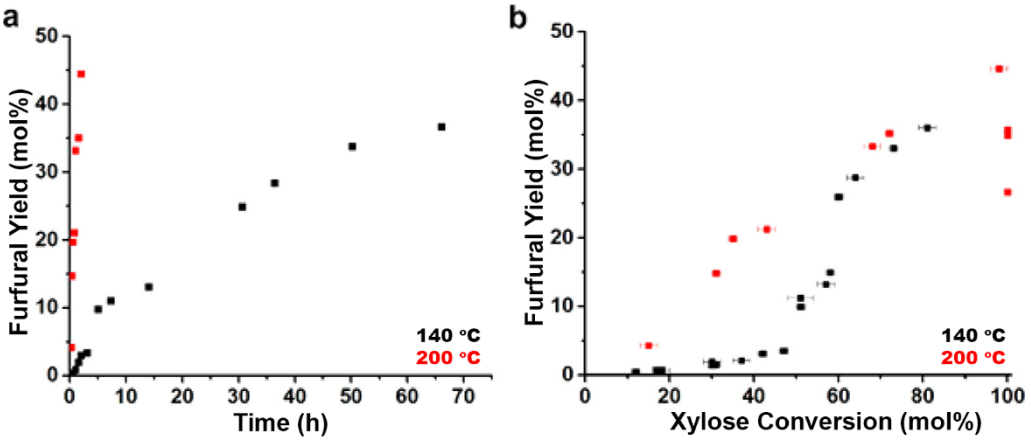

Figure 4.2 Yield of furfural (a) as a function of time and (b) as a function of conversion, for the dehydration reaction of xylose at 140 °C and 200 °C under traditional heating (350 mM xylose and 500 mM NH_4Cl).

Control experiments did not reveal traces of xylulose in our case. In contrast, MS and HPLC analysis of the crude reaction mixture showed the presence of high molecular weight species, compatible with sugar-like material after 2 h at 140 °C. The analysis of crude reaction mixtures at higher xylose conversion did not show the presence of these species; products at much higher molecular weight (compatible with highly condensed humic by-products) were detected instead. Intriguingly, the pH appeared to drop from 5 to 3 during the reaction both at 140 °C and 200 °C. The pH change was monitored by ^{1}H-NMR spectroscopy (Figure 4.3a) following the signal of the ammonium cation (NH_4^+).[24] The pH change is faster at higher temperature and can be rationalized by the formation of acidic species, such as formic acid, acetic acid, levulinic acid and furanoic acid, upon the decomposition of xylose, as were detected, in low concentrations, in the crude reaction mixture. The same pH change was obtained in control experiments adding comparable concentrations of acetic acid, propionic acid and formic acid to a 500 mM aqueous solution of NH_4Cl and it was not obtained upon heating the same solution (with no added acids) at 200 °C for 24 hours. This pH drop is connected to the shift in selectivity (*i.e.*, yield-conversion profile at low conversions) of the system, while at 200 °C the pH immediately drops to 3, resulting in a linear selectivity path. In the reaction performed at 140 °C there is a clear correspondence in the change of selectivity and the pH drop (Figure 4.3b). This relation is compatible with the formation of oligosaccharides at mild pH conditions, with the process reversing at pH = 3 because of the low stability of sugar oligomers at pH < 3.5.[25]

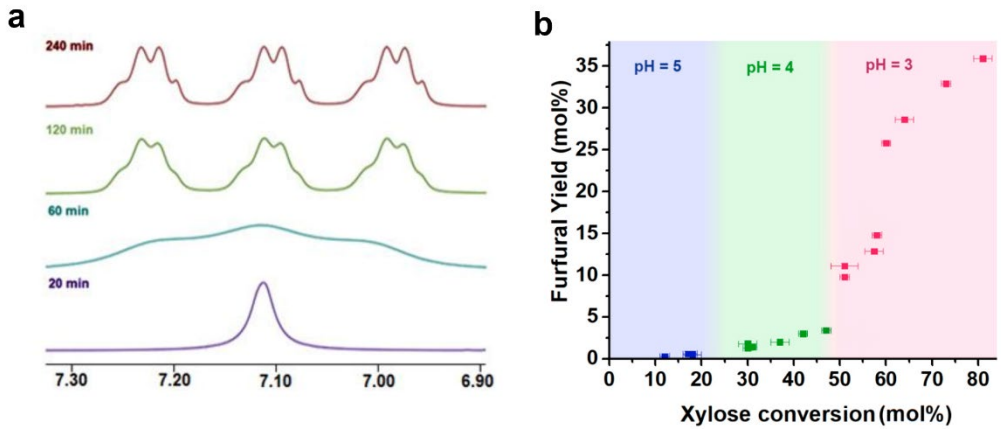

Figure 4.3 (a) Development of the multiplet of the NH_4^+ cation in the ^{1}H-NMR spectrum of the crude reaction mixture from the xylose dehydration (140 °C, traditional heating) (b) Yield of furfural as a function of conversion, for the dehydration reaction of xylose at 140 °C under traditional heating (350 mM xylose and 500 mM NH_4Cl) in relation with the pH drop, evaluated with pH paper.

4.2.2 Kinetic Analysis and Rate Enhancement

Moving from traditional to microwave heating enhanced the rate of the formation of furfural (Figure 4.4a), both at 140 °C and 200 °C. However, a much smaller difference in initial selectivity to furfural was observed between the runs at 140 and 200 °C (Figure 4.4b).

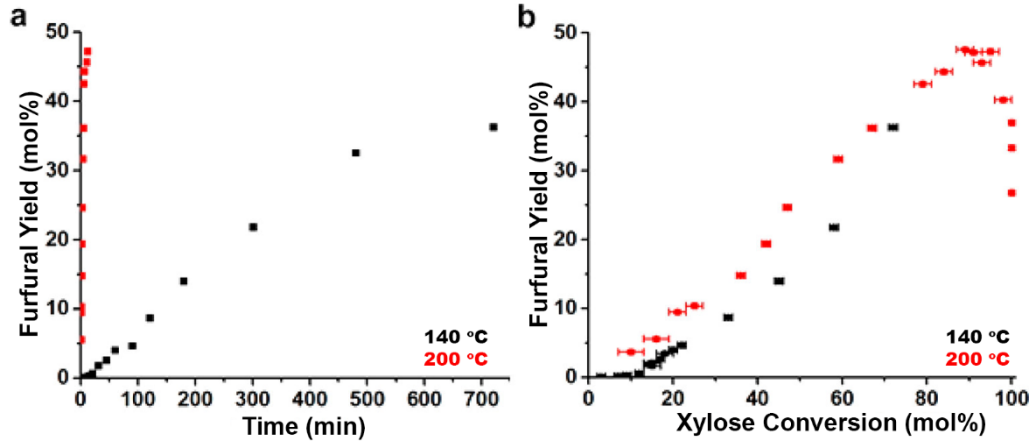

Figure 4.4 Yield of furfural (a) as a function of time and (b) as a function of conversion, for the dehydration reaction of xylose at 140 °C and 200 °C under traditional heating (350 mM xylose and 500 mM NH_4Cl).

The xylose dehydration reaction at 140 °C under microwave conditions showed a higher rate and a different conversion behavior compared with the same reaction performed at traditional heating (Figure 4.5a). Traditional heating led to a plateau between approx. 700-1600 min of reaction, which is not visible under microwave conditions. The pH drop from 5 to 3 already observed in traditional heating was again observed under microwave heating, however it occurred within the first 30 min of reaction at 140 °C, instead over 2 h. This difference may be rationalized by the rate enhancement generally observed under microwave heating. In general, the initial furfural selectivity is substantially influenced by the reaction temperature under traditional heating but not under microwave heating. At 200 °C, a clear rate enhancement was observed for the microwave heating, as expected (Figure 4.5b). Assuming first-order kinetics for the xylose conversion at 200 °C, the initial rate constant k was calculated from the initial slope of the early $\ln(X_0/X_t)$, where X_0 and X_t are the concentration of the xylose at time 0 and time t, respectively. The $k_{(200\ °C)}$ value amounts to 13.9 ± 0.4 min^{-1} for traditional heating and 197 ± 1 min^{-1} for microwave heating.

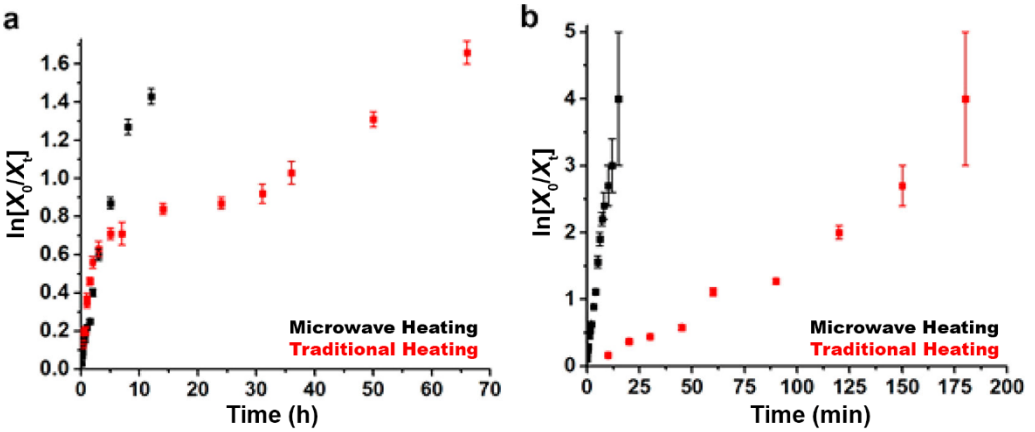

Figure 4.5 Comparison of the rates of the xylose dehydration reaction under traditional and microwave heating at (a) 140 °C and (b) 200 °C (350 mM xylose and 500 mM NH_4Cl).

4.2.3 Factors Affecting the Rate Enhancement

A number of elements were considered to explain the rate enhancement by microwave heating. Eventual temperature misreading, difference in heating profile, microwave irradiation power, and extent of liquid mixing were investigated. This rate enhancement cannot be attributed to different heating profiles, as control experiments still showed the formation of some furfural when the microwave irradiation was tuned to follow the heating profile of an experiment with conventional heating that did not produce any furfural (Figure 4.6). Any radiative, non-thermal effect has already been ruled out by Xiouras *et al*.[21] Therefore, the formation of local overheated regions within

the reaction vessel, where most of the reaction takes place, is assumed. Local overheating was also discussed by De Bruyn *et al.* and successfully modeled with COMSOL to be an effect of field inhomogeneity, confirming the consistently observed non-uniformity of the microwave field.[5,8,26] This was explored further through two sets of additional experiments.

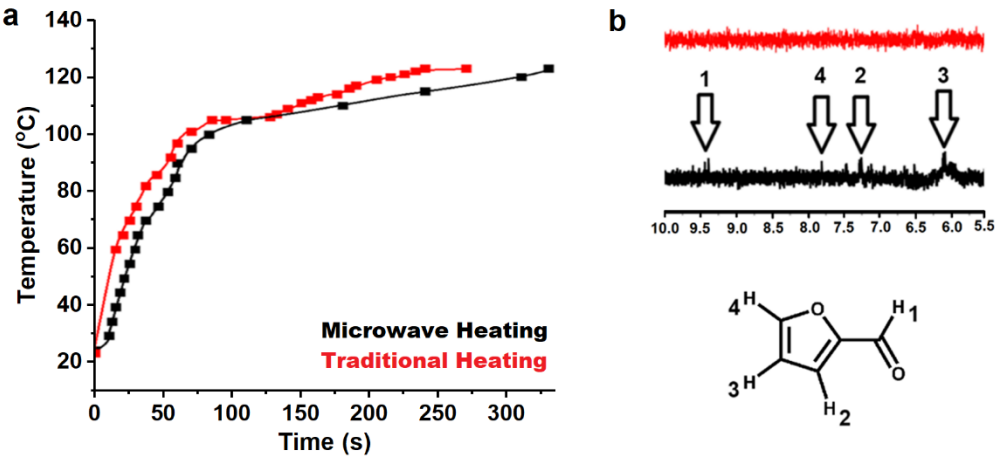

Figure 4.6 (a) Heating profiles for the reaction of xylose dehydration at traditional heating conditions (red line) and microwave heating conditions (black line), followed with a thermocouple sensor. (b) Qualitatively different behavior observed in the xylose dehydration reaction via ^{1}H-NMR spectroscopy (5 min) with comparable heating profiles between the two heating methods (same color coding). Peaks that can be assigned to furfural are visible in the crude reaction mixture at microwave heating conditions and not in the one at traditional heating conditions.

The effectiveness of microwave heating appears to require a minimum output power, as expected for the generation of local overheating. The reaction has been analyzed at different irradiation powers in an interval between 10 and 200 W. However, with everything else being constant (irradiation for 20 min at 180 °C under vigorous stirring of ca. 1000 rpm, optionally with active air cooling to keep the vessel temperature under control only at power output > 100 W), the microwave unit needs to be allowed to deliver an irradiation power above ca. 30 W to result in a high furfural yield of about 40 mol%, compared to the 5 mol% observed at low power or under traditional heating (Figure 4.7).

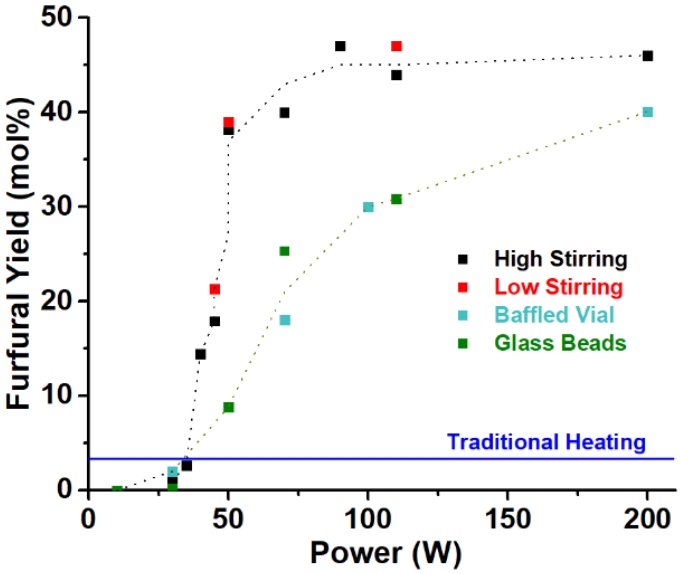

Figure 4.7 Effect of maximum irradiation power setting and of mixing conditions on the dehydration of xylose under microwave heating (20 min, 180 °C, 350 mM xylose and 500 mM NH_4Cl).

The effectiveness of microwave heating appears also to be attenuated by thorough mixing of the reaction medium, as expected if it would come from local overheating. Lowering the stirring rate from 1000 rpm to 400 rpm showed no change in the furfural yield profile. The small magnetic stirrer of the microwave unit is not very effective here as it pulls a sizable vortex in the liquid, resulting in a behavior not dependent on the stirring rate. Adding microwave-silent glass mixing beads in the vial, following a simple procedure described by Kappe *et al.* to prevent local overheating, keeping all the other parameters constant, lowered the furfural yield from 40 to 25 mol% at 70 W (Figure 4.7).[6] The mixing can also be improved by inserting baffles in the vessel.[27] The addition of three glass baffles appeared to shift the power threshold for high furfural yield to higher power level (from 30 to 70 W) and to reduce the maximum furfural yield from 40 to 18 mol% that is achievable at high maximum power (Figure 4.7). These effects are compatible with the hypothesis of local overheating and with previous results in literature, since it should indeed be partly annihilated upon improved mixing.[7,8] Such effect, which has a thermal origin, should not be observed if the effectiveness of microwaves would have been due to hypothetical non-thermal photonic excitation of the sugar or dipolar stabilization of the solvation sphere around the sugar, which is again proven to be inconsistent.[28]

Since microwave heating is inhomogeneous, the definition of the uncertainty on the temperature sensing (ΔT_{err}) is crucial.[6,7] Internal measurements with fiber optic sensors upon microwave heating showed large fluctuations,[8] so ΔT_{err} was first evaluated upon cooling (no microwave heating, with a thermocouple sensor) and then upon microwave heating using the autogenous pressure of water vapor as a cross reference. Upon cooling, so without any overheating expected, ΔT_{err} amounted to +0.35 (±1) °C. Upon microwave heating, ΔT_{err} showed a higher average of + 7 °C, but appeared to increase with target temperature from + 4 (± 1) at 140 °C to + 10 (± 4) °C at 200 °C, in this case ΔT_{err} is always >0 (Figure 4.1). Finally, the rate enhancement cannot be assigned simply to a higher bulk temperature of the liquid under microwave heating, for it would correspond to an effective bulk temperature that is 30 to 50 °C higher than measured. These values exceed both the standard deviations evaluated upon cooling (± 1 °C) and upon heating (± 7 °C). It would, furthermore, have resulted in an excessive vapor pressure and, eventually, a trip of the unit once it reaches the safety limit of 22.5 bar, corresponding to a steam pressure of 220 °C. These phenomena were not observed.

All these observations are consistent with the hypothesis of local overheating. Specifically, the thorough temperature calibration convincingly showed that the average liquid temperature derived from the vial pressure is slightly higher than the average temperature measured by the IR detector. Regrettably, the equipment used here did not allow us to measure temperature profiles throughout the vials. However, there is evidence in literature that has been provided through more sophisticated equipment. Thermographic analyses have suggested the formation of a hot core in the vessel, where the radiation is the most concentrated, under microwave heating.[29] This is compatible with the temperature gradients observed using multiple fiber optic sensors upon heating.[8] The existence of a gas-liquid interphase and the formation of dispersed hot spots near gas bubbles has also been explored as a possible explanation for the rising of inhomogeneity in the microwave field distribution.[5] Further analysis and experimental work could be performed to shed light on the origin of the local overheating at microwave conditions.

4.2.4 Kinetic Model with Local Overheating

To analyze the reaction kinetics, additional runs were carried out at intermediate temperatures (155, 170, and 185 °C) using the initial setup used for the two different heating methods (see above). The rate constants were determined as described above, in conditions of maximum furfural selectivity (approx. 50 mol%), and compared using an Arrhenius plot (Figure 4.8). Accordingly, the microwave heating resulted in a first-order rate constant that is 7-13 times higher than with traditional heating and an apparent activation energy that is about twice as high (Figure 4.8, Table 4.1). The complex behavior observed under traditional heating at 140 °C (Figure 4.5a), not

compatible with first-order kinetics, led us to exclude this specific point from the analysis.

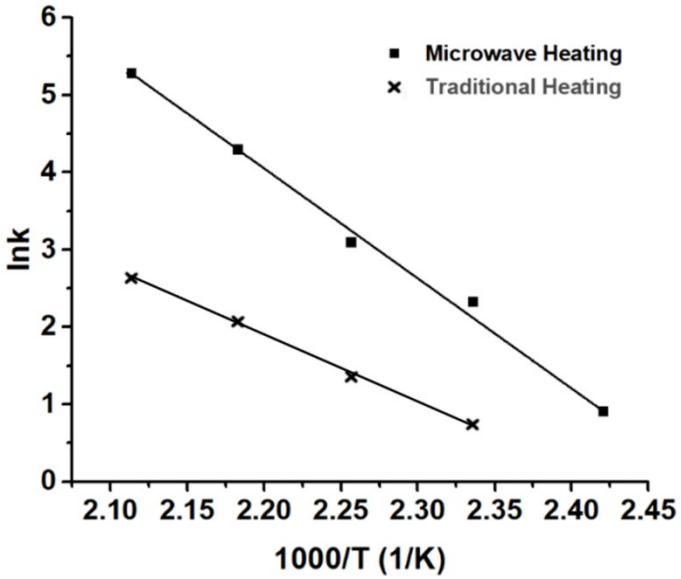

Figure 4.8 Arrhenius plot of the dehydration of xylose into furfural under traditional and microwave heating.

Table 4.1 Arrhenius fit parameters of the dehydration reaction of xylose into furfural under traditional and microwave heating as derived from the Arrhenius plots (Figure 4.8).

	$\ln k_0$	E_a (kJ/mol)	R^2
Microwave heating	35.3 ± 0.2	118.3 ± 0.4	0.998
Traditional heating	20.8 ± 0.5	71.4 ± 0.2	0.999

Related papers have concluded on the presence of a specific "microwave effect" from differences in rate and activation energy (Table 4.1).[1,2] One of them implied a different frequency of collisions under microwave irradiation, after assuming an identical pre-exponential factor for conventional and microwave heating.[2] If such an adjustment could be sensible in the presence of ferromagnetic materials, it should not apply here.[30] These kinetic data are also easily explained by local overheating. A kinetic model was developed that considers the reaction volume to be divided between a (large) fraction at the measured temperature and a (small) fraction at much higher temperature – the overheated fraction. This model leads to an apparent rate constant under microwave heating, k_{MW}, that is the volume-weighted average of the rate constants at the respective temperatures (Equation 4.1).

$$k_{MW} = k_0((1 - \alpha)e^{-\frac{E_a}{k_B T_1}} + \alpha e^{-\frac{E_a}{k_B T_2}}) \qquad \textbf{Equation 4.1}$$

In Equation 4.1 k_0 is the pre-exponential factor, k_B is the Boltzmann constant, E_a is the activation energy, α is the overheated volume fraction (defined between 0 and 1), T_1 is the bulk temperature and $T_2 > T_1$ is the temperature of the overheated fraction. Without any specific characterization available for the local overheating, the model assumes an average temperature difference ΔT between the bulk and the overheated region, so T_2 can be written as $T_2 = T_1 + \Delta T$. This approximation leads to the definition of a new equation (Equation 4.2), in which the rate enhancement obtained under microwave heating (k_{MW}/k_1) is expressed as a function of k_1.

$$\frac{k_{MW}}{k_1} = (1 - \alpha) + \alpha \left(\frac{k_1}{k_0}\right)^{-\frac{\Delta T}{T_1 + \Delta T}} \qquad \textbf{Equation 4.2}$$

The value of k_0 is extrapolated from the Arrhenius plot of the system under traditional heating as $\ln k_0$. To avoid excessive manipulation of the data, Equation 4.2 can be 'linearized' (Equation 4.3).

$$\ln k_{MW} - \ln k_1 = \ln((1 - \alpha) + \alpha\left(e^{\ln k_1 - \ln k_0}\right)^{-\frac{\Delta T}{T_1 + \Delta T}}) \qquad \textbf{Equation 4.3}$$

Initial fittings of the kinetic data using a α and ΔT as fitting parameters were not satisfactory and required ΔT to increase with increasing target temperature. A better fit was achieved by defining an "overheating factor" f as fitting parameter to define ΔT as $\Delta T = f(T_1 - 373.15\ K)$. The reference temperature was here chosen as 100 °C, because local overheating only develops beyond a minimum power output and there is no recorded effect of rate enhancement up to and including 100 °C where the average power output never exceeded 20 W. Obviously, the definition of two volume fractions with each their own temperature is an oversimplification, for local temperature gradients in the liquid are expected. The temperature distribution that has been visualized as hot core is here modeled as a single fraction of volume α with a single temperature T_2.[29] The choice of α and f was not completely arbitrary, and it was based on the existing literature on local overheating.[1,2,10-12] With a maximum 30% of overheated volume at maximum ΔT of 200 °C, α is defined between 0 and 0.3 and f is defined between 0 and 2. The rate enhancement $\ln k_{MW} - \ln k_1$ can then be fitted by setting α at an arbitrary value between 0.05 and 0.3 and optimizing f to fit the data. Good fits can be obtained for a variety of α and f combinations as illustrated in Figure 4.9.

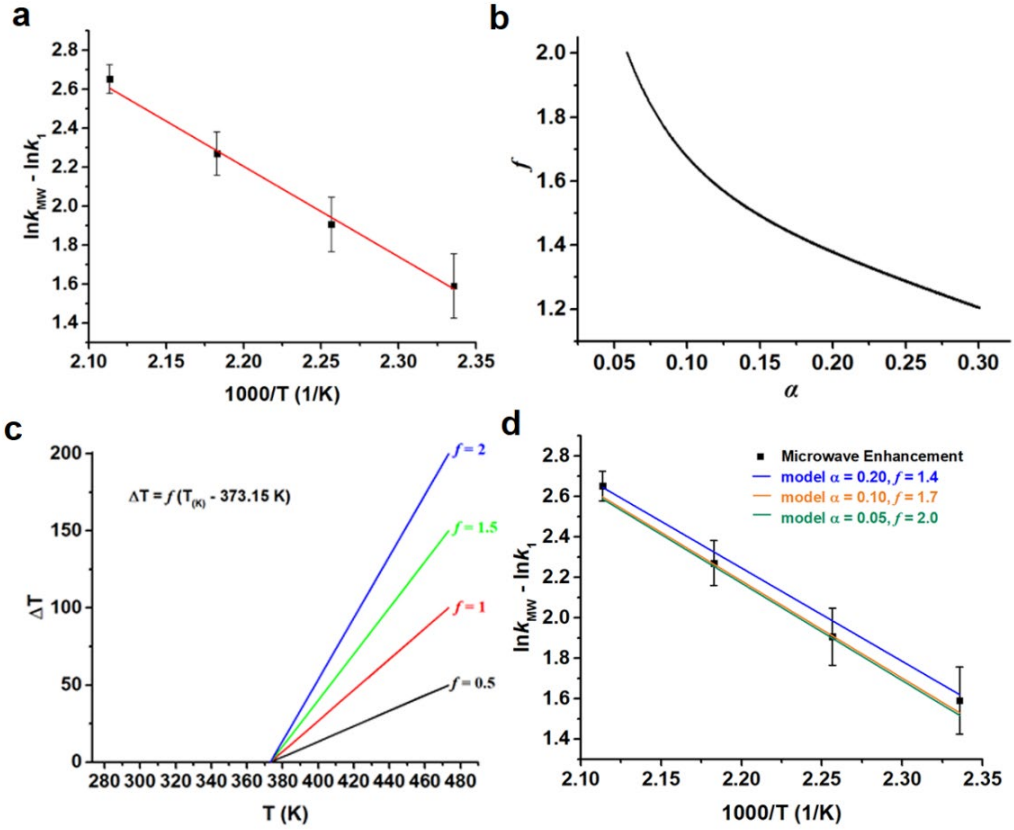

Figure 4.9 (a) Example of the fitting (solid line) of the experimental data (markers), with α arbitrarily set at 0.15 and f being fitted to 1.5. (b) Visualization of fitting pairs of the two parameters α and f, pictured within the boundaries defined in the text. (c) Relation between bulk temperature and ΔT, insurgence of local overheating over 100 °C (373.15 K) with different overheating factors. (d) Fitting the experimental data with different α and f pairs, chosen within the interval described in the text.

Obviously, more detailed thermographic studies similar to those reported by Scanche[29] should be performed to check the validity of the α and f values proposed here. Beyond kinetics and rate enhancement, local overheating can also explain the difference in the furfural selectivity profiles between traditional and microwave conditions observed in our system (see Figures 4.2b and 4.5b). Under microwave heating, the reaction does not truly take place at 140 °C but effectively proceeds at much higher temperature in the overheated areas (namely, 200 °C, based on the model if f = 1.5). Its selectivity

profile should therefore be compared with that of traditional heating at high temperature and, indeed, corresponds well with such profiles.

4.3 Conclusions

The present study confirms a significant rate enhancement in xylose dehydration to furfural under microwave heating. Several observations suggest that the rate enhancement is due to local overheating (possibly as a hot core) under microwave irradiation as the rate enhancement has only been observed beyond a threshold irradiation power. This power threshold was pushed to higher values ensuring a thorough mixing of the liquid phase, which was also achieved by addition of microwave-silent glass beads. The initial formation of sugar oligomers and the delay in pH drop, that is observed under traditional heating at low temperature, is insignificant at high temperature as well as at microwave-heated conditions at low and high temperatures. The hypothesis of local overheating is further supported by fitting the rate enhancement using a simple kinetic model that assumes two reactions zones, *i.e.*, a minor overheated zone amid a bulk liquid at target temperature, and two interlinked parameters, *i.e.*, a volume fraction α and a temperature overshoot factor f of overheating. Good fits were achieved with various combinations of α and f, between 0.05-0.30 and 1.2-2.0, respectively. In general, this study provides new insights to more clearly relate the often-observed rate enhancement of microwave heating to a thermal effect, *i.e.*, local overheating, without the need for a presumed and unspecified "microwave effect".

4.4 Experimental Section

4.4.1 Chemicals

D-(+)-Xylose (>99%), D_2O (99.9% atom D) and 3-(trimethylsilyl)propionic-2,2,3,3-d_4 acid sodium salt (TMSP, 98% atom D) were purchased from Sigma-Aldrich, ammonium chloride (NH_4Cl, 99%) was obtained from Normapur.

4.4.2 Methods and Equipment

All chemicals are commercially available and used without further purification. The reaction at microwave conditions and the ^{1}H-NMR spectra were performed using the equipment described in Chapter 3. HPLC chromatography (Agilent 1200) was performed with a Hiplex-Pb column operated at 70 °C with a Milli-Q water mobile phase at a flow rate of 0.6 mL/min and a refractive index detector (at 55 °C). IR spectroscopy was performed with a FT-IR spectrometer (Thermo Scientific Nicolet 6700) with a diamond ATR accessory (Thermo Optec Smart Orbit™). The temperature sensor of the

microwave reactor was calibrated following the same procedure described in Chapter 3. All of the data analysis and the fitting were performed using Origin 2016 (64 bit).

4.4.3 Xylose Dehydration under Traditional Heating

A solution (5 mL) of D-xylose (350 mM) and NH_4Cl (500 mM) was heated at various temperatures between 140 and 200 °C with the same equipment described in Chapter 3. The reaction mixing was performed with a magnetic stirrer (approx. 1000 rpm). The analysis of the samples was performed with the same procedure described in Chapter 3. The quantification performed with ^{1}H-NMR was occasionally verified with HPLC.

4.4.4 Xylose Dehydration under Microwave Heating

A solution (5 mL) of D-xylose (350 mM) and NH_4Cl (500 mM) was heated at various temperatures between 140 and 200 °C in the microwave reactor. The reaction mixing was performed with a magnetic stirrer (approx. 1000 rpm). The analysis of the samples was performed with the same procedure described in Chapter 3. The quantification performed with ^{1}H-NMR was occasionally verified with HPLC.

4.5 References

1. A. De la Hoz, Á. Díaz-Ortiz, A. Moreno, *Chem. Soc. Rev.* **2005**, *34*, 164-178.
2. Á. Díaz-Ortiz, P. Prieto, A. de la Hoz, *Chem. Rec.* **2019**, *19*, 85-97.
3. S. Horikoshi, T. Watanabe, A. Narita, Y. Suzuki, N. Serpone, *Sci. Rep.* **2018**, *8*, 1-10.
4. P. Bana, I. Greiner, *Aust. J. Chem.* **2017**, *70*, 776-785.
5. M. De Bruyn, V. L. Budarin, G. S. J. Sturm, G. D. Stefanidis, M. Radoiu, A. Stankiewicz, D. J. Macquarrie, *J. Am. Chem. Soc.* **2017**, *139*, 5431-5436.
6. C. O. Kappe, B. Pieber, D. Dallinger, *Angew. Chem., Int. Ed.* **2013**, *52*, 1088-1094.
7. C. O. Kappe, *Acc. Chem. Res.* **2013**, *46*, 1579-1587.
8. M. A. Herrero, J. M. Kremsner, C. O. Kappe, *J. Org. Chem.* **2008**, *73*, 36-47.
9. P. Bana, I. Greiner, *Aust. J. Chem.* **2016**, *69*, 865-871.
10. S. Curet, O. Rouaud, L. Boillereaux, *Chem. Eng. Process.* **2008**, *47*, 1656-1665.
11. X. Zhang, D. O. Hayward, D. M. P. Mingos, *Chem. Commun.* **1999**, 975–976.
12. P. Klán, J. Literák, S. Relich, *J. Photochem. Photobiol. A* **2001**, *143*, 49-57.
13. J. Asomaning, S. Haupt, M. Chae, D. C. Bressler, *Renew. Sustain. Energy Rev.* **2018**, *92*, 642-657.
14. P. Priecel, J. E. Perez Mejia, P. D. Carà, J. A. Lopez-Sanchez, *Green Chem.* **2018**, *56*, 243-299.
15. O. Ershova, K. Nieminen, H. Sixta, *ChemCatChem* **2017**, *9*, 3031-3040.
16. K. R. Enslow, A. T. Bell, *ChemCatChem* **2015**, *7*, 479-489.
17. O. Yemiş, G. Mazza, *Waste Biomass Valor.* **2019**, *10*, 1343-1353

18. I. K. M. Yu, D. C. W. Tsang, *Bioresour. Technol.* **2017**, *238*, 716-773.
19. J.-P. Lange, E. van der Heide, J. van Buijtenen, R. Price, *ChemSusChem* **2012**, *5*, 150-166.
20. R. Mariscal, P. Maireles-Torres, M. Ojeda, I. Sádaba, M. López Granados, *Energy Environ. Sci.* **2016**, *9*, 1144-1189.
21. C. Xiouras, N. Radacsi, G. Sturm, G. D. Stefanidis, *ChemSusChem* **2016**, *9*, 2159-2166.
22. B. Ashley, D. D. Lovingood, Y.-C. Chiu, H. Gao, J. Owens, G. F. Strouse, *Phys. Chem. Chem. Phys.* **2015**, *17*, 27317−27327.
23. O. Ershova, J. Kanervo, S. Hellstena, H. Sixta, *RSC Adv.* **2015**, *5*, 66727-66737.
24. M. Witanowski, *Pure Appl. Chem.* **1974**, *37*, 225-233.
25. H. Yuan, X. Yang, P. Chen, Y. Liu, G. Tang, Y. Zhao, *Sci. China Chem.* **2018**, *61*, 243-250.
26. G. S. J. Sturm, M. D. Verweij, T. van Gerven, A. I. Stankiewicz, G. D. Stefanidis, *Int. J. Heat Mass Transf.* **2012**, *55*, 3800−3811.
27. M. Chahartaghi, P. Eslami, A. Naminezhad, *Heat Mass Transfer* **2018**, *54*, 3771-3784.
28. M. Zhou, K. Cheng, H. Sun, G. Jia, *Sci. Rep.* **2018**, *8*, 1-10.
29. J.-S. Scanche, *Mol. Divers.* **2003**, *7*, 293-300.
30. E. Haque, N. A. Khan, J. H. Park, S. H. Jhung, *Chem. Eur. J.* **2010**, *16*, 1046-1052.

Chapter 5

Selective Extraction of Xylose from Acidic Hydrolysate–from Fundamentals to Process

Xylose is a promising feedstock for the fuel and chemical industry. This chapter proposes an integrated process to recover and purify xylose from an acidic hydrolysate stream, e.g., coming from pretreated lignocellulose. This process consists of selectively extracting the xylose as the diboronate ester and back-extracting it into a clean aqueous solution. 85% xylose extraction efficiency using toluene/phenyl boronic acid in a single stage is reported. Furthermore, the extraction procedure is compatible with acidic and basic xylose feed (from pH 1 to 12), does not need a phase transfer agent (such as Aliquat), is strongly selective for xylose, and proceeds best with aromatic solvents. The structure of the diboronate ester is demonstrated by means of NMR spectroscopy and evidence for the intermediate formation of a monoboronate ester are shown. The release of xylose from the diboronate ester is explored, and an integrated process for xylose purification is proposed and its boundaries are discussed.

Part of this chapter has been published in: L. Ricciardi, W. Verboom, J.-P. Lange, J. Huskens, *ACS Sus. Chem. Eng.* **2021**, *9*, 6632-6638.

5.1 Introduction

Xylose is the second most abundant sugar in nature, after glucose. Xylose is a valuable raw material in the sweetener, aroma, and flavoring industries, and it is a promising starting material for the production of chemicals and fuels, for example, by its conversion to furfural.[1–4] Xylose is present in lignocellulosic biomass mainly as glucuronoxylan in hardwoods and as glucoronoarabinoxylan in grasses and softwood.[4,5] Xylose syrup can be extracted from lignocellulosic biomass by means of various pretreatment or fractionation processes.[4,5] Recovering xylose from its complex syrup typically employs time and/or energy-demanding techniques, such as water evaporation and crystallization, or requires costly and complex setups like chromatographic separation.[6] Other approaches, such as liquid−liquid extraction, have been reported but remain challenging because of the high solubility of sugars in aqueous medium.[3,7–9] One of the most common approaches for the liquid−liquid extraction of sugars from an aqueous medium proceeds by the formation of hydrophobic boronate esters of the saccharides.[3,9–15] In principle, this can provide a concentrated sugar solution in organic solvent, which can be directly processed without any post-treatment.[12]

Xylose liquid−liquid extraction and sugar liquid−liquid extraction, in general, are commonly performed at basic pH with an equimolar concentration of a hydrophobic boronic acid (BA), for example, phenylboronic acid (PBA), and a phase transfer agent (*e.g.*, the lipophilic quaternary ammonium salt Aliquat 336, *aka* Aliquat) to form a hydrophobic ion-pair complex.[3,10–12,15–17] The need for a basic pH (pH > 9) has been rationalized by considering the optimal conditions for the formation of the tetrahedral, negatively charged form of the BA, which forms stable boronate ester bonds with sugars in water.[3,9–13] This negatively charged ester can be then extracted into the organic phase through the interaction with the positively charged Aliquat.[11,14] Because of the pH limitation, this process cannot be readily applied to acidic hydrolysates that are commonly obtained from biomass pretreatment.[4] The aim of this work is to extract xylose from an acidic hydrolysate as a neutral boronate ester, which obviates the use of a phase transfer agent. Earlier studies have reported the neutral diester of PBA and xylose.[9]

The compatibility of this ester with the acidic xylose feed that is delivered by numerous pretreatment processes is shown and the observed pH independence of the extraction in the absence of Aliquat is rationalized by discussing the coupled equilibria involved in this system. The high extraction selectivity for xylose over other sugars present in the xylose feed is demonstrated and the recovery of xylose from the boronate ester by

back-extraction, to propose a conceptual process design for the purification of xylose, is investigated.

5.2 Results and Discussion

In order to develop an extraction process to isolate xylose from an acidic hydrolysate, several elements need to be taken into account. Xylose needs to be extracted selectively from a mixture that contains multiple sugars, and the extraction should be achievable at acidic pH to avoid costly pH changes. The organic solvent used to extract the xylose into the organic phase should favor extraction but also allow back-extraction into water. Such a process can be designed around a hydrophobic and charge-neutral boronate diester of xylose (Figure 5.1). The efficiency and selectivity of the extraction will be discussed, as well as the solvent dependence and sugar selectivity. The limitations of the method to achieve a full process are explored as well.

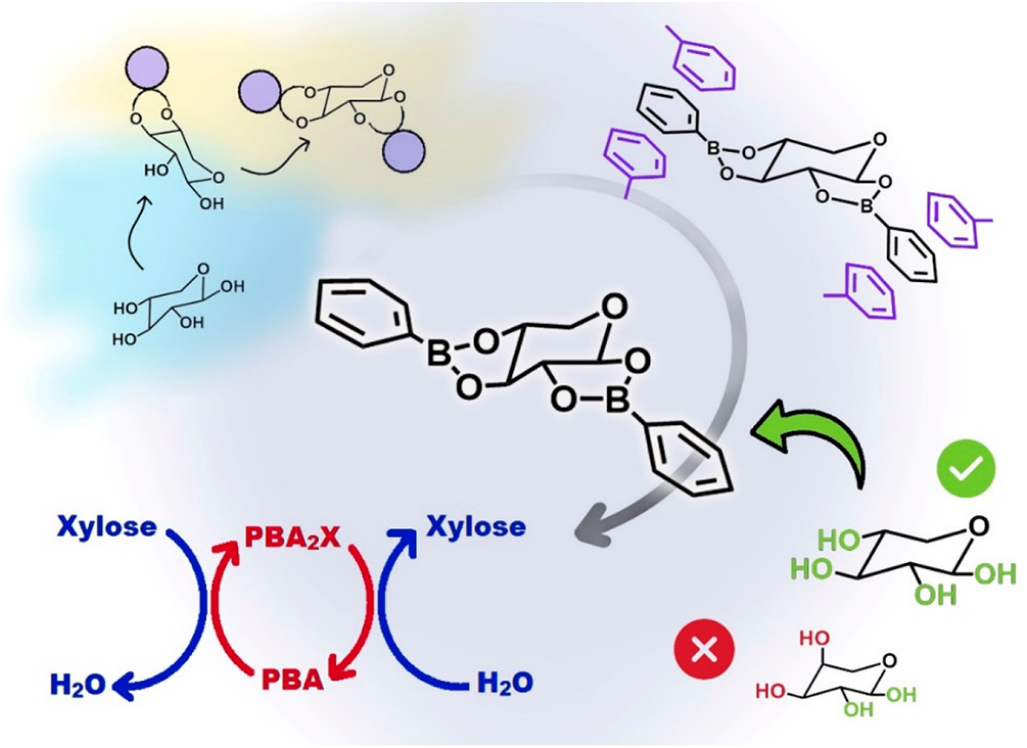

Figure 5.1 Conceptualization of the xylose extraction process, toward industrial application. Following the central black arrow, from the top left to the bottom left: the two-step mechanism of extraction of xylose into the organic phase as a boronate diester; the visualization of the π–π interaction of the diester in an aromatic solvent, showing the stabilization of the diester in the organic phase; the configuration-based

sugar selectivity of the extraction, rooted in the necessity of having pairs of OH groups in *cis* configuration for the formation of a boronate diester; the combination of all these elements into a process of selective xylose extraction from the acidic feed (left) leading to purified xylose (right).

5.2.1 Xylose Extraction without Phase Transfer Agent

Earlier studies have reported the possibility to extract xylose into toluene at neutral pH by the formation of a hydrophobic, charge-neutral sugar-boronate diester.[9] This procedure did not require the assistance of Aliquat as a phase transfer agent. Stretching these conditions to the typical acidic pH encountered in hydrolysates is possible, by using an acidic (pH = 1) aqueous xylose solution (350 mM, 5.2 w%) and an equivalent volume of toluene/PBA solution with various PBA concentrations, in the absence of Aliquat (Figure 5.2).

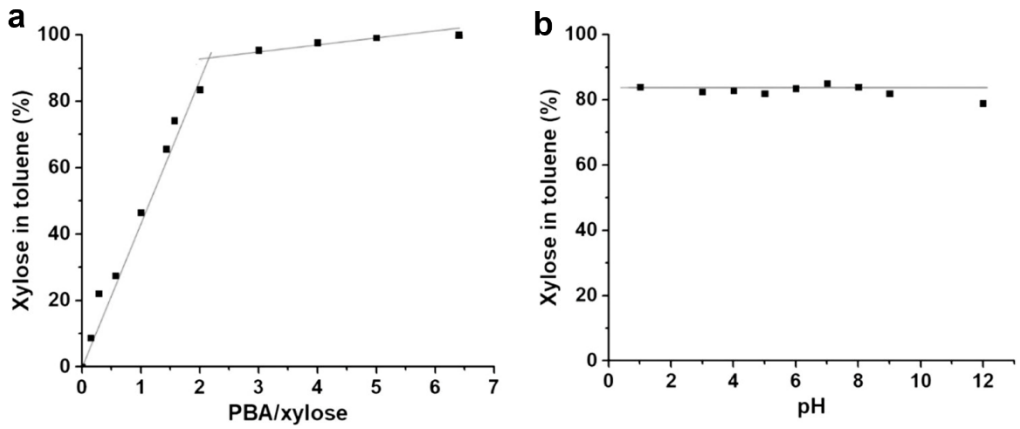

Figure 5.2 Fraction of xylose extracted into toluene (conditions: 1:1 water–toluene, xylose 350 mM, room temperature), at various PBA/xylose ratios at pH = 1 (a) and at various pH's at PBA/xylose = 2 (b).

After reaching equilibrium, the two phases were analyzed by ^{1}H-NMR spectroscopy to determine the concentration of xylose in the aqueous phase and of the boronate ester in the organic phase. When working at a PBA−xylose ratio of 2:1, approximately 85% of the xylose is extracted into the organic phase. At PBA/xylose ratios > 4, nearly 100% is extracted. Figure 5.2a indicates an inflection point at a PBA/xylose ratio of 2:1. Comparison with literature data[9,17,18] and further experimental analysis using 2D-NMR, FTIR, and MS confirmed the extracted species to be the (neutral) boronate diester of xylose and two units of PBA (PBA_2X). The efficiency of the extraction appeared to be pH-independent between pH 1 and 12 (Figure 5.2b). In this pH range, the nature of the xylose boronate diester remained unchanged. This wide pH range in which the

extraction functions supports the role of a neutral hydrophobic species in the extraction equilibrium. Under acidic conditions and in the absence of Aliquat, the extraction is promoted by the strong hydrophobic nature of the PBA units in the diester in the charge-neutral trigonal state. This implies that the affinity of the PBA units for the organic phase is the driving force for the extraction into the organic phase.

5.2.2 Equilibria Involved in the Extraction of Xylose

The extraction process takes time, and transient turbidity was observed during the experiments. Both literature indications[3] and control experiments suggest that, in all cases, equilibrium between the organic and aqueous phases is reached after a maximum of 1−2 h at room temperature. In all cases, the extraction process can be divided into three distinct stages. At the early stages of the process, the biphasic system is composed of two clear solutions. When the mixing starts, the upper toluene phase becomes turbid within the first 30 min. This turbidity disappears after 1.5−2 h to leave again a clear biphasic system. Thereafter, the biphasic extraction system remained stable for some 500 h.

When operated at higher temperature, the process still showed the transient development of a turbid toluene phase, though the extraction reached completion with two clear phases within a shorter time, *e.g.*, approximately 20 min at 70 °C (Figure 5.3). The analysis of the two phases at the end of the extraction (2:1 PBA/xylose, pH 1) showed free xylose in the aqueous phase (approximately 15%) and PBA_2X in the toluene phase (approximately 85%), with no monoester intermediate (PBAX) being detected. However, analysis (both with ^{1}H-NMR and MS) of the turbid toluene phase, obtained by stopping the extraction at an early stage, strongly suggests the formation of a PBAX boronate monoester intermediate.

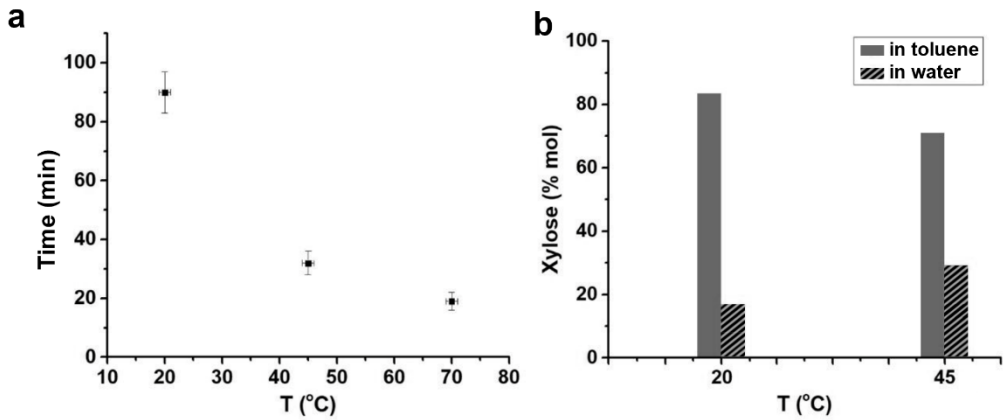

Figure 5.3 Xylose extraction, 1:1 toluene-water (pH = 1), starting xylose concentration 350 mM, [PBA] in toluene 700 mM, performed at temperature > 20 °C. (a) The time between the beginning of the extraction and the reaching of the equilibrium decreases when operating at higher temperatures, with the turbidity observed disappearing earlier in the process. If the sampling for the analysis is done at room temperature the extraction efficiency does not influence. (b) If the sampling is performed at different temperatures the partition of the sugar in the two phases is influenced, with more of the sugar residing in the aqueous phase at higher temperatures.

The presence of a putative intermediate monoester (PBAX) suggests a two-step extraction process (Figure 5.4a): the first molecule of PBA binds xylose at the water/toluene interface and forms a monoester, which resides as an amphiphile at the interface between the two phases, causing turbidity, probably due to the formation of an emulsion. It eventually binds to a second unit of PBA to form the diester PBA_2X which is well soluble in toluene. Aliquat has been shown to be ineffective at nonalkaline pH.[13,16] To verify this experimentally, solutions of xylose (350 mM) at different pH values were brought into contact with an equal volume of a solution of PBA in toluene (700 mM, 8.5 w %) to which Aliquat was added as the chloride salt (700 mM, 28 w%).

When the organic phase containing Aliquat was brought into contact with the aqueous phase at pH = 7, the Cl^- anion migrated to the aqueous phase, as evidenced by dropwise addition of an aqueous solution of $AgNO_3$ and the visualization of the precipitation of AgCl. In the meantime, the pH dropped from 7 to 4. However, the PBA resided mainly in the organic phase, as shown by NMR. When lowering the Aliquat concentration in toluene from 700 mM to 200 mM, after reaching equilibrium, consistent xylose extraction can be detected, even though the efficiency is lowered. This behavior can be rationalized assuming that the deprotonated PBA anion is exchanged with Cl^- and scavenged from the aqueous phase by Aliquat. At basic pH, the water-soluble boronate

anion reacts with xylose to form a boronate monoester anion in the aqueous phase, and this is then extracted to the toluene phase with the assistance of Aliquat (Figure 5.4c). At neutral/acidic pH (when pH < pK_a), however, no water-soluble boronate anion forms in the aqueous phase (Figure 5.4b), which renders the Aliquat phase transfer inoperable.[11,14] PBA resides predominantly in the organic phase as neutral species, and the Aliquat exchanges its chloride anion with an OH^-, which is bound by PBA, with concomitant acidification of the water phase. This causes the PBA to be inaccessible for extraction of the xylose (Figure 5.4b).

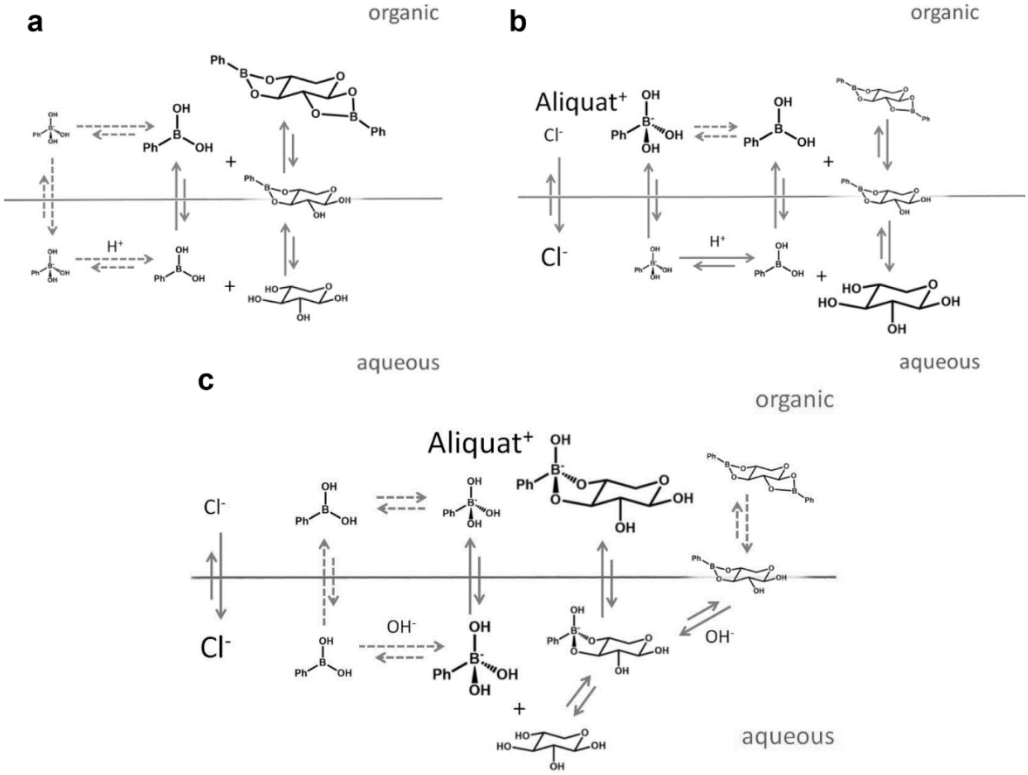

Figure 5.4 Equilibria involved in the biphasic water–toluene system in the presence of xylose and PBA and in the absence (a) or presence (b) of Aliquat, at acidic pH (or more generally at pH values below the pK_a of PBA), or at pH > pK_a (c). Different species are represented in the panels with a relative size that reflects their abundance at this pH. The dashed arrows indicate equilibria that play no role in the extraction under the given conditions but are shown for comparability with other conditions. The absence of Aliquat (a) leads to the preferential formation of the xylose diester with PBA, while the addition of Aliquat (b) promotes retention of xylose in the water phase and PBA partitioning into the organic phase. (c) Common pathway of sugar extraction, where a

negatively charged sugar-boronate monoester is formed in the aqueous phase and then extracted into the organic phase.

In accordance, when a lower amount of Aliquat is used, only a comparable fraction of PBA is inactivated. Although more work would be needed to assess all equilibria, the following *rationale* is proposed. At basic pH, all boronates are already quaternary and charged; also in the two options (free and sugar-bound boronate), the sugar-bound one then goes preferentially into the organic phase (but only as the monoester, a diester-bis-anion is too polar and/or gives too much internal charge repulsion in the organic solvent). The preference for binding OH^- to the boron center does not play a role in this case in predicting this preference, as the high pH sets both in this quaternary state. In neutral/acidic medium, in contrast, the coupled sugar binding/OH coordination dictates the species populations; apparently the speciation lies less on the side of the sugar-bound complex than on the side of the PBA.

5.2.3 Effect of Organic Solvent Type on the Extraction Efficiency

The extraction was performed with different organic solvents to study the effect of the solvent type on the extraction efficiency. Xylose in water, at pH = 1, was contacted with an equal volume of an organic solvent with PBA (PBA/xylose = 2:1), and the fractions of diester that partitioned into the organic phase upon a single extraction step were analyzed by ^{1}H-NMR. Aromatic, nonaromatic, and one mixture were tested, and the results are shown in Figure 5.5, in which the extraction efficiencies are plotted as a function of the solvents' dielectric constant. As the boronate diester with PBA contains an aromatic hydrophobic part, aromatic solvents were found to be more effective than nonaromatic ones, irrespective of their polarity. Among the aromatic solvents, the presence of an electron-withdrawing group (*i.e.*, nitrobenzene) enhances xylose extraction into the organic phase, while the presence of an electron-donating group (*i.e.*, anisole) reduces it. Among the nonaromatic solvents, partial mixing and emulsification with the aqueous phase (*e.g.*, 1-octanol) are detrimental for the extraction. Using a combination of an aromatic solvent with a nonaromatic one (1:1 toluene−*γ*-valerolactone (GVL); triangles in Figure 5.5) suppresses the extraction efficiency compared to pure toluene. From this set of experiments, it can be concluded that π−π stacking plays an important role in the partitioning of PBA_2X into the organic phase. Moreover, these results confirm that the affinity of the PBA units for the organic phase, at acidic conditions, is the driving force for the sugar extraction.

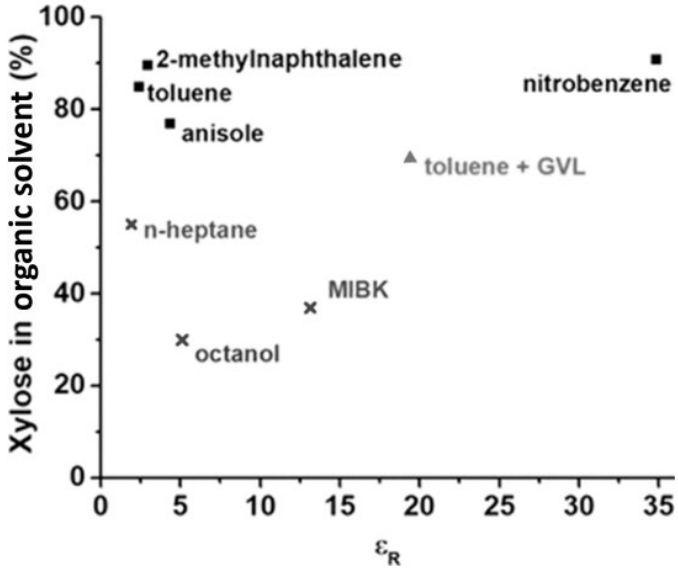

Figure 5.5 Fraction of xylose in the organic phase after extraction (1:1 water–organic, 350 mM xylose, 700 mM PBA, pH = 1 from H_2SO_4) *versus* the dielectric constant of the organic solvent of choice. Crosses, squares, and triangles represent nonaromatic, aromatic, and mixed aromatic/nonaromatic solvents, respectively.

5.2.4 Selectivity for Xylose Extraction from Pure Solutions and a Model Hydrolysate

The high structural variability of sugars strongly affects their ability to bind to boronic acids.[13,15,18,19] To investigate the effect of the sugar structure on the extraction efficiency different common sugars (*i.e.*, glucose, fructose, arabinose, galactose, sucrose) were studied using the same extraction protocol (Figure 5.6). The selection of the monosaccharides in this analysis is based on their abundance in lignocellulosic hydrolysates.[20–22] Specifically, these monosaccharides are found, at different relative w%, as building blocks of polysaccharides in hemicellulose.[4,20–22] Xylose presents two pairs of OH groups which both occur in an equatorial position, favorable for binding PBA, as discussed above. Fructose and glucose also present two pairs of OH groups eligible for binding PBA but have an additional OH group that is left unbound. This free OH group is hydrophilic and thus reduces the affinity of these diesters for the apolar organic phase. Arabinose, galactose, and sucrose present only one pair of equatorial OH groups and can only bind one PBA molecule, leaving two, three, or six OH groups unbound, respectively, leading to decreasing extraction efficiencies (Figure 5.7). Interestingly, the extraction selectivity for xylose is maintained at temperatures as high as 90 °C.

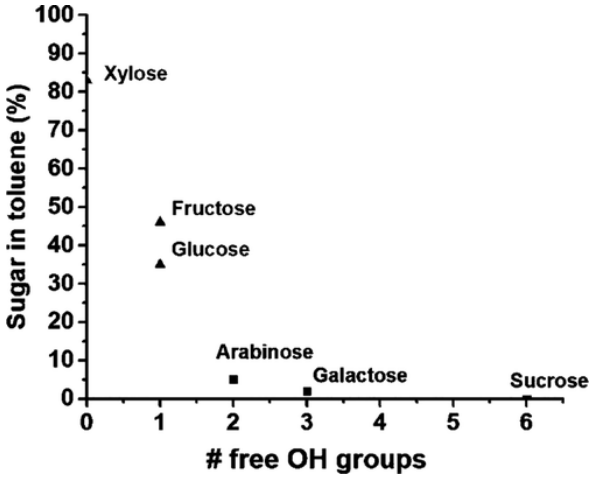

Figure 5.6 Fraction of sugar in the toluene phase after extraction (1:1 water–toluene, 350 mM of sugar, 700 mM PBA, pH = 1 from H_2SO_4) *versus* the number of OH groups left free after the binding of PBA to form a boronate mono/diester. Sugar boronate monoesters and diesters are shown as squares and triangles, respectively.

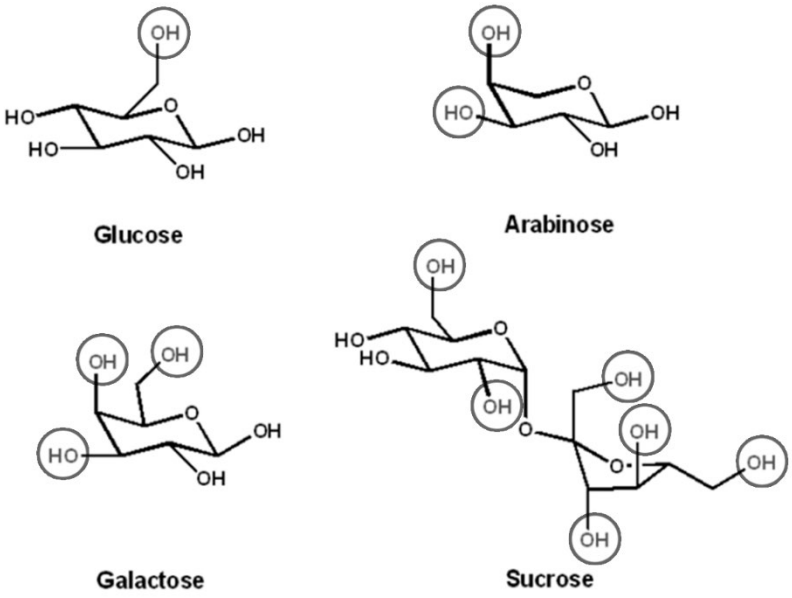

Figure 5.7 Structures of some of the sugars used in this study, put in the most favorable configuration for binding PBA. The OH groups that are left unbound are highlighted with a circle.

The extraction selectivity reported here significantly deviates from the one reported in the literature at basic pH in the presence of a phase transfer agent.[15] Most sugars present one pair of equatorial OH groups that can bind PBA and form an anionic sugar boronate ester at high pH. The negative charge and the proximity of the bulky Aliquat further hinders the binding of a second boronate anion to an equatorial OH pair that would eventually remain. Nevertheless, the ion pairing with Aliquat overcomes the hydrophilicity of the esters and makes them partition into the organic phase without regard to the number of free OH groups. Hence, no significant sugar selectivity was observed under such conditions.[3]

To further demonstrate the value of the extraction selectivity at low pH, the extraction of xylose from a mixture of sugars was attempted (Figure 5.8). Such a mixture is supposed to represent a hydrolysate obtained by dilute acid pretreatment of lignocellulose.[20-22] A model pretreatment hydrolysate, representative for a xylose-rich hydrolysate obtained from hardwood and/or agricultural residues at mild conditions of temperature and acidity, was prepared by mixing 52% xylose, 35% arabinose, 6% galactose, and 3% glucose, and dissolving this mixture in water at 5 w% total sugar concentration. Acidification to pH = 3 was achieved by using acetic acid, a common coproduct of pretreatment.[4,20–22] Upon application of the extraction protocol (see above, using acetic acid and a 2:1 PBA/sugar molar ratio), the aqueous phase appeared to retain most of the initial arabinose and galactose but no xylose anymore (Figure 5.8). In contrast, the toluene phase contained > 95% of xylose in the form of PBA_2X. Xylose could be extracted to high percentages because arabinose and galactose did not bind it, and the extraction was effectively operated at a PBA/xylose ratio of around 4:1, which was shown to lead to > 95% xylose extraction (Figure 5.2a). The limited amount of glucose present in the model hydrolysate and the competition with a more suitable sugar (*i.e.*, xylose) led to no detectable extraction of glucose.

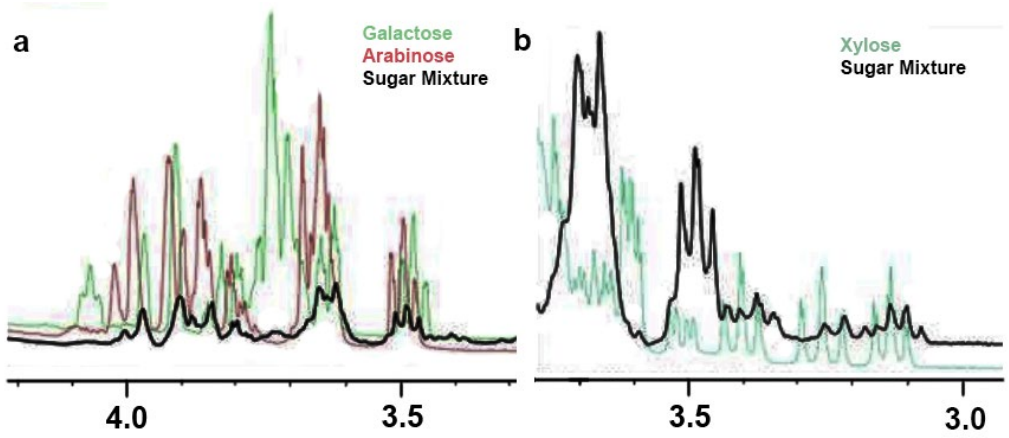

Figure 5.8 ^{1}H-NMR spectra of the aqueous phase (pH = 3 from acetic acid) of the sugar mixture after the extraction compared to (a) the ^{1}H-NMR spectra of arabinose and galactose and (b) the ^{1}H-NMR spectrum of xylose

5.2.5 Integrated Process to Isolate Xylose

So far, the discussion has been limited to the extraction of xylose from the hydrolysate. For industrial application, however, the recovery of the xylose from the extracted boronate diester and of the extraction solvent also needs to be investigated. An obvious approach consists of back-extracting the xylose with an acidic aqueous solution.[3] Accordingly, an integrated extraction process would contact the xylose-containing hydrolysate with a solution of solvent and phenylboronic acid (PBA), usually in counter-current operation, to form the xylose diboronate ester and entrain it upward with the solvent phase, while the resulting xylose-lean hydrolysate is withdrawn at the bottom of the column. The solvent/ester solution is subsequently contacted with an acidic aqueous phase to hydrolyze the ester and back-extract the resulting xylose into the water phase. Such a scheme is typically practiced using two extraction columns in a series as shown in Figure 5.9a. However, both steps could be integrated into a single extraction column with a lower section performing the extraction step and an upper part performing the back-extraction (Figure 5.9b). Such a column would comprise a side-feed for the hydrolysate, a side-draw for the aqueous xylose product stream, and a solvent/PBA recycle from top to bottom. Overall, the process would ideally be carried out at elevated temperature, *e.g.*, 60−90 °C, to proceed swiftly. Back-extraction experiments from toluene/PBA were executed and appeared to be challenging: > 10 extraction stages were required to recover > 80% of the xylose. The extraction efficiency of the toluene/BPA system, 85% in a single stage, turned out to hinder the back-extraction. In contrast, the use of a less efficient extraction mixture such as *n*-heptane/BPA (45% in a single stage, see Figure 5.4 panels a and b) allowed a much

easier back-extraction of xylose. For an efficient process, therefore, the combined efficiencies of solvent extraction and back-extraction need to be considered.

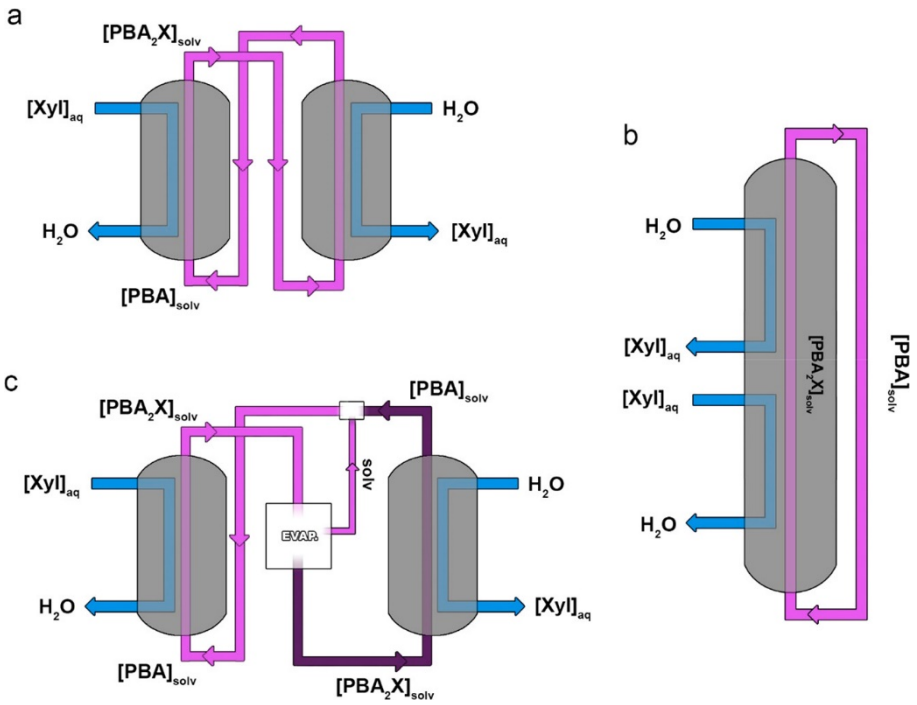

Figure 5.9 Conceptual process schemes for producing clean xylose solution by extraction and back-extraction: conventional scheme (a), integrated scheme (b), and scheme with interstage concentration (c).

The process concepts described in Figure 5.9 will work in counter-current operations, differently than lab scale experiments. The overall efficiency of counter-current operation is typically expressed as the concentration ratio in solvent and feed, C_s/C_f, and related to the single-stage efficiency E and the number of stages n (Equation 5.1).

$$\frac{C_s}{C_f} = \frac{(E-1)}{(E^{n+1}-1)} \qquad \textbf{Equation 5.1}$$

This ratio can then be converted into extraction yield (Equation 5.2).

$$Y = 1 - \frac{C_s}{C_f} = \frac{E(E^n-1)}{(E^{n+1}-1)} \qquad \textbf{Equation 5.2}$$

Applying the same reasoning to the back-extraction leads to n' stages and for the back-extraction yield to be rewritten as function of the extraction efficiency E', with $E' = E^{-1}$ (Equation 5.3).

$$Y' = \frac{E'(E'^{n'}-1)}{(E'^{n'+1}-1)} \qquad \textbf{Equation 5.3}$$

Consequently, the overall yield *Y*" of extraction followed by back-extraction can be expressed with Equation 5.4.

$$Y'' = Y \cdot Y' = E \cdot \frac{(E^{n}-1)(E^{n'}-1)}{(E^{n-1}-1)(E^{n'-1}-1)} \qquad \textbf{Equation 5.4}$$

Based on Equation 5.4 and its limitations (diluted feed, back-extraction in the same medium as the feed and at the same flow rate as the feed), the overall efficiency of extraction and back-extraction, in the same medium as the feed, can be calculated using 20 stages to be freely distributed between extraction and back-extraction. The maximum overall efficiency did not really depend on the partition coefficient *K* observed in single-stage extraction as long as the solvent/feed ratio (*S*/*F*) was adjusted to reach, but not exceed, 50% extraction in a single stage, considering $E = KS/F$. Hence, the process is free to use a large variety of extraction solvents and can be optimized on other performance parameters than extraction efficiency. Recovery and concentration are not the sole critical factors for the economic viability of such a process. Losses of solvent and PBA in both aqueous streams, *i.e.*, in the xylose-lean hydrolysate and in the xylose-rich product stream, also need to be minimized. Loss of toluene should not expect to be very critical owing to its low solubility in water of 0.05 w% (at 25 °C). Loss of PBA could be more substantial, since it dissolves in water up to 1 w% (at 25 °C). Analysis of the aqueous phase after extraction revealed indeed the presence of 0.9 w% PBA. Appropriate measures should be considered to mitigate these losses. While achieving a respectable yield, such an extraction/back-extraction scheme still delivers a product stream that is slightly more diluted than the feed stream. This drawback can be improved upon inserting a solvent reconcentration step, *e.g.*, by partial evaporation, before the back-extraction (Figure 5.9c). In the case modeled in Figure 5.10, the evaporation of 50% of the solvent delivers the 82% recovery at 8.2% concentration, *i.e.*, 64% higher than present in the feed stream. This would obviously increase the energy consumption of the process, but much less than upon evaporation of a comparable volume of water to concentrate the hydrolysate or the final xylose aqueous product stream, for the heat of evaporation of hydrocarbon solvents is less than a fifth of that of water, namely 0.3 kJ/mL *versus* 2.2 kJ/mL.

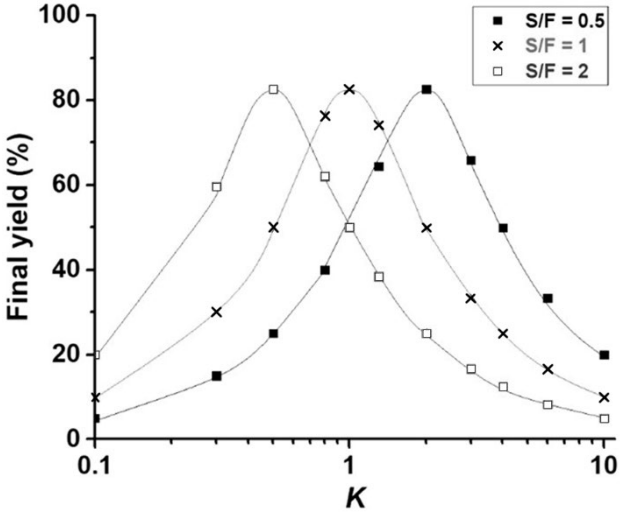

Figure 5.10 Yield of combined extraction/back-extraction under counter-current operation (assumptions: medium and flow rate of feed and back-extraction medium are identical, 10 extraction stages and 10 back-extraction stages).

Economic considerations could be used to define the optimum solvent reconcentration level. Gori et al.[9] have proposed another approach to recover the xylose from a PBA_2X/solvent stream. It involves the transesterification of PBA_2X with another diol (*e.g.*, ethylene glycol) to produce a PBA-glycol ester and to precipitate xylose from the solution. The xylose can then be advantageously used as crystalline xylose, be redissolved in water, or be transferred to a polar organic solvent for further processing. Once the crystalline xylose is recovered, the resulting PBA-glycol ester (PBA-EG) can then be hydrolyzed with an acidic aqueous solution to form a decantable PBA phase for recycling.[9] However, the resulting acidic aqueous glycol solution needs further workup, *e.g.*, by water evaporation, to allow recycling of the glycol for the next run. All these steps eventually make the xylose recovery quite complicated. This approach seems particularly elegant when one targets crystalline xylose or when one wishes to transfer the xylose into a nonaqueous solvent. It is, however, fairly complex for transferring xylose back to water. A deeper process modeling study would be needed to compare it to the method proposed here in terms of energy demand and equipment cost and component losses.

5.3 Conclusions

This study proposes an integrated process to recover and purify xylose from an acidic hydrolysate stream, *e.g.*, coming from steam expulsion or dilute acid pretreatment of lignocellulose. This process consists of selectively extracting the xylose as the boronate

diester directly from the acidic hydrolysate and back-extracting it into a clean aqueous solution. The structure of the xylose-PBA diester is demonstrated by means of various methods and provided strong evidence for the intermediate formation of an uncharged monoester. Analysis of the many equilibria and species involved supports the successful extraction of xylose into an organic solvent as the boronate diester in the absence of a phase transfer agent. Compared to Aliquat-mediated extraction at basic pH, the current procedure simplifies the extraction process considerably as an acidic hydrolysate feed can be used directly and no phase transfer agent is needed. The extraction selectivity for xylose *versus* other sugars that may also be present in the xylose feed is demonstrated and explained. Thanks to its high selectivity for xylose and its efficiency at all pH values, the present approach presents a significant improvement over prior art, *i.e.*, over alkaline extraction with Aliquat as the phase transfer agent. Initial analyses of extraction and back-extraction efficiencies provide a good prospect for the future development into a process to purify and isolate xylose from more complex feeds. In future work, the ease of fully removing the organic solvent from the isolated xylose will need to be assessed, also depending whether the intended use is for food or further chemical conversion, the latter being intended here. Also, a more detailed analysis of the capital and operating costs of a process based on this extraction will be conducted, and a comparison to other ways to isolate xylose, such as by moving bed chromatography.

5.4 Experimental Section

5.4.1 Chemicals

D-(+)-xylose (> 99%), D-(+)-glucose (> 99%), D-(−)-fructose (> 99%), L-(+)-arabinose (> 99%), D-(+)-galactose (> 99%), D-(+)-sucrose (> 99.5%), D_2O (99.9% atom D), toluene-d_8 (99% atom D), DMSO-d_6 (99% atom D), dioxane (99.8%), 3-(trimethylsilyl)propionic-2,2,3,3-d_4 acid sodium salt (TMSP, 98% atom D), Aliquat 336, *γ*-valerolactone (99%), nitrobenzene (99%), anisole (99%), methylisobutylketone (> 99%), 1-octanol (> 99%), *n*-heptane (> 99%), and 2-methylnaphthalene (98%) were purchased from Sigma-Aldrich, while phenylboronic acid (99%) was obtained from Alfa Aesar.

5.4.2 Methods and Equipment

All chemicals are commercially available and were used without further purification. ^{1}H-NMR spectra were recorded as described in Chapter 3. The ^{1}H-NMR characterization of PBAX and PBA_2X was performed in DMSO-d_6 to ensure the possibility to directly compare all the esters with xylose. IR spectra and MS spectrometry were recorded as described in Chapter 4. In all cases, stirring was performed with a magnetic stirrer at 1000 rpm at room temperature.

5.4.3 PBA-Mediated Extractions

Equal volumes of an aqueous sugar solution and a solution of PBA in organic solvent were put into contact and stirred at room temperature for a maximum time of 2 h. Solutions of D-xylose (350 mM) in water (pH = 1, 7, and 10) and PBA and Aliquat 336 in toluene (both at equimolar conditions and in excess of PBA) were used to study the effect of Aliquat 336 on the extraction (only in this case the total time was prolonged to 24 h). Solutions of D-xylose (350 mM) in water (pH varying from 1 to 9) and a PBA solution in toluene (700 mM) were used to study the effect of pH. A solution of D-xylose (350 mM) in water (pH = 1 from H_2SO_4) and PBA solutions in toluene at various concentrations were used to study the effect of different xylose-PBA ratios. A solution of D-xylose (350 mM) in water (pH = 1 from H_2SO_4) and PBA solutions (700 mM) in various organic solvents were used to explore the effect of the organic solvent on the extraction. Solutions of various sugars (350 mM) in water (pH = 1 from H_2SO_4) and a PBA solution in toluene (700 mM) were used to analyze the behavior of different sugars in the extraction process. In all cases, both phases were analyzed by ^{1}H-NMR spectroscopy as described above.

5.4.4 Isolation and Analysis of PBAX and PBA_2X

In the case of PBA_2X, a solution of D-xylose (350 mM) in water (5 mL; pH = 1 from H_2SO_4) and a PBA solution in toluene (5 mL; 700 mM) were mixed for 2 h at room temperature. In the case of PBAX, a solution of D-xylose (350 mM) in water (5 mL; pH = 6 from H_2SO_4) and a PBA solution in toluene (5 mL; 350 mM) were mixed for 30 min. After separating the two phases, the solvents were removed with a continuous stream of dry N_2. The solid samples obtained were characterized with ^{1}H-NMR spectroscopy (in DMSO-d_6) and MS spectrometry.

5.4.5 Xylose Extraction from Complex Matrix

A mixture of different sugars, based on the composition of hemicellulose derived from rice husk,[20–22] in water (pH = 3 from acetic acid) and a solution of PBA in toluene (700 mM) were mixed for a total time of 2 h. The two phases were analyzed with ^{1}H-NMR spectroscopy as described above.

5.5 References

1. M. Yadav, D. K. Mishra, J.-S. Hwang, *Appl. Catal. A* **2012**, *425−426*, 110−116.
2. P. Gallezot, *Chem. Soc. Rev.* **2012**, *41*, 1538−1558.
3. N. Sánchez-Bastardo, I. Delidovich, E. Alonso, *ACS Sus. Chem. Eng.* **2018**, *6*, 11930−11938.

4. J.-P. Lange, E. Van der Heide, J. Van Buijtenen, R. Price, *ChemSusChem* **2012**, *5*, 150−166.
5. X. Li, Y. Chen, J. Nielsen, *Curr. Opin. Biotechnol.* **2019**, *57*, 56−65.
6. S. Ramaswamy, J.-H. Huang, B. V. Ramarao, *Separation and Purification Technologies in Biorefineries*, Wiley, Chichester (UK), **2013**.
7. P. N. Vashist, R. B. Beckmann, *Ind. Eng. Chem.* **1968**, *60*, 43−51.
8. O. G. Sas, I. Domínguez, B. González, Á. Domínguez, *J. Environ. Manage.* **2018**, *228*, 475−482.
9. S. S. Gori, M. V. R. Raju, D. A. Fonseca, J. Satyavolu, C. T. Burns, M. H. Nantz, *ACS Sus. Chem. Eng.* **2015**, *3*, 2452−2457.
10. T. C. R. Brennan, S. Datta, H. W. Blanch, B. A. Simmons, B. M. Holmes, *Bioenergy Res.* **2010**, *3*, 123−133.
11. G. J. Griffin, L. Shu, *J. Chem. Technol. Biotechnol.* 2004, 79, 505−511.
12. B. Li, P. Relue, S. Varanasi, *Green Chem.* **2012**, *14*, 2436−2444.
13. J. A. Peters, *Coord. Chem. Rev.* **2014**, *268*, 1−22.
14. G. J. Griffin, *Sep. Sci. Technol.* **2005**, *40*, 2337−2351.
15. M. Matsumoto, K. Ueba, K. Kondo, *Sep. Purif. Technol.* **2005**, *43*, 269−274.
16. M. Dowlut, D. G. Hall, *J. Am. Chem. Soc.* **2006**, *128*, 4226−4227.
17. Y. Furikado, T. Nagahata, T. Okamoto, T. Sugaya, S. Iwatsuki, M. Inamo, H. D. Takagi, A. Odani, K. Ishihara, *Chem. Eur. J.* **2014**, *20*, 13194−13202.
18. P. J. Wood, I. R. Siddiqui, *Carbohydr. Res.* **1974**, *33*, 97−104.
19. P. J. Wood, I. R. Siddiqui, *Carbohydr. Res.* **1974**, *36*, 247−256.
20. R. Macrae, R. K. Robinson, J. M. Sadler, M. J. *Encyclopedia of Food Science, Food Technology and Nutrition, 2nd ed.*, Academic Press, Cambridge (Massachusetts), **2003**, pp 3060−3071.
21. B. Ward, *Molecular Medical Microbiology, 2nd ed.*, Academic Press, Cambridge (Massachusetts), **2014**, pp 201−233.
22. S. S. Adav, S. K. Sze, *Biotechnology and Biology of Trichoderma*, Elsevier, Amsterdam, **2014**, pp 103−111.

Chapter 6

Selectivity Switch by Phase Switch - The Key to a High-Yield Furfural Process

This work shows the effective conversion of xylose into furfural, with selectivities >90 mol%, in an aqueous-organic three-solvent system, composed of an apolar aromatic solvent, a polar organic solvent and acidic water to catalyze the formation of furfural. This is coupled with a pre-extraction step of xylose as a boronic diester into a promising integrated process for valorizing diluted xylose-hydrolysate. This process promises facile recovery of furfural and good recycling of all solvent components. Use of the boronic diester was found irrelevant for the high selectivity, as its hydrolysis under the reaction conditions is fast. Surprisingly, the >90 mol% selectivity requires the three-solvent system to transition from biphasic to monophasic at the reaction conditions. The phenylboronic acid (PBA) used to extract xylose, was found instrumental to this transition; PBA-lean media (<20 mM PBA) remain biphasic under the reaction conditions and deliver only 70 mol% selectivity. Water partial pressure measurements across the phase transition temperature confirm the occurrence of the phase transition. The increase of the apolar nature of the reaction medium when transitioning from biphasic to monophasic operation, reached upon mixing of the aromatic solvent with the water-polar organic phase, is likely responsible for the improved selectivity. The presence of an aromatic solvent in the mixture is important, probably for its interaction with PBA that is instrumental to achieve the phase transition. A 1:1:1 toluene-sulfolane-water (pH =1) mixture and [PBA] >20 mM resulted in the highest observed xylose-to-furfural selectivity (95 mol%).

Part of this chapter has been published in: L. Ricciardi, W. Verboom, J.-P. Lange, J. Huskens, *Green Chem.* **2021**, *in press*.

6.1 Introduction

Furfural is currently produced by acid-catalyzed dehydration of xylose present in lignocellulosic biomass.[1-4] However, the xylose-to-furfural selectivity is severely limited by side-reactions, in particular the formation of solid humic by-products, observed consistently over several reaction conditions.[1-5] To address these problems and enhance the production of furfural, various strategies have introduced an organic solvent in the process.[5-12] A common strategy to improve the efficiency of xylose dehydration is to perform the reaction in a biphasic system,[5-10] with the aim to extract furfural as soon as it is formed and thereby protect it from degradation.[10] Accordingly, the xylose-to-furfural selectivity is raised to 65-70 mol%, which is a significant improvement over the 50 mol% observed when xylose is dehydrated in water.[10] Alternatively, the reaction can be performed under monophasic conditions, using polar aprotic solvents (*e.g.*, DMSO and sulfolane), optionally with limited amounts of water, delivering furfural with a selectivity up to 80-85 mol%.[14-19] An explanation for this improved selectivity is that aprotic organic solvents suppress the formation of acyclic sugar, which is more prone to degradation, while the limited amount of water directly interacts with the sugar influencing the mechanism of dehydration.[14,15] However, this approach requires the xylose to be recovered from the dilute aqueous feed, which severely increases the cost of the sugar.[1,2] Additionally, these solvents cannot be considered green, based on their detrimental effect on human health and hazard for the environment, and their separation from water streams requires a high energy input.[20] In the context of fructose dehydration to hydroxymethylfurfural (HMF) under biphasic conditions, Román-Leshkov and Dumesic introduced the use of a polar organic solvent (*e.g.,* 1-butanol) that gave a monophasic system at the reaction conditions.[13] However, the mutual solubility of water and the organic solvent at higher temperatures resulted in the formation of more degradation products, possibly due to rehydration.[13]

This Chapter studies the use of a three-solvent mixture, using water (with acid to induce reaction), an apolar, aromatic organic solvent, and a polar aprotic solvent, in the conversion of xylose to furfural, with the aim to integrate this step into a process with a pre-extraction step of xylose as a boronic diester (Figure 6.1). Chapter 5 describes the extraction of xylose from an acidic aqueous feed into an organic aromatic solvent as the boronic diester (PBA_2X) and its conversion at biphasic operation. In the present study, a temperature-dependent switching from biphasic to monophasic conditions is observed upon adding a third, polar aprotic, solvent, in the presence of phenylboronic acid (PBA). A simultaneous strong effect on the xylose-to-furfural selectivity is found to be connected with this switch in phase behavior. The conditions under which this phase transition occurs is explored and a tentative rationalization for the effect on the selectivity is offered. Based on these findings, an onset to an integrated process scheme

is provided, benefitting from both the diester extraction and the highly selective monophasic conversion, and allowing for the separation of the solvents from the aqueous waste stream and the recycling of both solvents and additives.

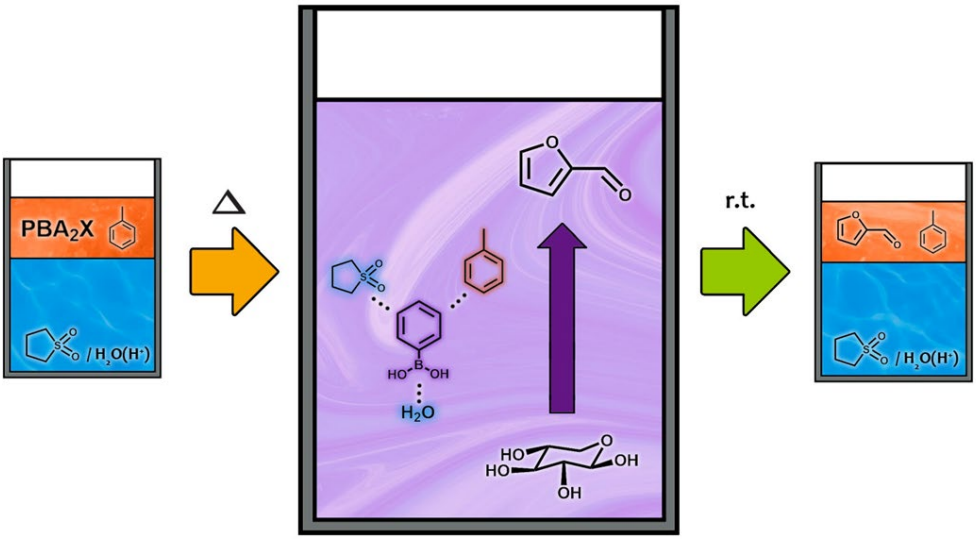

Figure 6.1 Conceptual representation of the solvent composition of the system and its phase behavior, during preparation of a boronic ester feed (of xylose and PBA) in an aromatic solvent, PBA-induced transition to monophasic at the reaction temperature, and separation of the produced furfural during work-up.

6.2 Results and Discussion

6.2.1 Selectivity switch in the dehydration of xylose to furfural in a three-solvent system

When aiming for a process to convert xylose from biomass into furfural, the extraction of xylose from an acidic aqueous hydrolysate will deliver a toluene phase containing PBA_2X.[20] This extraction allows naturally to consider a biphasic system to convert the xylose upon back-extraction into acidic water, but the xylose-to-furfural selectivity under biphasic operation is typically only about 70%, as shown in Chapter 3. Therefore, considerations on adapting the solvent in which to convert the back-extracted xylose are needed. In this Chapter, a solution of PBA_2X in toluene is used. However, it has to be noted that choosing the diester as the starting material is not an essential element to provide the selectivity observed in this process. As it will be shown, (i) the hydrolysis of the diester in a solvent mixture that contains water is fast compared to the conversion of released xylose into furfural, and (ii) it is free PBA (not its ester) that

provides the control over the temperature-induced biphasic to monophasic transition that in its turn provides the high selectivity. Many experiments were therefore conducted by simply adding the xylose to the water phase and PBA to toluene before mixing the solvents, this to allow, for example, variation of the xylose-PBA ratio.

Performing the hydrolysis and conversion of PBA_2X in a 1:1:1 toluene-sulfolane-water (water at pH = 1, 97 mM of PBA_2X in the reaction mixture) system led to an unexpectedly high furfural selectivity of approx. 95 mol% at full xylose conversion, after approx. 3.5 h (Figure 6.2). At room temperature, the mixture was biphasic, with the toluene forming the organic phase and the sulfolane-water mixture as the polar aqueous phase. However, at the reaction temperature (180 °C), formation of a single phase was observed. In contrast, operation in 1:1 toluene-water (pH 1), which is biphasic at the reaction temperature, resulted in only 70 mol% selectivity.[11] To understand the origin of the high furfural selectivity in the former case, the progress of the reaction was followed in time (Figure 6.2), showing a fast (< 30 min) release of the sugar from its boronate ester and partitioning into the aqueous phase (upon analysis at room temperature at which the mixtures are always biphasic), followed by a slower conversion of the released xylose into furfural. Remarkably, the xylose-to-furfural selectivity stayed >90 mol% over the entire course of the reaction until full conversion. The fast hydrolysis of the boronate ester form of the xylose, PBA_2X, into xylose in water, which is practically complete within the first 30 min, indicates that the use of PBA_2X as the starting material is not essential to achieve the observed selectivity. Indeed, performing the reaction in the same solvent mixture, but starting from free xylose in water (pH = 1) and PBA in toluene (with a xylose concentration in the system of 97 mM and a PBA concentration of 194 mM), gave the same furfural selectivity.

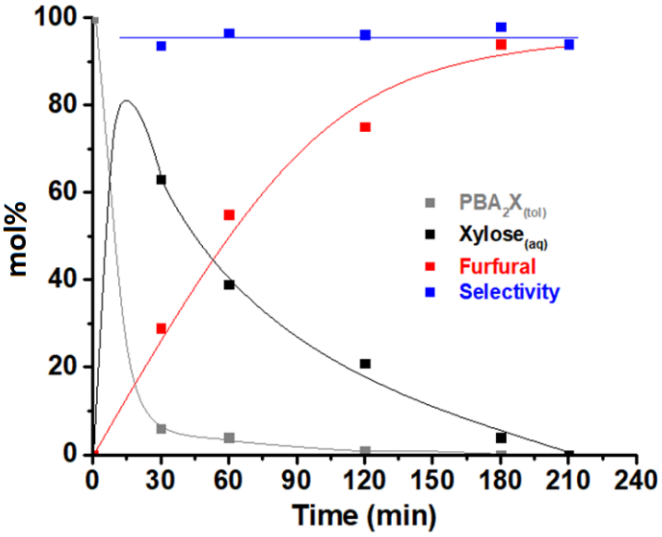

Figure 6.2 Relative concentrations (in mol% of the starting total xylose concentration of 97 mM) of furfural, xylose and unconverted PBA_2X, and the selectivity toward furfural *versus* time. Reaction performed in a 1:1:1 toluene-sulfolane-water (pH = 1) system at 180 °C. Values calculated from NMR analysis of aqueous and toluene phases at room temperature (lines are to guide the eye).

In contrast, performing the reaction starting from free xylose in water (pH = 1), using the same solvent system and experimental conditions, but in the absence of PBA, gave only a 70 mol% yield of furfural, comparable to the selectivity obtained under commonly applied water-toluene biphasic conditions. This suggests that the PBA, originating from the hydrolysis of PBA_2X, is an essential component to obtain the high selectivity, even though ester formation is not. To investigate the effect of the reaction medium and the role of PBA in it, the xylose dehydration reaction was performed at a constant xylose concentration and using the same experimental conditions and solvent system. PBA was added to the toluene phase reaching concentrations in the reaction mixture that varied from 0 to 233 mM (Figure 6.3). While the final furfural selectivity was always close to 70 mol% at [PBA] < 20 mM in the reaction mixture, it increased markedly and in a stepwise manner to > 90 mol% at PBA concentrations in the reaction mixture above 20 mM.

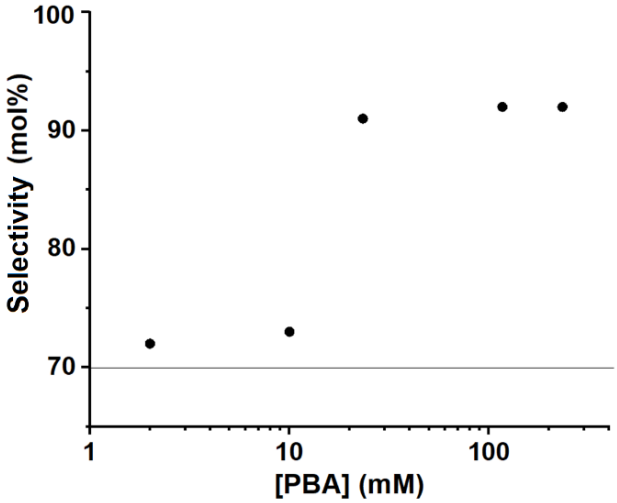

Figure 6.3 Xylose-to-furfural selectivity (mol%) *versus* PBA concentration (mM) in the reaction mixture; reaction performed at 180 °C for 3-4 h (full conversion achieved in all cases) in a 1:1:1 toluene-sulfolane-water (pH = 1) solvent system with free xylose (97 mM in the reaction mixture) and free PBA at varying concentrations. The horizontal line at approx. 70 mol% represents the selectivity obtained at a PBA concentration of 0 mM.

6.2.2 Phase Change of the Three-Solvent Mixture as a Function of PBA Concentration and Temperature

The sharp selectivity transition observed above triggered us to investigate the phase behavior of the reaction mixture as a function of PBA concentration and reaction temperature. Visual observation of the number of phases of the reaction mixtures was performed, and the xylose-to-furfural selectivity was assessed (Figure 6.4). Datapoints were found distributed over those with biphasic and monophasic behavior, and a dividing line became apparent. Complementary experiments in glass capillaries containing the solvent-PBA mixtures (without xylose) indeed showed that the 1:1:1 toluene-sulfolane-water (pH = 1) system transitions from biphasic to monophasic, depending on the temperature and the PBA concentration. Furthermore, these experiments showed no partial mixing prior to the phase transition from biphasic to monophasic. The transition itself is very fast and occurs in a 2-3 s time interval. After the transition, the single phase is clear and does not cause diffraction of light, which is a good indication that the single phase is not an emulsion. Upon cooling, the monophasic system turns back to biphasic at the same transition temperature. Apparently, the higher the PBA concentration, the lower the temperature needed to transition from biphasic to monophasic. All points in Figure 6.4 that correspond to

monophasic operation (above the dashed line) gave xylose-to-furfural selectivities ranging from 89-96%, while the reactions under biphasic operation (below the line) gave selectivities between 65-73% (Table 6.1). In neither regime a dependence of the selectivity on the PBA concentration is observed. Thus, it can be concluded that the step in the selectivity graph observed in Figure 6.3 coincides with the conversion from a two-phase to a one-phase reaction mixture, which can be viewed in Figure 6.4 as going horizontally from left to right at a reaction temperature of 180 °C.

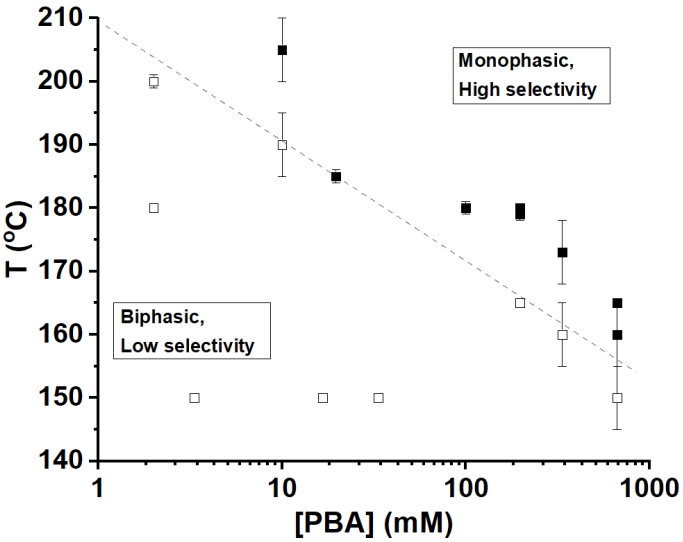

Figure 6.4 Determination (by visual inspection) of the phase behavior of the 1:1:1 toluene-sulfolane-water (pH = 1) three-solvent system as a function of the PBA concentration in the reaction mixture and the reaction temperature, in the absence of xylose. The markers represent experimental points at which the number of phases was determined, with the solid and open symbols indicating monophasic and biphasic conditions at the observation temperature, respectively. For the data points with a small error bar for the temperature, the determination of the transition was achieved applying a gradual temperature variation to the mixture in glass capillaries. In all other cases, the transition temperature was determined at a larger scale using pressure-resistant vials, with no gradual temperature variation, hence the larger error bars. The dashed line serves as a guide to the eye, indicating the transition in phase behavior.

Table 6.1 Xylose-to-furfural selectivity for a selection of points reported in Figure 6.4.

Temperature (°C)	[PBA] (mM)	X-to-F selectivity mol%
150	3.3	63
150	667	65
150	67	67
200	2	67
150	17	71
180	2	73
165	667	89
205	10	91
180	100	95
180	197	96

6.2.3 Colorimetric Study of the Relative Concentration of BBA

Increasing the temperature promotes uptake of PBA in the aqueous-organic phase just before reaching the phase switching temperature (Chapter 5, Figure 5.3b). The relative concentrations of boronic acid in the two phases, prior to the phase transition, appear to be strongly temperature-dependent. The partitioning as a function of temperature was investigated using a colored analogue of PBA, 10-bromoanthracene-9-boronic acid (BBA), which allowed us to visualize the relative concentrations from the color intensity (Figure 6.5). This analysis shows that there is a drastic increase of the boronic acid concentration in the aqueous phase at T > 150 °C. For PBA, the uptake in the water-organic solvent is probably already enhanced at lower temperature because PBA is less hydrophobic than the colored derivative, which is supported by the fact that some PBA can already be observed in the water phase at room temperature, whereas the colored one cannot. PBA in itself can be seen as an amphiphile, having an aromatic moiety that interacts well with the aromatic organic solvent, and a polar and ionizable headgroup that interacts well with water and polar solvents. The promoted dissolution of the boronic acid in the aqueous phase at elevated temperature is in part due to the increased importance of entropy on the partitioning but may also indicate an improved interaction with the water-organic mixture. This improved interaction in turn might promote the observed biphasic-to-monophasic transition. From the observed independence of the selectivity on the PBA concentration under monophasic operation mentioned before, it can be concluded that the PBA itself is present in too low amounts to affect the overall solvent polarity, so that its role is primarily in effectuating the phase transition.

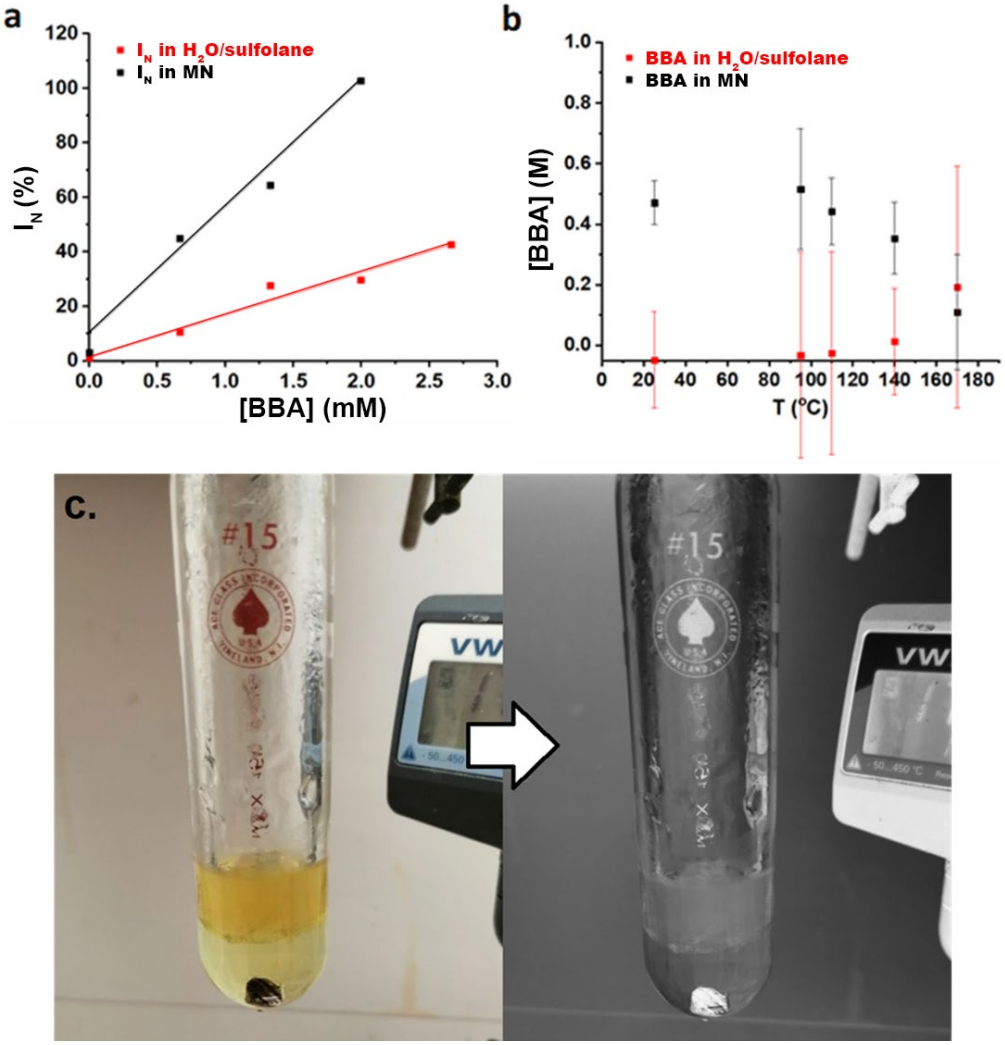

Figure 6.5 (a) Calibration curves to relate the concentration of 10-bromoanthracene-9-boronic acid (BBA) to the normalized color intensity, evaluated by analyzing photographs of the solutions with ImageJ. (b) Relative concentrations, in MN and in water/sulfolane, of BBA with increasing temperature. (c) Characteristic photographs processing for the analysis.

6.2.4 Phase Behavior Change and Water Partial Pressure

With the aim to get insight into the interactions between the three different solvents in the system and in particular about the solubilization of the water in it, eventual

anomalies in the water partial pressure as the system transitions from biphasic to monophasic were looked for. To this end, the water partial pressure at a 1:1:1 mixture of 1-methylnaphthalene, sulfolane and water (pH = 1) containing PBA at various concentrations (at 0, 23 and 117 mM in the mixture) was analyzed at temperatures ranging between 170 and 190 °C. The result of this data analysis is a P *versus* T set of average datapoints (for each PBA concentration), for each T, with SEMs both on temperature and pressure. To evaluate the deviation from the 'standard' behavior, the values at 0 mM of PBA were subtracted from the ones at 23 mM and 117 mM of PBA and plotted against T (°C) (Figure 6.6). Furthermore, to evaluate the statistical significance of this deviation, for each Δ*P* the *p*-value, *i.e.*, the probability of obtaining results at least as extreme as the observed results of a statistical hypothesis test, assuming that the null hypothesis is correct, was calculated using Equations 6.2, 6.3 and 6.4 and shown in Table 6.2.[21] First, the confidence interval (*CI*) was determined for each Δ*P*, with a confidence level of 95% (Equation 6.1).

$$CI = \frac{(\Delta P + \sigma_{\Delta P}) - (\Delta P - \sigma_{\Delta P})}{2 \cdot 1.96} \qquad \textbf{Equation 6.1}$$

Knowing *CI* and the value of Δ*P*, the *z*-value, *i.e.,* the ratio between an observed value and the confidence interval of the said value, a measure of the difference of what is observed from the mean value, was calculated in its absolute value (Equation 6.2).

$$z = \left| \frac{\Delta P}{CI} \right| \qquad \textbf{Equation 6.2}$$

Finally, using the *z*-value for each Δ*P*, the *p*-value was determined (Equation 6.3).

$$p = e^{(-0.717z + 0.416z^2)} \qquad \textbf{Equation 6.3}$$

In this study, 1-methylnaphthalene was used instead of toluene because its lower vapor pressure will not significantly mask eventual changes in the water partial pressure. A statistically significant difference in the water partial pressures between the cases with and without PBA developed once the temperature exceeded 180 °C, and the systems that contained PBA showed a slightly higher water partial pressure (Figure 6.6 and Table 6.2). This data is in agreement with the occurrence of a transition to monophasic at 180 °C, and it indicates that the monophasic mixture accommodates water less well than the polar aqueous phase under biphasic conditions. Qualitatively, the poorer accommodation of water in the monophasic case corresponds with the mixture that has to hold the water possessing a higher extent of organic solvent (comparing water in sulfolane to water in sulfolane plus 1-methylnaphthalene under biphasic and monophasic conditions, respectively).

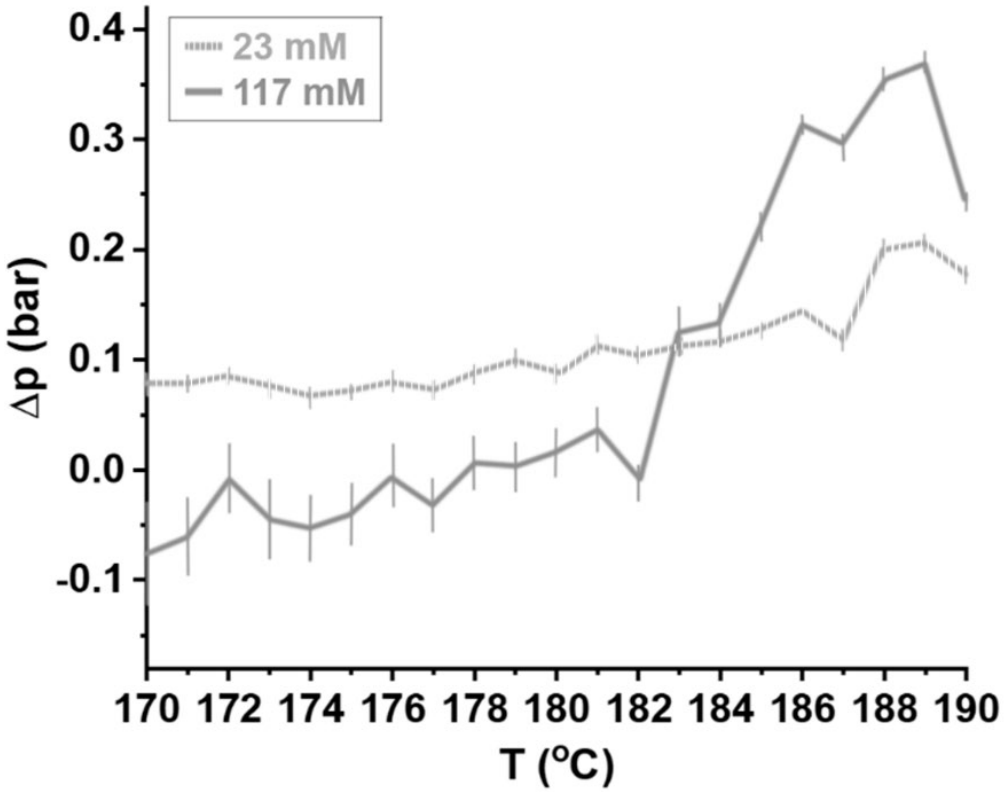

Figure 6.6 Difference in recorded pressure (Δ*P*) between the run with no PBA and the run with PBA at 23 mM and 117 mM in the temperature range between 170 and 190 °C. The error bars on Δ*P* represent the standard error of the mean (SEM). This figure shows the case in which the window was kept at 0.5 degrees.

Table 6.2 Values of Δ*P* coupled with the SEM and the respective *p*-value.

	23 mM PBA			117 mM PBA		
T (°C)	**Δ*P* (bar)**	**$\sigma_{\Delta P}$ (bar)**	***p*-value**	**Δ*P* (bar)**	**$\sigma_{\Delta P}$ (bar)**	***p*-value**
170	0.0718	0.0277	5.99E-07	-0.0816	0.0932	0.0858
171	0.0730	0.0262	7.97E-08	-0.0663	0.0721	0.0710
172	0.0793	0.0253	1.96E-09	-0.0128	0.0661	0.7171
173	0.0692	0.0283	2.26E-06	-0.0514	0.0741	0.1750
174	0.0604	0.0272	1.63E-05	-0.0588	0.0632	0.0678
175	0.0655	0.0247	3.00E-07	- 0.0461	0.0582	0.1209
176	0.0742	0.0258	3.14E-08	-0.0105	0.0592	0.7406
177	0.0666	0.0236	5.59E-08	-0.0374	0.0517	0.1571
178	0.0811	0.0243	1.56E-10	0.0014	0.0524	0.9617
179	0.0959	0.0241	4.20E-14	-0.0030	0.0513	0.9170
180	0.0824	0.0239	4.25E-11	0.0100	0.0476	0.6926
181	0.1086	0.0235	1.92E-18	0.0314	0.0434	0.1561
182	0.0989	0.0235	1.57E-15	-0.0172	0.0379	0.3789
183	0.1077	0.0214	2.04E-21	0.1199	0.0469	8.2052E-07
184	0.1133	0.0208	1.38E-24	0.1288	0.0379	8.2114E-11
185	0.1213	0.0202	1.72E-29	0.2161	0.0295	2.3216E-42
186	0.1390	0.0208	1.01E-35	0.3088	0.0254	1.355E-110
187	0.1118	0.0244	4.35E-18	0.2884	0.0271	8.5617E-86
188	0.1966	0.0227	5.63E-58	0.3503	0.0265	6.917E-130
189	0.2015	0.0214	7.54E-68	0.3658	0.0246	1.663E-163
190	0.1707	0.0255	6.63E-36	0.2378	0.0253	6.5834E-68

6.2.5 Effects of Water Contents and Solvent Composition

To further characterize the effects of solvent composition on the system, experiments were performed keeping the aqueous phase (at pH = 1), but varying the polar and apolar organic solvents to compose the final three-solvent system, at a constant reaction temperature of 180 °C (Table 1; full xylose conversion was always achieved). The behavior of the different solvent mixtures containing toluene and a polar organic solvent shows a clear qualitative difference at room temperature and at the reaction temperature. However, all these systems are biphasic at room temperature the relative volumes of the two phases differ from system to system. Dioxane partitions equally between water and toluene, ɣ-valerolactone (GVL) mixes exclusively with toluene, and DMSO and sulfolane mix exclusively with water. This behavior relates well to the relative polarities of the organic solvents expressed *e.g.*, in terms of water-octanol partition coefficient log*P* (Table 6.3).

Table 6.3 Xylose-to-furfural selectivity at full xylose conversion in various 1:1:1 apolar-polar-aqueous three-solvent systems (180 °C, pH = 1). In all cases the reaction was stopped at a time point shortly after full xylose conversion. The solvent polarity of the polar solvent is represented here by the water-octanol partition coefficient (-log*P*). The column named 'NoP' refers to the number of phases at the reaction temperature.

Apolar solvent	Polar solvent	-log*P*	NoP	Sel.[a]	t (h)
Toluene	DMSO	1.35	1	90	3
Toluene	Sulfolane	0.77	1	95	3.5
Toluene	Dioxane	0.42	2	60	3
Toluene	GVL	0.27	2	65	4
Nitrobenzene	DMSO	1.35	1	95	2
MN	DMSO	1.35	1	87	3
MN	Sulfolane	0.77	1	89	3.5

[a] Selectivity expressed in mol%.

The choice of the polar solvent shows to be a crucial variable, with high selectivities obtained in the case of the most polar solvents, DMSO and sulfolane, and lower selectivities obtained in the case of the less polar ones, dioxane and GVL. When keeping the polar organic solvent sufficiently polar, changing the aromatic counterpart did not seem to affect the final selectivity as much. These results further underline the results shown above that the crucial element influencing the xylose-to-furfural selectivity is the presence of a polar organic solvent in combination with an aromatic one so that a three-solvent mixture is obtained, that transitions to monophasic at the reaction temperature, which is indeed observed in the case of DMSO and sulfolane, but not in the case of dioxane and GVL. The case of 1-methylnaphthalene-sulfolane-water (pH = 1) is specifically valuable as it allows easy distillation of furfural from the solvent mixture (specifically, 1-methylnaphthalene and sulfolane, obtained after phase separation achieved by cooling the reaction mixture), and it will be discussed in the process concept below. These results relate well with literature, in which most organic solvents and solvent mixtures show to favor high furfural selectivity.[14-17] Comparing different solvent systems for xylose dehydration shows that fully organic (monophasic) and mostly organic transient monophasic conditions perform better than traditional biphasic conditions. Specifically, using a 1:1 mixture of water and 1-butanol, which is monophasic above 125 °C, for performing xylose dehydration to furfural results in an approx. 8 mol% selectivity improvement from traditional biphasic conditions (Table 6.4). Closest to our finding, Román-Leshkov and Dumesic showed that, also in the case of fructose dehydration to HMF, an improvement in selectivity was observed when using a water/1-butanol system.[13] Overall, the comparison shows that the three-

solvent system proposed in this work gives a better furfural selectivity at milder temperatures than any of the systems reported earlier.[14-17,22]

Table 6.4 Comparison of literature data about xylose dehydration performed in different solvent systems and the results obtained in this work using transient monophasic systems. Complete xylose conversion is reached in all cases. The column named 'N' refers to the number of phases at the reaction temperature.

Solv. 1	Solv. 2	Solv. 3	N	v:v	Cat.	S[a]	[X][b]	T[c]	Ref.
Water			1		H_2SO_4	45	350	200	2
DMSO			1		MCM-SO_3H	82	600	140	3
Water	Toluene		2	1:1	H_2SO_4	69	175	200	Ch. 3
Water	DMSO		1	1:1	$SnCl_4$/LiCl	60	100	140	4
Water	1-Butanol		1	1:1	H_2SO_4	77	175	200	here
Water	DMSO		1	1:1	H_2SO_4	79	97	180	here
Water	Sulfolane		1	1:1	H_2SO_4	80	97	180	here
Water	Toluene	Sulfolane	1	1:1:1	H_2SO_4	95	97	180	here

[a] Selectivity expressed in mol%.

[b] Concentration expressed in mM.

[c] Temperature expressed in mM.

The water content and the apolar nature of the phase in which the dehydration takes place, appear to affect the xylose-to-furfural selectivity, as has also been reported for related systems. For instance, molecular dynamics simulations on the interaction of sugars (*e.g.*, glucose) in progressively more organic solvent mixtures of water with DMSO, THF and DMF, reveal that these solvents compete with water in forming the first solvation shell around the sugar, even when added in relatively low amounts (< 40-50 v%).[23] This promotes the dehydration of sugars by altering the relative stability of initial and transition states.[14-17,24,25] Additionally, high amounts of polar organic co-solvent are reported to form water-rich local domains, influencing the energy barrier for the reaction.[26] These findings agree qualitatively with our high selectivity observed when increasing the fraction of organic solvent after the transition to monophasic. On the other hand, it is difficult to rationalize solely by the water content why our monophasic operation, with one-third water in the mixture, performs also better than in a polar-organic solvent/mixture with less water. Yet, selectivity is also and foremost controlled by the good solubilization and protection of the produced furfural and by suppression of the formation of humins. Possibly, the reaction operates under more apolar conditions, by merging not only more water but also a more apolar organic solvent into the mixture, than is achieved in the polar-organic case. Such an enhanced apolar character of the phase in which the dehydration occurs, would favor solubilization and stabilization of the furfural, as well as a concomitantly better

suppression of the formation of acyclic sugar, both leading to a better selectivity. Furthermore, control experiments show that performing the reaction in monophasic 1:1 DMSO-water or sulfolane-water systems, without the aromatic solvent but with the same initial PBA_2X concentration, leads to lower xylose-to-furfural selectivities (Table 6.4), confirming that the apolar nature of the mixture is important as well, not just the water content in it.

6.2.6 Conceptual Integration of Xylose Extraction and Monophasic Conversion into a Furfural Manufacturing Process

The three-solvent xylose-to-furfural conversion can be combined with a xylose-boronate ester extraction approach, to convert diluted xylose hydrolysate to furfural at high yield and with low energy demand. For the purpose of this study, a hydrolysate stream containing 4-5 w% of xylose is chosen, as encountered in industrial processing of biomass. Operating at higher xylose concentration is not favorable because it requires reconcentration of the xylose syrup and results in a lower xylose-to-furfural selectivity. In a first step, the xylose is extracted as the boronate diester by contacting the hydrolysate with a 1-methylnaphthalene (MN)/PBA solution. The resulting organic/boronate diester solution is mixed with an acidic sulfolane/water solution and heated to the reaction temperature to hydrolyse the ester and convert the released xylose into furfural. Sulfolane is chosen over DMSO due to its higher stability at high temperature.[27] The reactor effluent is then cooled to allow phase separation into a MN/PBA/furfural organic phase and a sulfolane/water/furfural phase. The furfural is separated from the organic phase by means of distillation, resulting into a furfural distillate, *i.e.*, the desired product stream, and a MN/PBA bottom stream, which is to be recycled to the xylose extraction column. The sulfolane/water phase is sent to a distillation column to remove the unrecovered furfural before recycling it to the dehydration reactor. Indeed, much of the unextracted furfural can be distilled off as heterogeneous azeotrope with water that spontaneously splits into a water phase containing 8 w% furfural and a furfural phase containing 6 w% water.[1,28] It is worth noting that this scheme does not require deep furfural recovery from the aqueous phase since some furfural can be recycled back to the dehydration step. The water product stream will need to be recycled to balance the water consumed to hydrolyze PBA_2X to free xylose (Figure 6.7).

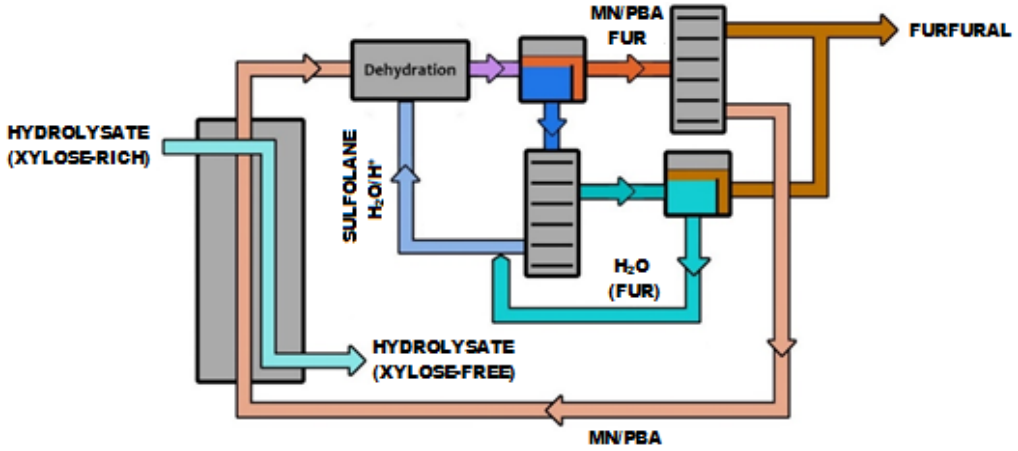

Figure 6.7 Conceptual process for the two-step furfural production based on the integration of xylose extraction as the boronate diester from an acidic hydrolysate followed by conversion of the xylose into furfural in a highly efficient monophasic three-solvent mixture.

The viability of this process concept will depend on the efficiency in closing the two recycle streams. Most critically, it will not allow significant losses of MN, PBA and sulfolane in the clean hydrolysate. To this end, it will not allow significant slip of sulfolane into the MN/PBA phase of the decanter, as eventual sulfolane contamination will likely end up in the clean hydrolysate stream. If the losses of sulfolane, MN and PBA are not negligible, a small finishing step is to be considered, *e.g.*, by adsorption, to further purify the clean hydrolysate and recover the lost sulfolane, MN and PBA. It has to be noted that the sequence of xylose extraction followed by dehydration allows to leave a number of hydrolysis by-products in the hydrolysate and, thereby, to produce furfural with a much higher purity. Boric acid has indeed been shown to extract xylose with high selectivity and leave behind most of the hexoses impurities and the acetic acid that are also formed during the hydrolysis step, limiting the efforts in the purification of both reagent and product stream.[29]

6.2.6.1 Partition in the Decanter

The product work-up section is dictated by the behavior of the liquid/liquid split of the different components (Table 6.5). The phase separation was found to develop swiftly. The distribution of the main components (produced furfural, the three solvents and PBA) in the three-solvent system was analyzed by preparing a MN solution of furfural (350 mM) and PBA (590 mM) to model the reaction effluent. 1 mL of this solution was then contacted with 2 mL of a 1:1 (v/v) mixture of water (pH = 1) and sulfolane. Accordingly, about 40% of the furfural was found in the MN-rich phase together with

minor amounts of sulfolane (7% on intake) and water. The water/sulfolane phase contained then the remaining 60% of the furfural, together with modest amounts of PBA and negligible amounts of MN that will eventually build-up to steady-state in the recycle loop. These two phases need to be worked up to recover the furfural, recycle the sulfolane and MN/PBA, and eliminate excess water formed by the dehydration reaction.

Table 6.5 Partitioning of the various system components and losses in a 1:1:1 (v/v/v) MN/sulfolane/water (pH = 1) solvent system.

Component	$[conc]_{wat+S}$	$[conc]_{MN}$	$w\%_{wat-S}$	$w\%_{MN}$	K_d[a] [X]	P_{mol}[b]
Furfural	103 mM	144 mM	0.88	1.3	0.72	1.43
Water	27.6 M	92 mM[c]	44	0.15[c]	300	601
Sulfolane	5.1 M	370 mM	54	4.0	27.3	13.8
PBA	125 mM	340 mM	1.3	3.7	0.37	0.74
MN	3 mM	7.0 M	0.04	91	0.0004	0.0009

[a] Water/organic partition, as the volume of the polar phase is the double of the apolar one, this value implies a dilution.

[b] This water/organic partition factor considers the amounts (in mmol) in the phases and not the concentrations, correcting for the fact that the polar phase is twice the volume of the apolar one.

[c] A non-negligible amount of water is dispersed in the MN phase.

6.2.6.2 Furfural Recovery

Considering atmospheric boiling, furfural could easily be distilled off from the MN/PBA phase. This can be visualized by evaluating the distillation resistance of a specific species from a certain solvent.[29] The distillation resistance (Ω) from 1-methylnaphthalene, taking in account the w% of furfural in the phase, is Ω = 0.0157 °C^{-1}. Taking into account the evaluated w% of water mentioned in Table 6.5, the distillation resistance grows to Ω = 0.0167 °C^{-1}. These distillation resistances are negligible, as industrial distillation trains can typically work up to Ω = 10-15 °C^{-1}.[30] The entrainment of some sulfolane (4 w%) in the MN/PBA phase should not affect the distillation since sulfolane also has a higher boiling point than furfural. Recovering furfural from the aqueous/sulfolane phase is more challenging. However, much could be distilled off as an azeotrope with water, likely together with excess water which boils just a few degrees higher than the water/furfural azeotrope.[1] Alternatively, furfural could be extracted by repurposing the clean MN/PBA. Control experiments showed that five extractions of the polar phase with a clean aromatic phase (MN) resulted in an approx. 90 mol% recovery of furfural. Furfural will be recovered to the extent that is

economically attractive, and the remaining fraction will be recycled to the dehydration reactor.

6.2.6.3 MN/PBA Recycle

The MN/PBA that comes out from the furfural distillation column as the bottom stream can be directly recycled to the extraction column. There, the hydrolysate could extract, dissolve and entrain some of the MN, PBA and sulfolane present in the recycle stream. The loss of MN and PBA will be negligible, considering their low solubility limits in water (0.003 w% and 1 w%, respectively). Minor amounts of sulfolane will likely get be extracted by the hydrolysate, considering the high water/MN partition coefficient seen in Table 2. If economically critical, the sulfolane and PBA lost in the hydrolysate could be recovered by adsorption over a bed of active carbon. Of course, the boronic acid of choice could still be modified to lower its solubility in water and, thereby, its loss in the hydrolysate.

6.2.6.4 Sulfolane Recycle

Recycling most of the sulfolane does not present significant challenges. Once most of the furfural is distilled off together with excess water, the sulfolane/water (pH = 1) bottom stream can be directly recycled to the dehydration reactor. Small amounts of furfural and MN will not affect the reaction operation and will eventually build up to a steady state. The application of such a process concept promises the production of furfural with a selectivity approx. 20 mol% higher than traditional industrial approaches, thus providing less waste.[1]

6.2.6.5 Preliminary Economics

The process concept prosed here delivers a higher selectivity in furfural than the alternative concept based on dehydration in a single-phase aqueous medium or dehydration in biphasic water/organic media. However, the selectivity improvement is accompanied by an increase in process complexity to close the various recycles. It should then be investigated whether the selectivity benefit is likely to pay for the increased process complexity.

Very preliminary, though insightful calculations have been developed to answer this question. They have been based on approach for preliminary economic screening proposed by Lange *et al.*,[31] and formulated as balancing the incomes and costs of the process according to the Equation 6.4.

$$Yield_{product} * Price_{product} > Price_{feed} + Cost_{conversion} \quad \textbf{Equation 6.4}$$

With the yield expressed as a ration of the tons of product over the ones of feed and the prices and costs expressed in $/ton. First, the equation was used to estimate the price of xylose. Single-step biomass pretreatment is assumed, with the production of a cellulosic pulp and aqueous xylose stream with 60 w% carbohydrate yield with a standard conversion cost of 200 $/ton feed. The calculated carbohydrate cost is of 467 (±98) $/ton, which is set to be equal for the pulp and the xylose by assuming that both would share the same outlet, *e.g.,* fuel ethanol after hydrolysis of the cellulose/xylose mixture followed by co-fermentation. Such carbohydrate price is clearly higher than the ~300 $/ton encountered for sugar syrup derived from starch or sugar crops. However this is consistent with the fact that cellulosic ethanol is more expensive than crop ethanol.

This xylose price is then used together with furfural market price of 1400 $/ton and furfural yield of 70 and 95 mol%, *i.e.,* 45 and 61 w%, to estimate the maximal conversion cost that it can be afforded using the equation above. With 70 mol% xylose-to-furfural selectivity, the biphasic process is estimated to afford a conversion cost of 161 (±140) $/ton, which falls within the range of a single process step. Hence, the biphasic process has reasonable chances of being affordable. Interestingly, the 95 mol% yield of the xylose extraction concept could afford a conversion cost of 385 (±162) $/ton, *i.e.,* could afford about two process steps instead of one. The overall conversion cost advantage amounts to 224 (±22) $/ton, with a small uncertainty that results from the fact that the uncertainties of both scenarios are fully correlated; both need to use the same high/low xylose and furfural prices. The premises used for these calculations are summarized in Table 6.6.

Table 6.6 Premises for preliminary economics.

	Unit	Value	Comment/source
Biomass price	$/ton	80 (±20)	
Furfural price	$/ton	1400 (±200)	
Conversion cost	$/ton	200 (±50)	For a single process step
Carbohydrate yield	w% on biomass	60 (±5)	
Furfural yield	w% on xylose	45 (±3)/61 (±3)	Based on yields of 70/95 mol%, resp.

6.3 Conclusions

This Chapter demonstrates the possibility to convert xylose-diboronate ester, the product of xylose extraction, to furfural with > 90 mol% yield by applying a three-solvent system that forms a single phase at the reaction temperature. Obtaining a single phase appeared essential to obtain the high selectivity, and its occurrence is

dependent on PBA concentration and temperature. Interaction between PBA and the aromatic solvent is a likely trigger for the phase transition. Although not fully clear, the increased apolar nature of the solvent mixture in which the dehydration occurs, achieved upon monophasic operation, contributes to the observed improved selectivity. High selectivities, at and above approx. 90 mol%, become feasible with a variety of solvent combinations and PBA concentrations. Specifically, the highest xylose-to-furfural selectivity (95 mol%) is obtained in a 1:1:1 sulfolane-toluene-water (pH = 1) system, using a PBA diester of xylose as the starting compound. The reaction conditions allow the use of solvents that ease the furfural recovery by splitting into two liquid phases upon cooling and allow easy distillation of the furfural from the media. A conceptual process design for furfural production, based on these findings, and a further analysis of the various losses and a preliminary economic analysis, have been presented. This approach is potentially preferable to conventional biphasic systems (due to the high selectivity) and to the alternative monophasic organic operation (due to the minimal distillation duties required). The produced furfural can be recovered from the system with negligible losses of the solvents in the product and waste streams, and thus this process design minimizes waste and maximizes recyclability. Additional research is needed to validate and upscale such process design, with the possibility of implementing the use of biobased and fully biodegradable solvent alternatives.[20]

6.4 Experimental Section

6.4.1 Chemicals

D-(+)-Xylose (>99%), D_2O (99.9% atom D), toluene-d_8 (99% atom D), dioxane (99.8%), 3-(trimethylsilyl)propionic-2,2,3,3-d_4 acid sodium salt (TMSP, 98% atom D), dimethylsulfoxide (DMSO, 99%), sulfolane (99%), 10-bromoanthracene-9-boronic acid (BBA, 99%), ɣ-valerolactone (GVL, 99%), nitrobenzene (99%), 1-butanol (98%), 1-methylnaphthalene (98%) were purchased from Sigma-Aldrich, while phenylboronic acid (PBA, 99%) and tetramethylsilane were obtained from Alfa Aesar. PBA_2X was obtained as described in Chapter 5.

6.4.2 Methods and Equipment

All chemicals were used without further purification. ^{1}H-NMR spectra were recorded as in Chapter 3, with tetramethylsilane as an additional standard in case of the organic phases. In all cases the reactions were performed using a heating mantle, stirring was done with a magnetic stirrer at 1000 rpm.

6.4.3 Xylose Conversion to Furfural

A 1:1:1 v/v/v solvent mixture (each 2 mL) of an aromatic solvent (toluene, nitrobenzene, or 1-methylnaphthalene), a polar organic solvent (DMSO, sulfolane, GVL, or dioxane) and water (pH = 1 from added H_2SO_4), containing a total concentration of xylose of 97 mM (either in its free form or as PBA diester) was heated between 150 °C and 205 °C, for reaction times varying between 0.5 and 16 h. In the case of the experiments performed with free xylose as a starting material, PBA was also added to the mixture, at concentrations between 0 mM and 667 mM. To ensure maximum comparability between all the various experiments, the same total amount of solution (6 mL) was always used. Alternatively, 2 mL of an aqueous xylose solution (350 mM, pH = 1 from H_2SO_4) was mixed with 2 mL of a polar organic solvent (1-butanol, DMSO, sulfolane) and heated at temperatures between 180 °C and 200 °C between 3 and 5 h. Prior the analysis with ^{1}H-NMR spectroscopy, all the reactions were stopped and cooled to room temperature.

6.4.4 Determination of the Phase Behavior of the Three-Solvent System

A Pyrex capillary tube was filled with equal volumes of a PBA solution in toluene (from 6 mM to 750 mM), sulfolane and water (pH = 1 from H_2SO_4) for a total volume of approx. 1 mL. The capillary was sealed with a blowtorch (oxyacetylene flame), cooled to room temperature and then put into an oven, where the temperature was accurately controlled (from 25 °C to 220 °C). The observed transition from biphasic to monophasic was photographed and filmed. Alternatively, the same solvent mixture, for a total volume of 6 mL, was placed in a high pressure-proof hard glass vessel (ACE Glass Incorporated) and heated using a heating mantle (from 140 °C to 210 °C). In this case, the assessment of the phase behavior is less precise and resulted in a wider range of temperatures for the transition to occur.

6.4.5 Colorimetric Analysis of BBA Concentration

5 mL of various solutions with BBA concentrations between 0.6 M to 2.6 M, both in MN and in a 1:1 sulfolane-water (pH = 1) mixture, were heated up to 180 °C. A 1:1:1 solvent mixture (each solvent 2 mL) of 1-methylnaphthalene, sulfolane, and water (pH = 1) containing 0.5 M of BBA was heated between 25 and 180 °C. Photographs of these solutions were taken, at the mentioned temperature using the integrated camera of a smartphone and analyzed in ImageJ. The relative intensity (I) of the portion of the picture under analysis was evaluated using the function “histograms” of ImageJ. Each photograph was imported in ImageJ and the image type was changed from RGB to 8xbit, to eliminate the effect of the hue on the analysis. The picture was then inverted, to maximize the difference in intensity between signal and background (Figure 6.5c).

The normalized intensity (I_N) was calculated as a difference of the area in which the signal and the background are expected, both divided by the value of the background (I_{BG}), to minimize the picture-to-picture fluctuations in luminosity and exposure (Equation 6.5).

$$I_N = 100 \cdot \left(\frac{I_{BBA}}{I_{BG}} - 1\right) \qquad \textbf{Equation 6.5}$$

The standard error on the said intensity was evaluated dividing the standard deviation by the square root of the number of pixels of the selection, both of which are obtained as raw data from ImageJ. In the calibration process, each of these values was coupled to a known concentration, and these relationships were used to obtain a linear fit, to evaluate of the concentrations in the cases under analysis. The errors on each measurement were evaluated using standard error propagation theory.

6.4.6 Evaluation of the Partial Vapor Pressure of Water

Three different 1:1:1 solvent mixtures (each solvent 25 mL) of 1-methylnaphthalene, sulfolane, and water (pH = 1) containing 0 mM, 23 mM or 117 mM of PBA were heated from 25 °C to 190 °C in an autoclave reactor of 200 mL, equipped with a pressure sensor and two thermocouples (one to measure the temperature of the liquid phase, one to measure the temperature of the gas phase). Temperature and pressure were monitored continuously in a time window between 3 and 5 h. All measurements were performed three times. The obtained data were analyzed using MatLab. The raw data for the 3 different runs at each concentration were grouped together in a P *versus* T array. A temperature window of 0.5 °C was applied to the data set to divide the data in small groups (*e.g.*, all the data between 99.5 °C and 100.5 °C were grouped together and labeled "100 °C"). These data subgroups were averaged. The standard errors of the mean (SEM) of the subgroups were also evaluated. As every T point is related to a P value, the same procedure was also applied point by point to the pressure dataset.

6.5 References

1. J.-P. Lange, E. van der Heide, J. van Buijtenen, R. Price, *ChemSusChem* **2012**, *5*, 150-166.
2. R. Mariscal, P. Maireles-Torres, M. Ojeda, I. Sádaba, M. López Granados, *Energy Environ. Sci.* **2016**, *9*, 1144-1189.
3. M. M. Antunes, S. Lima, A. Fernandes, M. Pillinger, M. F. Ribeiro, A. A. Valente, *Appl. Catal. A* **2012**, *417–418*, 243–252.
4. P. Priecel, J. E. Perez Mejia, P. D. Carà, J. A. Lopez-Sanchez, *Green Chem.* **2018**, *596*, 243-299.
5. Y. Román-Leshkov, J. N. Chheda, J. A. Dumesic, *Science* **2006**, *312*, 1933-1937.

6. F. Delbecq, Y. Takahashi, T. Kondo, C. C. Corbas, E. R. Ramos, C. Len, *Catal. Commun.* **2018**, *110*, 74-78.
7. R. Weingarten, J. Cho, W. C. Conner, Jr., G. W. Huber, *Green Chem.* **2010**, *12*, 1423-1429.
8. G. G. Millán, S. Hellsten, A. W. T. King, J.-P. Pokki, J. Llorca, H. Sixta, *J. Ind. Eng. Chem.* **2019**, *72*, 354-363.
9. A. Parejas, V. Montes, J. Hidalgo-Carrillo, E. Sánchez-López, A. Marinas, F. J. Urbano, *Molecules* **2017**, *22*, 2257-2275.
10. B. Li, S. Varanasi, P. Relue, *Green Chem.* **2013**, *15*, 2149-2157.
11. Y. Nie, Q. Hou, W. Li, C. Bai, X. Bai, M. Ju, *Molecules* **2019**, *24*, 594-612.
12. C. Lansalot-Matras, C. Moreau, *Catal. Commun.* **2003**, *4*, 517– 520.
13. Y. Román-Leshkov, J. A. Dumesic, *Top Catal.* **2009**, *52*, 297-303.
14. L. Shuai, J. Luterbacher, *ChemSusChem* **2016**, *9*,133–155.
15. B. R. Caes, R. T. Raines, *ChemSusChem* **2011**, *4*, 353–356.
16. A. H. Motagamwala, K. Huang, C. T. Maravelias, J. A. Dumesic, *Energy Environ. Sci.* **2019**, *12*, 2212—2222.
17. A. H. Motagamwala, W. Won, C. Sener, D. Martin Alonso, C. T. Maravelias, J. A. Dumesic, *Sci. Adv.* **2018**, *4*, 9722-9730.
18. A. S. Dias, M. Pillinger, A. A. Valente, *J. Catal.* **2005**, *229*, 414–423.
19. W. Wang, H. Li, J. Ren, R. Sun, J, Zheng, G. Sun, S. Liu, *Chin. J. Catal.* **2014**, *35*, 741–747.
20. F. Gao, R. Bai, F. Ferlin, L. Vaccaro, M. Li, Y. Gu, *Green Chem.* **2020**, *22*, 6240-6257.
21. J.-T. Lin, *Appl. Statist.*, **1989**, *38*, 69-70.
22. C. Sener, A. H. Motagamwala, D. Martin Alonso, J. A. Dumesic, *ChemSusChem* **2018**, *11*, 2321 –2331.
23. V. Vasudevana, S. H. Mushrif, *RSC Adv.* **2015**, *5*, 20756-20763.
24. M. A. Mellmer, C. Sanpitakseree, B. Demir, P. Bai, K. Ma, M. Neurock, J. A. Dumesic, *Nat. Catal.* **2018**, *1*, 199–207.
25. J. J. Varghese, S. H. Mushrif, *React. Chem. Eng.* **2019**, *4*, 165-206.
26. T. W. Walker, A. K. Chew, H. Li, B. Demir, Z. C. Zhang, G. W. Huber, R. C. Van Lehn, J. A. Dumesic, *Energy Environ. Sci.* **2018**, *11*, 617-628.
27. D. L. Head, C. G. McCarty, *Tetrahedron* **1973**, *16*, 1405-1408.
28. I. Agirrezabal-Telleria, I. Gandarias, P.L. Arias, *Bioresour. Technol.* **2013**, *143*, 258–264.
29. R. Xing, W. Qi, G. W. Huber, *Energy Environ. Sci.* **2011**, *4*, 2193-2205.
30. J.-P. Lange, *ChemSusChem* **2017**, *10*, 245–252.
31. J.-P. Lange, *Catal. Sci. Technol.* **2016**, *6*, 4759–4767.

Chapter 7

Effect of Ionic Strength on Furfural Synthesis – Process Concept and Kinetic Modeling

The effects of ionic strength on the dehydration of xylose, applied as the diester with phenylboronate, PBA (PBA_2X), to furfural under biphasic conditions have been explored to maximize the xylose-to-furfural selectivity and to allow implementation in an industrial process. Experimental results obtained in reactions at 200 °C in a 1:1 v/v organic-aqueous biphasic system (composed of either 1-methylnaphthalene (MN) or toluene and water at pH = 1 from H_2SO_4) indicate an increased xylose-to-furfural selectivity (from approx. 70 mol% to approx. 90 mol%) when increasing the ionic strength (by addition of Na_2SO_4) from 0.1 M to 6.1 M. Comparing the reactivity of PBA_2X to free xylose at the same ionic strength of 3.1 M shows a xylose-to-furfural selectivity increase from approx. 75 mol%, when starting from free xylose, to 88 mol%, when starting from PBA_2X. The effect of the sulfate anion is compared to that of chloride, showing little to no difference both in the conversion rate and in the selectivity. Switching from mono- to divalent cations exhibited an increase in the rate of conversion, but no effect on the selectivity. Based on the experimental data, a process concept is proposed, which combines xylose extraction from a xylose-rich biomass hydrolysate industrial feed with selective furfural production at high-ionic strength biphasic conditions (using MN as organic solvent). The validity of the process concept is supported by additional data on partitioning, which show that a product stream can be created by means of distillation. The losses in the process cycle are found to be marginal. Furthermore, this study includes a kinetic model that comprehensively describes the dehydration of xylose from PBA_2X taking into account all the steps of the process (hydrolysis, partitioning and dehydration), to pin-point the effect of changing the nature of the solvent system (different solvents and ionic strengths) and the interaction between the two phases (various mixing conditions) on each of these steps. Moreover, this model allows to simulate the evolution of the concentrations of all relevant species in the system, at various reaction conditions, providing further insight into the mechanism. Both the experimental data and the model confirm that, at high ionic strengths, starting from PBA_2X results in higher xylose-to-furfural conversions and selectivities when compared with using free xylose as a starting material. This is possibly ascribed to effects on the sugar conformation when obtained from the hydrolysis of PBA_2X. In overview, these results promise an industrial implementation of high ionic strength biphasic operations, which result in a high xylose-to-furfural selectivity.

7.1 Introduction

Optimizing the conditions of the dehydration of xylose to furfural, to increase the xylose-to-furfural selectivity, is of key importance in the field of biomass processing and biofuel production.[1-3] The benchmark of this selectivity improvement is the acid-catalyzed reaction, run at fully monophasic aqueous conditions, which results into a xylose-to-furfural selectivity of approx. 45-50 mol%.[1-3] Generally, as discussed also in Chapter 4, this selectivity can be improved up to 65-70 mol% by moving from fully aqueous monophasic to aqueous-organic biphasic conditions, due to the continuous extraction of the newly formed furfural into the organic phase (*e.g.,* toluene or 1-methylnaphthalene).[1,4]

Both under monophasic and biphasic conditions , the addition of inorganic salts to the aqueous phase results in higher xylose conversion rates and improved xylose-to-furfural selectivities.[5-11] Specifically, using aqueous solutions of inorganic salts affects the reaction mechanism and its kinetics in comparison with pure water.[8,9] Both the rate of xylose consumption and that of furfural production increase upon salt addition, and different salts result in different maximal xylose-to-furfural selectivities.[8.9] In the case of halide salts, these effects are dependent both on the cation and the anion.[7-14] It has also been reported that divalent cations interact more strongly with saccharides than monovalent ones.[15,16] Combs *et al.* report that alkaline earth metal cations interact with glucose, forming bidentate complexes, which accelerated its transformation.[17] In the specific context of biphasic operation, the presence of salt in the aqueous phase will also alter the partitioning of the newly formed furfural, with a positive effect on its reactive extraction and hence its selectivity.[18,19]

However, industrial application of solvent systems with added salt is limited, as the addition of salt to the xylose-rich hydrolysate stream would make later separation from the water phase challenging, impairing the salt recyclability and the treatment of the waste water, prior to disposal.[1,20] One way to solve this problem is to selectively remove xylose from the sugar-hydrolysate, to isolate the hydrolysate stream from the reaction step. Chapter 5 has shown the development of a process for the liquid-liquid extraction of xylose from a sugar-rich hydrolysate stream by the formation of an organic-soluble diester of xylose (X) and phenylboronate (PBA), PBA_2X, under acidic biphasic conditions. In all the previously mentioned studies, the starting material used is free xylose in water.[5-19]

This Chapter explores the combination of the extraction process described in Chapter 5 and biphasic operation, employing a aqueous phase at high ionic strength, with the aim to boost the xylose-to-furfural selectivity and enable salt recycling. The working hypothesis is that moving from low to high ionic strength, by adding salt to PBA_2X in an

aqueous-organic biphasic system, will affect the partitioning of both furfural and PBA_2X between the two phases, as well as the release of xylose in the aqueous phase, both with a positive effect on selectivity. High ionic strengths are obtained using sulfate salts of both mono- and divalent cations but also chlorides that are more widely studied in literature.[9,12] Based on these findings, an initial process concept that implements the xylose extraction from lignocellulosic hydrolysate is provided. Furthermore, a model encompassing both kinetic and thermodynamic aspects is formulated to rationalize the effects of ionic strength, solvent system and mixing on the various steps of the mechanism of xylose dehydration from PBA_2X.

7.2 Results and Discussion

The dehydration of xylose, starting from PBA_2X in a biphasic system was conducted at different ionic strengths of the water phase. Using the PBA_2X diester as the starting material adds a hydrolysis step in the reaction scheme (Scheme 7.1), needed to liberate the xylose into the aqueous phase, which will then undergo acid-catalyzed dehydration. Adding salt to the reaction mixture influences not only the process of xylose dehydration and the partitioning of furfural between the two phases, but also the equilibrium of the formation/hydrolysis of PBA_2X, thus affecting the reaction kinetics. This is visualized in Scheme 7.1 using colored arrows, green for the steps that are positively influenced by the presence of salt, red for the one that is negatively influenced. Specifically, each mole of PBA_2X hydrolysis in water requires four moles of water to obtain free xylose and PBA, this is disfavored as high salinity results in a decreased water activity.[21,22] On the contrary, the reaction of xylose dehydration produces three moles of water per mole of xylose, and it is promoted at high salt concentrations. In practice, the partition coefficient for the diester cannot be measured and, therefore, the partitioning + formation/hydrolysis of the diester need to be combined when modeling the kinetics of the process (see below).

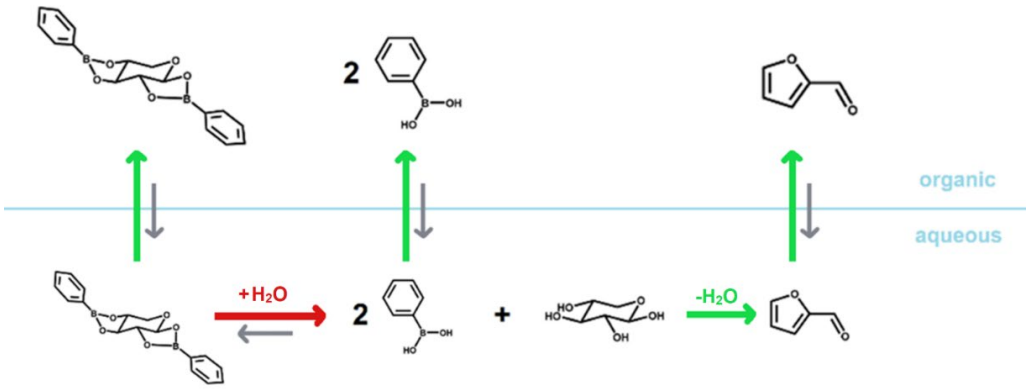

Scheme 7.1 Reaction scheme for the dehydration of xylose, starting from PBA_2X, to furfural in a biphasic system. Green arrows represent the steps that are positively influenced by the presence of salt, red arrows represent steps that are negatively influenced by the presence of salt.

7.2.1 Effect of Adding Salt to the Aqueous Phase

The dehydration of xylose, using PBA_2X as the starting material, was performed at 200 °C and at different ionic strengths of the water phase reached by adding Na_2SO_4 in a 1:1 v/v water-toluene biphasic system (pH = 1 from H_2SO_4, ionic strength 0.1 M). Specifically, the experiments were performed at ionic strengths of 0.1 M (no salt), 1.6 M, 3.1 M and 6.1 M. The conversion rate and the selectivity were assessed by measuring the concentrations of furfural and unreacted xylose (in free form and diester form) in the crude reaction mixture by ^{1}H-NMR spectroscopy. All reactions were followed in a time window of 4 h. In this chapter, salt concentrations are reported using ionic strength, *I* (Equation 7.1), which incorporates both the concentrations and the valences of the ions.

$$I = \frac{1}{2}\sum_{i=1}^{n} c_i z_i^2 \qquad \textbf{Equation 7.1}$$

Here c_i is the molar concentration of the ion *i* (M), and z_i is its valence.

Figure 7.1 (panels a to d) shows the overall xylose conversion, based on the concentration of PBA_2X in the organic phase and free xylose in the aqueous one, the yield of furfural, obtained from the concentration of furfural in both phases, and the xylose-to-furfural selectivity, calculated from the ratio of furfural yield and xylose conversion, at different ionic strengths. In general, increasing the ionic strength results into two main trends: the xylose-to-furfural selectivity increases from approx. 70 to 90 mol%, and the rate of xylose conversion decreases from 55 to 25 mol% after 1 h.

Moreover, the furfural selectivity stays constant over time at all ionic strengths, indicating that the reactions that lead to by-products proceed in parallel with the dehydration.

Figure 7.1e shows the apparent reaction rate constant, *k*, for the conversion of xylose at the two extremes of the range of ionic strengths explored (*i.e.*, 0.1 and 6.1 M). These *k* values are evaluated by fitting the data points to Equation 7.2, which is derived considering the reaction of dehydration as first order in xylose.

$$X\% = 100 \cdot (1 - \mathrm{e}^{k(t - t_{lag})}) \qquad \textbf{Equation 7.2}$$

X% is the calculated xylose conversion at time *t*, *k* is the kinetic constant for xylose conversion and t_{lag} is a lag time implemented in the formula to consider the time it takes for the system to reach the reaction temperature (200 °C), typically between 0.1 and 0.2 h. The results of this analysis (Figure 7.1f) show that, when starting from PBA_2X, the rate of the xylose consumption decreases when increasing the ionic strength, in contrast to rate-enhancing effects reported for monophasic aqueous operation with added salt.[8,9] This slower conversion can be rationalized by a more favorable uptake of the diester in the organic phase and a slower hydrolysis of the ester in water (Scheme 7.1) as a result of the added salt, thus reducing the availability of free xylose in the water phase.

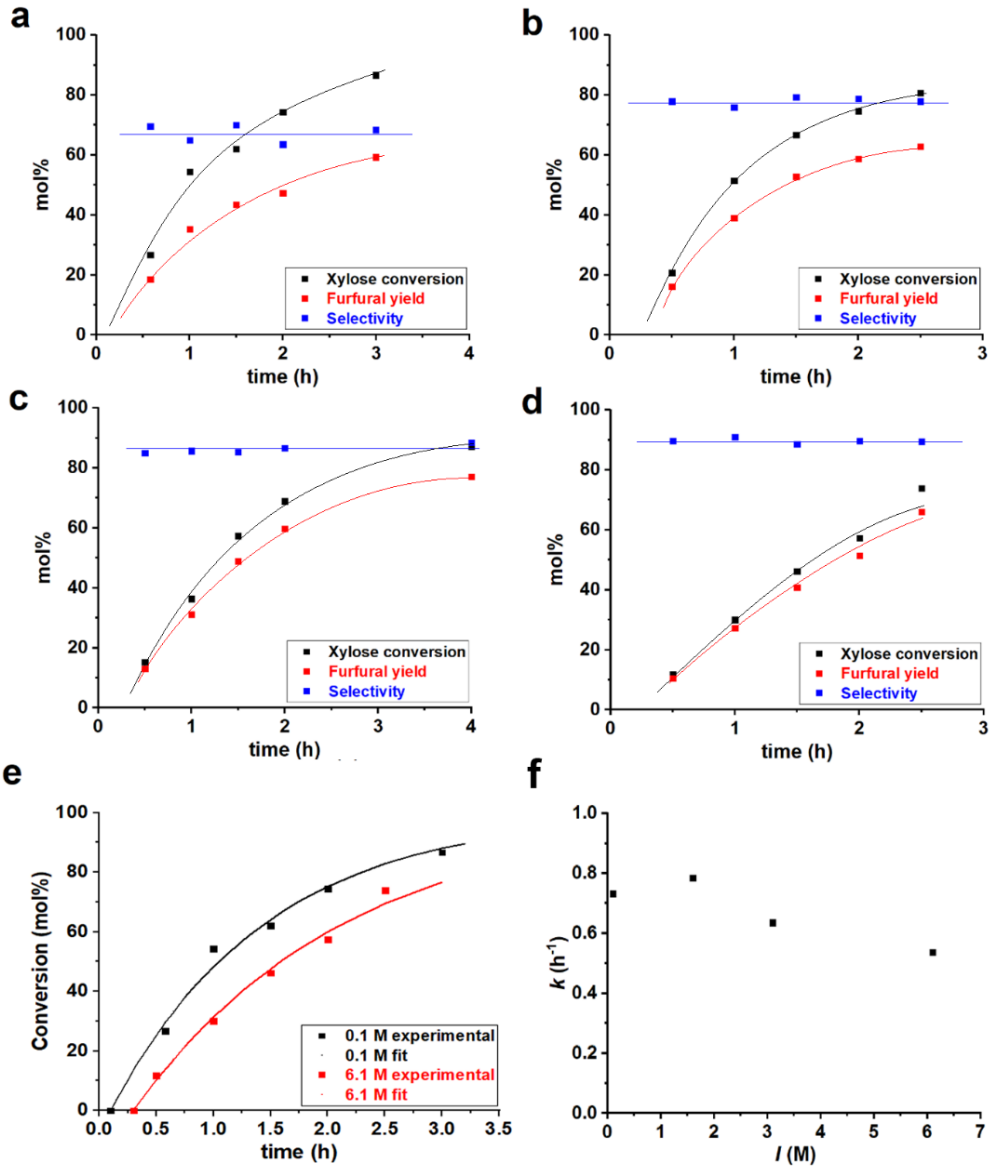

Figure 7.1 (a-d) Xylose conversion, furfural yield and and xylose-to-furfural selectivity (mol%) *versus* time. Reaction performed in a 1:1 toluene-water (pH = 1) biphasic system at 200 °C starting from PBA_2X in the organic phase, with (a) no added salt (ionic strength of 0.1 M), (b) at 1.6 M, (c) at 3.1 M and (d) at 6.1 M, lines are to guide the eye. (e) Example of the fit of the experimental data of xylose conversion, fit performed for the data set at 0.1 M and 6.1 M ionic strength. (f) Apparent rate constant k (h^{-1}) of the

dehydration of xylose performed starting from PBA_2X in a 1:1 toluene-water (pH = 1) biphasic system at 200 °C as a function of the ionic strength of the aqueous phase.

The apparent rate constant *k* is convoluted by the partitioning of the diester between the organic and aqueous phases, and by the rates of hydrolysis of the diester and the subsequent conversion of the released xylose by dehydration. To explore the effect of the mixing rate on the mass transfer of the diester between the two phases, experiments were performed with PBA_2X as starting material and at 3.1 M ionic strength at three different mixing regimes. Specifically, one set of experiments was performed in the absence of mixing, one at regular mixing (regularly sized magnetic bar in comparison to the vessel diameter, 1000 rpm), and one at vigorous mixing (using an oval-shaped magnetic stirrer, 1000 rpm). All reactions were performed at 200 °C and followed over a time window of 4 h (Figure 7.2).

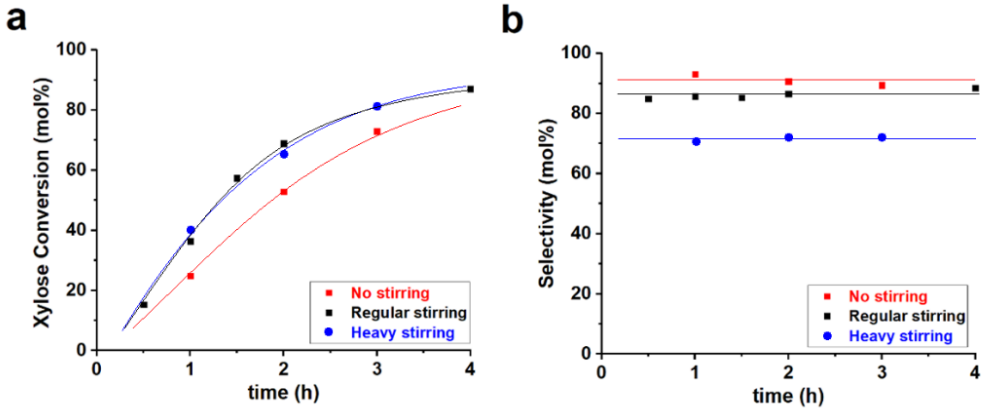

Figure 7.2 (a) Xylose conversion (mol%) and (b) xylose-to-furfural selectivity *versus* time for the dehydration reaction of xylose performed starting from PBA_2X in a 1:1 toluene-water (pH = 1) biphasic system at 200 °C at various mixing rates. Lines are to guide the eye.

Interestingly, no stirring resulted in an even slower rate of conversion, with little to no effect on the selectivity, while moving from regular to heavy stirring did not seem to affect the conversion rate but resulted in a significant drop in selectivity. The rate dependence can be rationalized by considering that the stirring speed affects the phase transfer of PBA_2X from the organic into the aqueous phase (as shown in Scheme 7.1). To investigate the effect on selectivity, further analysis of the reaction mixtures after the reaction was performed with ^{1}H-NMR. Only in the case of heavy stirring, a peak was observed at around 10 ppm, indicative of the presence of a carboxylic acid, probably due to formation of furoic acid.[2]

While Na_2SO_4 is used so far, literature mainly reports the use of halide salts, specifically chlorides.[9,12,23] Therefore, the dehydration of xylose, starting from PBA_2X, was also performed with added NaCl, in a 1:1 biphasic system of toluene and water (pH = 1 from HCl). The reaction time was fixed at 2 h and the ionic strength was varied again between 0.1 M and 6.1 M (Figure 7.3a and 7.3b). Additionally, the dehydration reaction was carried out using $MgSO_4$ and $MgCl_2$ at different ionic strengths, keeping all the other conditions the same as before (Figure 7.3c and 7.3d).

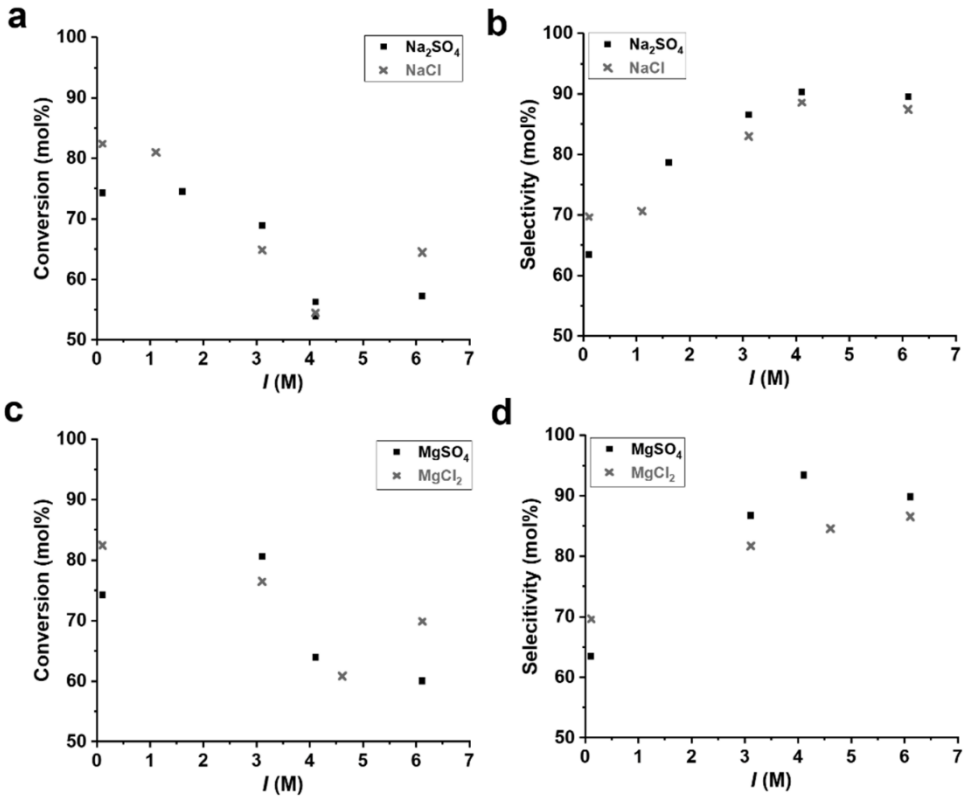

Figure 7.3 (a,c) Xylose conversion (mol%) and (b,d) xylose-to-furfural selectivity as a function of ionic strength, for the xylose dehydration performed starting from PBA_2X for 2 h in a 1:1 toluene-water (pH = 1) biphasic system at 200 °C. Ionic strengths were set by Na_2SO_4 (a/b, squares), NaCl (a/b, crosses), $MgSO_4$ (c/d, squares) and $MgCl_2$ (c/d, crosses).

Carrying out the reaction using NaCl and Na_2SO_4, resulted in small differences in conversion (<10 mol%), and these minor differences do not follow any specific trend. Similarly, the selectivities were comparable for the two systems. A slightly higher conversion was observed for magnesium salts over the sodium salts, paired with a

slightly higher furfural yield (approx. 5-10 mol% more), but with no effect on selectivity. As in the case of sodium salts, the differences observed between magnesium chloride and sulfate salts stay within a 10 mol% margin, and do not follow any specific trend. It is known that divalent cations interact more strongly with the OH groups of a sugar in water, through the formation of a bidentate complex between the cations and the OH pairs of the sugar.[15,16] This influences the reactivity of the sugar, resulting in higher rates of conversion when using divalent cations, as reported by Ershova *et al*.[9] In the present case, this behavior is preserved, indicating that starting from PBA_2X only affects the hydrolysis of PBA_2X to xylose into the aqueous phase. Additional experiments are needed to confirm and assess the significance of the observed trends and discontinuities.

7.2.2 Process Concept

Based on these data, a process concept for a possible industrial application can be developed. To do so, as mentioned already in Chapter 6, toluene needs to be substituted with 1-methylnaphthalene (MN), a high-boiling aromatic solvent that allows easy furfural distillation. As a proof of concept, the dehydration of xylose, starting from PBA_2X, was performed in a 1:1 v/v MN-water (pH = 1 from H_2SO_4) mixture at an ionic strength of 3.1 M, using Na_2SO_4 (Figure 7.4). The reaction in MN appears to be slightly slower (80 mol% *versus* 87 mol% conversion after 4 h) and less selective (75 mol% *versus* 85 mol%) than the one in toluene, in accordance with the results reported in Chapter 6. Nevertheless, the xylose-to-furfural selectivity is still high (75 mol%), in comparison with operations in water-MN biphasic systems with no added salt (approx. 65 mol%), and raising the ionic strength further could result in even higher selectivity improvements.

To investigate the possible losses of the different components in the biphasic system, the partitioning of PBA, furfural, water, and MN in the biphasic system were studied. The relative concentrations are reported in Table 7.1. The high ionic strength favors the partitioning of furfural and PBA into the organic phase, with approx. 80-90 mol% of both the components in the MN phase. To evaluate the losses of Na_2SO_4 and H_2SO_4 in the organic phase, elemental analysis was performed on a sample of the MN phase, after reaching full xylose conversion, indicating Na and S at 0.009 w% and 0.006 w%, respectively. This is compatible with a loss of 0.22-0.24 % of the total amounts of both Na_2SO_4 and H_2SO_4, which could be explained by imperfect L/L separation and the presence of water droplets (which contains the acid and the salt) dispersed in the organic phase.

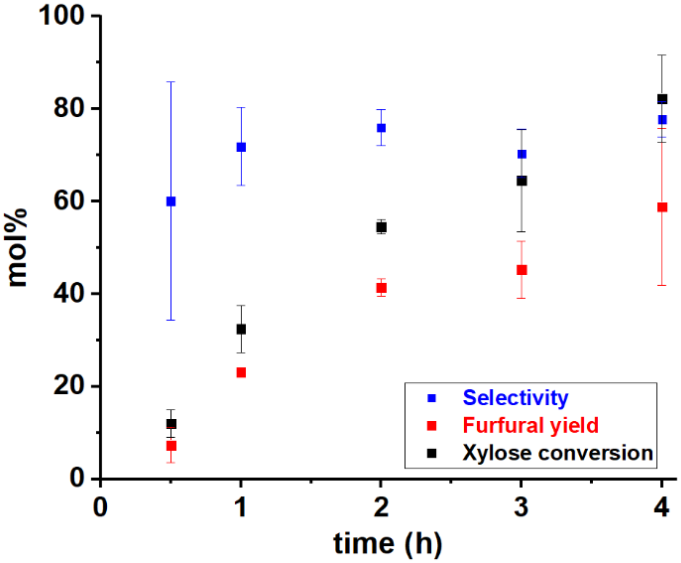

Figure 7.4 Furfural yield, xylose conversion and xylose-to-furfural selectivity (mol%) *versus* time. Reaction performed starting from PBA_2X in a 1:1 MN-water (pH = 1) biphasic system at 200 °C at an ionic strength of 3.1 M Na_2SO_4. The error bars represent the standard error of the measurement, evaluated after triplicating the analysis.

Table 7.1 Partitioning of the various system components and losses in a 1:1 v-v MN/water (pH = 1) solvent system, *I* = 3.1 M.

	Aqueous Phase	Organic Phase
PBA	129 mM (22 mol%)	566 mM (78 mol%)
Furfural	46 mM (12 mol%)	352 mM (88 mol%)
MN	2 mM	7.03 M
Water	55.0 M	66 mM

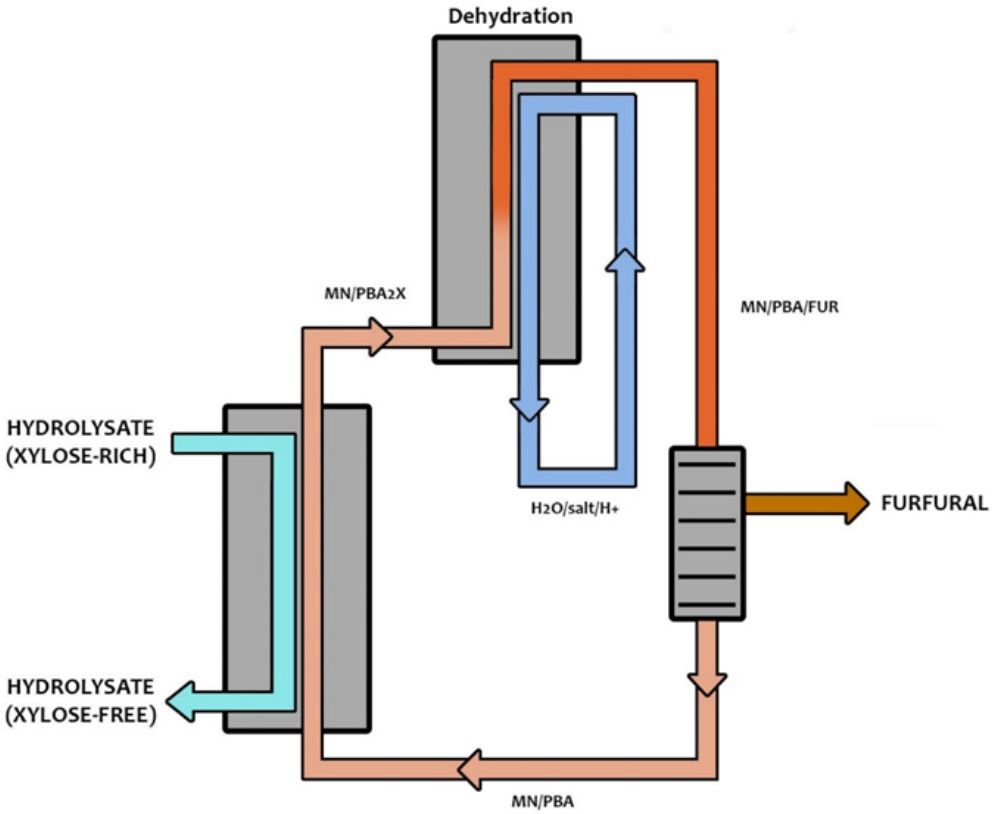

Figure 7.5 Conceptual process for the two-step furfural production based on the integration of xylose extraction as the boronate diester from an acidic hydrolysate followed by conversion of xylose into furfural in a biphasic system with a highly salted aqueous phase.

All these considerations lead to the development of a process concept, illustrated in Figure 7.5. In a first step where the hydrolysate is contacted with a MN/PBA solution, xylose is extracted from a xylose-rich hydrolysate as its boronate diester, as described in Chapter 5. The resulting organic/boronate diester phase is then heated to the reaction temperature and contacted with an acidic aqueous phase at high salt concentration to hydrolyze the boronate ester and convert the released xylose into furfural. The effluent furfural-containing stream is then sent to a distillation column to recover the furfural as distillate and a MN/PBA stream as bottom stream, that can be recycled to perform a new cycle of xylose extraction. The water produced in the dehydration reaction is to be recycled with additional fresh water to balance the water

used in the hydrolysis of PBA_2X. Possibly, much of the leftover furfural in the aqueous phase can be distilled as an azeotrope with water, as already discussed in Chapter 6.[1,2,21]

7.2.3 Kinetic Model

As shown in Scheme 7.1, the xylose dehydration from PBA_2X can be separated into multiple steps. The first step is the partitioning of PBA_2X between the organic and the aqueous phases, which is followed by the hydrolysis of the diester to free xylose and PBA in water, the dehydration of free xylose into furfural, with the possible formation of by-products, and finally, the partition of liberated PBA and furfural between the organic and aqueous phases. The first two steps (partitioning and hydrolysis of the diester) are equilibria, while the xylose dehydration step is not reversible, as the rehydration of furfural and all the intermediates causes degradation.[1,2]

It is complicated to experimentally separate the first two steps, as the ^{1}H-NMR analysis only allows to determine the concentration of PBA_2X in the organic phase and free xylose in the aqueous phase. The diester is not observed in the water phase, probably because its solubility is too low. Formally, a monoester may temporarily form at the biphasic interface (see Chapter 5) but it is not visible after stirring. The hydrolysis of PBA_2X generates PBA, which partitions between the two phases, and the majority goes into the organic phase (at least at room temperature at which the analysis is performed). For these reasons, here the partitioning of PBA_2X and its subsequent hydrolysis is described by a single, joint thermodynamic constant *K*, which is defined based on the measurable concentrations and which is dependent on the organic solvent and on the ionic strength of the water phase (Equation 7.3). The concentration of PBA_2X is taken in the organic phase (and assumed negligible in the water phase), and the concentration of xylose is taken in the water phase (and is absent in the organic phase). For PBA, however, this occurs in both phases and therefore the total amount of PBA divided by the total volume is taken into consideration, *i.e.*, the volume-weighed concentration average over the two phases, called the "overall concentration" $[PBA]_{ov}$. The thermodynamic constant *K* defined in Equation 7.3 can be related to two rate constants, of the formation and hydrolysis of the diester, k_{1f} and k_{1h}, respectively.

$$K = \frac{k_{1f}}{k_{1h}} = \frac{[\mathrm{PBA_2X}]_{org}}{[\mathrm{X}]_{aq}[PBA]_{ov}{}^2} \qquad \textbf{Equation 7.3}$$

The reaction step, *i.e.*, the dehydration of free xylose in water, is defined by the kinetic constant k_2. So, the xylose dehydration from PBA_2X can be modeled as presented in Scheme 7.2, with each step of the process related to a rate constant.

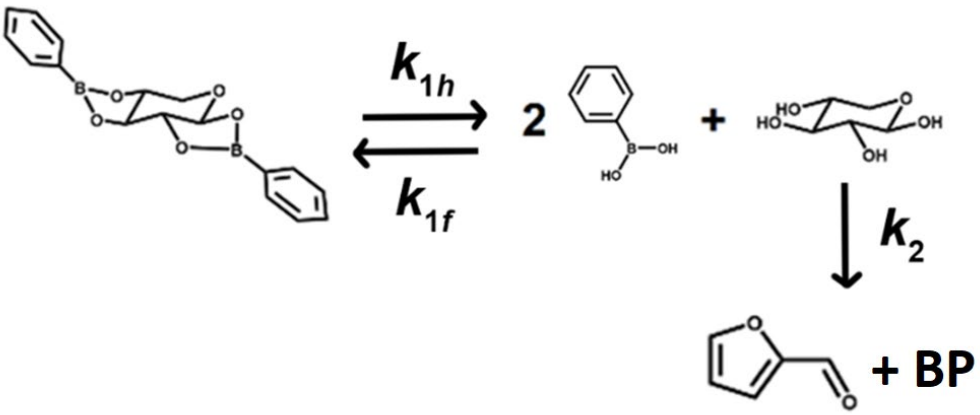

Scheme 7.2 Kinetic scheme for the dehydration of xylose to furfural (and by-products, BP) from its diester form.

Based on Scheme 7.2, the three rate constants (k_{1f}, k_{1h} and k_2) can be used to describe the evolution of the concentration of free xylose in water with time (Equation 7.4).

$$\frac{d[\mathrm{X}]_{aq}}{dt} = k_{1h}[\mathrm{PBA_2X}]_{org} - k_{1f}[\mathrm{X}]_{aq}[\mathrm{PBA}]_{ov}^2 - k_2[\mathrm{X}]_{aq} \qquad \textbf{Equation 7.4}$$

The first term of the equation describes the hydrolysis of PBA_2X, the second the diester formation, and the third the xylose dehydration reaction. Similarly, for PBA_2X, Equation 7.5 describes the evolution of the concentration of PBA_2X with time.

$$\frac{d[\mathrm{PBA_2X}]_{org}}{dt} = k_{1f}[\mathrm{X}]_{aq}[\mathrm{PBA}]_{ov}^2 - k_{1h}[\mathrm{PBA_2X}]_{org} \qquad \textbf{Equation 7.5}$$

Through Equations 7.4 and 7.5, the evolution of the concentration of these two species can be evaluated in the desired time window, using the known initial concentrations of PBA_2X and xylose. The concentration of PBA can then be calculated at any point of time from its mass balance, knowing the total amounts of PBA in the system and that of the PBA_2X diester in the total volume.

The calculated conversion, X_{calc}, can be calculated from Equation 7.6, where the initial concentrations are indicated with the suffix "0".

$$X_{calc} = \frac{[\mathrm{PBA_2X}]_{org} + [\mathrm{X}]_{aq}}{[\mathrm{PBA_2X}]_{org,0} + [\mathrm{X}]_{aq,0}} \qquad \textbf{Equation 7.6}$$

Because furfural is found in both phases, its overall concentration is defined, as in the case of PBA, by dividing the total amount by the total volume. In the model, however,

the furfural concentration is not expressed explicitly, because the selectivity remains constant over time for every run. Therefore, the rate constant for the formation of furfural can be obtained later directly by multiplying the experimental selectivity of a particular run multiplied by the modeled reaction rate constant k_2.

The model simulations start from the initial concentrations of free xylose, PBA and PBA_2X. Depending on whether an experiment is run by putting the diester in the organic phase, or by putting xylose in the water phase and PBA in the organic phase, this leads to different starting points even though the total concentrations of all constituents (xylose and PBA) can be the same. From the equations given above, all species concentrations can be calculated at any point in time, using the starting conditions of a given experimental run. Since the conversion takes hours and that an apparent lag time of approx. 0.1 h occurs, 0.01 h is taken as the time interval between time points in our simulations. In case partitioning of any species would turn out to be faster than this time constant, it can safely be assumed to be in equilibrium at any point in time, and hence that its kinetics does not affect the modeled reaction rate constant k_2.

The model was set to fit the experimental conversion data by least-squares minimization, performed in Excel, while varying the three fit parameters, k_{1h}, K, and k_2 (k_{1f} is calculated from $K \cdot k_{1h}$, Equation 7.3). The data were fitted using a single lag time, optimized at 0.1 h, irrespective of starting feed (PBA_2X or X+PBA) and medium (water, toluene/water or MN/water). This simplification was based on the expectation that the lag time is a consequence of the temperature ramp-up process.

The three fit parameters k_{1h}, K, and k_2 were optimized independently or kept the same across a set of data series depending on the relation between the experimental cases. For example, all data series for water-toluene biphasic systems at the same ionic strength were fitted altogether with the same values of k_{1h}, K, and k_2, regardless to the starting conditions (i.e., free xylose, free xylose and PBA, PBA_2X). For studying effects of stirring speed, only k_{1h} was varied, while K and k_2 were kept the same over the different runs.

First, all cases in toluene-water biphasic operation were considered, with three different starting conditions (xylose in water and no PBA, xylose in water and PBA in toluene, and PBA_2X in toluene) and at two ionic strengths (0.1 and 3.1 M), yielding in total 6 cases. For all cases, the model was fitted to the conversion data, with two sets of constants fitted jointly for each ionic strength. The experimental and fitted data are shown in Figure 7.6, while Table 7.2 gives the two sets of optimized fit parameters. Figure 7.6 shows the good fit to the experimental data in all cases. Notably, the lag time of 0.1 h is well visible in panels a-d, while the pronounced induction period observed

upon starting from the diester in the organic phase (panels e-f) is properly reproduced by the model.

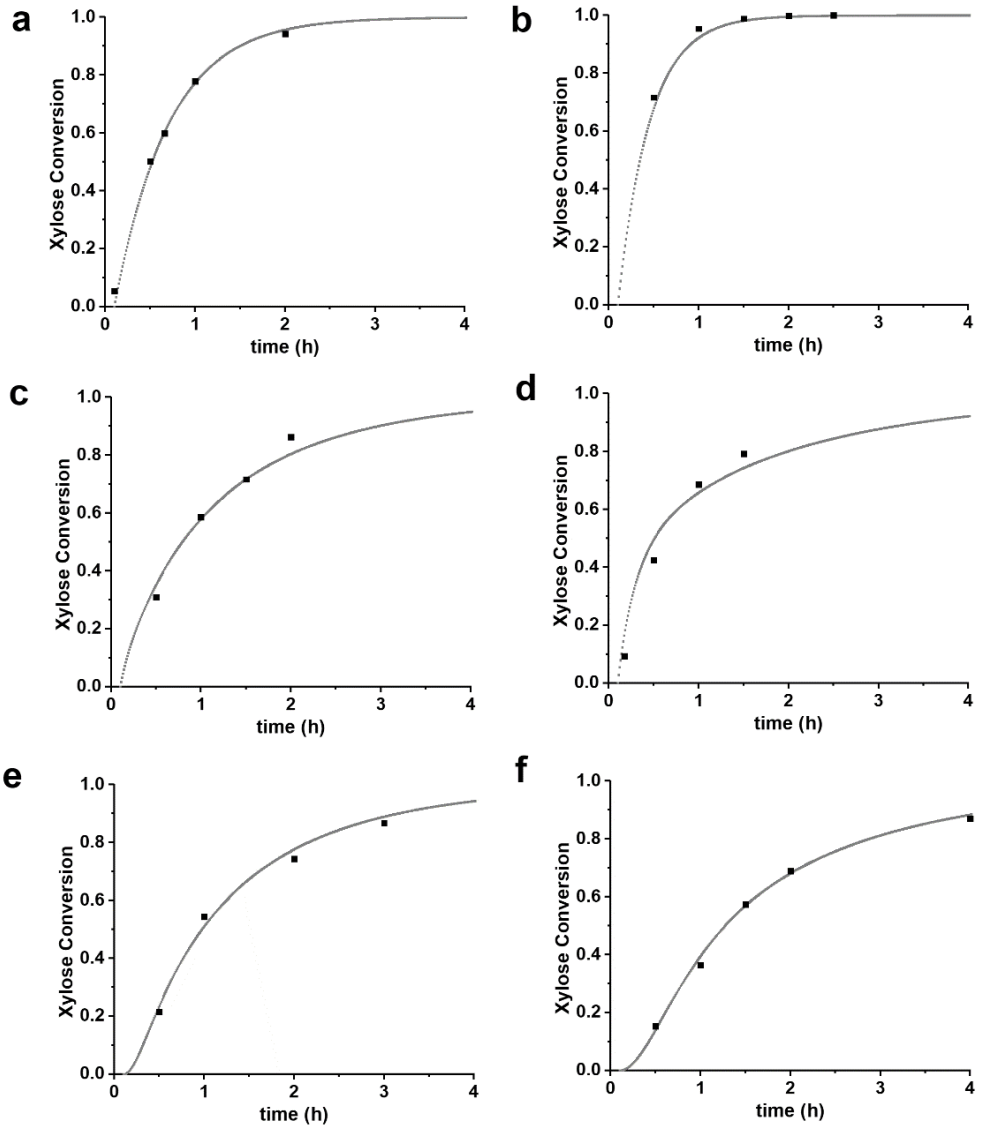

Figure 7.6 Xylose conversion *versus* time, comparison between the experimental points (dots) and the fitted model (line) for the reactions performed in a 1:1 toluene-water (pH = 1) biphasic system at 200 °C from (a) 320 mM free xylose in water, no PBA, no salt, (b) 320 mM free xylose in water, no PBA, *I* = 3.1 M (Na_2SO_4), (c) 320 mM free

xylose in water, 640 mM PBA in toluene, no salt, (d) 320 mM free xylose in water, 640 mM PBA in toluene, I = 3.1 M (Na_2SO_4), (e) 320 mM PBA_2X in toluene, no salt and (f) 320 mM PBA_2X in toluene, I = 3.1 M (Na_2SO_4).

Table 7.2 Fitted values of the kinetic model parameters for the xylose dehydration reaction at 200 °C in a 1:1 toluene-water (pH = 1), biphasic system at different ionic strengths, I.

I (M)	k_{1h} (h^{-1})	k_{1f} ($h^{-1}M^{-2}$)	K (M^{-2})	k_2 (h^{-1})
0.1 (no salt)	4.15	55.50	13.37	1.64
3.1	1.04	36.09	34.65	2.81

Figure 7.6 and Table 7.2 show that a high ionic strength accelerates the xylose dehydration, resulting in a higher k_2, which is in agreement with the literature.[7-9] High ionic strengths also result in an increased K (by a factor 2.6), as expected for a classical desalting effect. Kinetically, the salt effect is even stronger, as seen in particular in k_{1h} (4.0 times lower at 3.1 M when compared to 0.1 M ionic strength), which represents the combined partitioning plus ester hydrolysis, and its reverse reaction's rate constant is lowered as well (by a factor 1.5). Hence, the model confirms that the apparent slower reaction at high salt when starting from the diester in the organic phase, can be attributed purely to the inhibited phase transfer and hydrolysis of the ester in water, even while the reaction rate constant of the liberated xylose is enhanced.

After the optimization of the parameter sets, the model simulations of all species concentrations over time can be viewed. It is interesting to follow the differences in the trends of the concentration of free xylose in water at different initial conditions (Figure 7.7). The case with PBA_2X as the starting material is compared to the one with free xylose (in water) with a 2:1 molar ratio of PBA (in toluene) (Figure 7.7a). When starting from PBA_2X, the xylose concentration initially increases and, after reaching a maximum at around 0.5 h, starts to decrease, as more and more xylose is being converted. In contrast, when starting from free xylose in water, the concentration of xylose in water drops steadily. After about 0.5 h, the two curves become strongly comparable because the ester partitioning and hydrolysis/formation have equilibrated and are following the pace of conversion, although the delay (of approx. 0.15 h) in the case starting from the diester is still apparent.

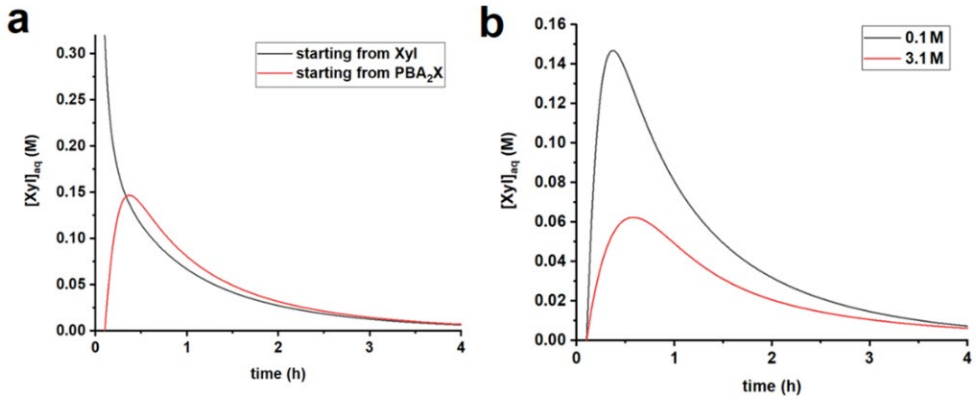

Figure 7.7 Comparison of the development of the free xylose concentration in water *versus*. time (a) starting from free sugar in water and PBA in toluene, or with PBA_2X in toluene, both at 0.1 M ionic strength, and (b) starting with PBA_2X in toluene at 0.1 M or at 3.1 M ionic strength. Curves are obtained from the model simulations.

Comparing the cases with PBA_2X as a starting material, but at different ionic strengths (Figure 7.7b), shows that, at any given time, the total amount of free xylose present in the aqueous phase is considerably lower at high salt, as a result of the more favorable partitioning of the diester into the organic phase as explained above. As explained above, this results in a slower apparent conversion at high salt, caused by the fact that the xylose concentration is lowered by approx. a factor 2.5 (at the maximum), while the reaction rate constant is enhanced by only a factor 1.7.

Subsequently, toluene is compared with 1-methylnaphthalene (MN) and the effect of the stirring speed looked at, all at 3.1 M ionic strength. Three different stirring speeds were used, leading to six cases in total (Figure 7.8). The rate constant k_2 is kept the same for all the six scenarios, as the xylose dehydration happens in the aqueous phase and should be independent of the organic phase as well as the water-organic interface (*i.e.*, stirring rate). The partitioning of the diester, however, is solvent dependent and its formation/hydrolysis rate should depend on the organic/water interface (*i.e.*, stirring rate). To reflect this, the fit parameter K is different for toluene and MN, but constant for all cases in one of these solvents, while the rate constants k_{1h} and k_{1f} can vary in each separate case, due to the variation of the stirring conditions. All these cases were fitted as explained above, and good fits were obtained in all cases (Figure 7.8). The fitted parameters are given in Table 7.3.

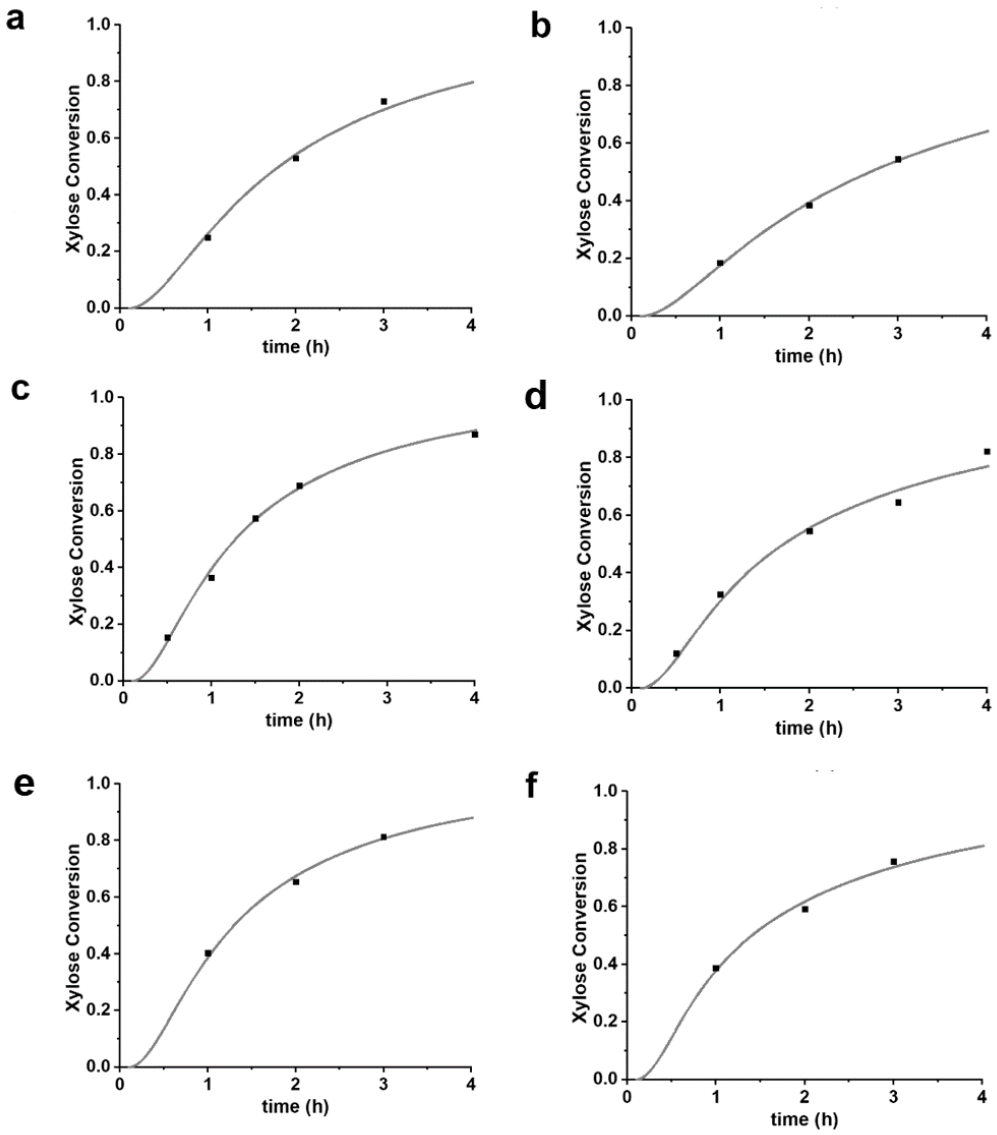

Figure 7.8 Xylose conversion *versus* time, comparison between the experimental points (dots) and the model fits (lines) for the xylose dehydration reaction starting from PBA_2X (320 mM in organic solvent) performed in a biphasic system at 200 °C, 3.1 M ionic strength with no (a,b), normal (c,d) or heavy (e,f) stirring and in 1:1 toluene-water (a/c/e) or in a 1:1 MN-water (b/d/f) biphasic system.

Table 7.3 Fitted values of the kinetic model parameters for the xylose dehydration reaction performed at 200 °C at 3.1 M ionic strength in a 1:1 organic-aqueous biphasic system composed of water (pH = 1) and either toluene or MN, at various stirring conditions.

Stirring	Organic solvent	k_{1h} (h^{-1})	k_{1f} ($h^{-1}M^{-2}$)	K (M^{-2})	k_2 (h^{-1})
no	Toluene	0.56	19.33	34.65	2.81
regular	Toluene	1.04	36.09	34.65	2.81
heavy	Toluene	1.00	34.74	34.65	2.81
no	MN	0.35	29.47	83.66	2.81
regular	MN	0.73	60.90	83.66	2.81
heavy	MN	1.12	93.90	83.66	2.81

Table 7.3 shows that K increases when moving from toluene to MN, while keeping I constant. This agrees with previous data on the extraction process (Chapter 5) and can be rationalized by a stronger interaction between MN and the diester. This depresses the hydrolysis of the ester and, consequently, the apparent xylose conversion is slower in MN, even though the rate constant is the same.

The stirring speed has a pronounced effect on the rate constants of the diester partitioning and hydrolysis/formation for both solvents. Overall, an increased stirring speed increases both rate constants k_{1h} and k_{1f}, indicating that the phase transfer is limiting the overall rate of hydrolysis. Switching from no stirring to regular stirring resulted in an about 2-fold increase of k_{1h} and k_{1f} for both solvents. For toluene there was no effect of increasing the stirring speed further. In contrast, for MN, the highest stirring speed increased the rate constants further. These effects are also witnessed when looking at the free xylose concentrations obtained from the simulations (Figure 7.9).

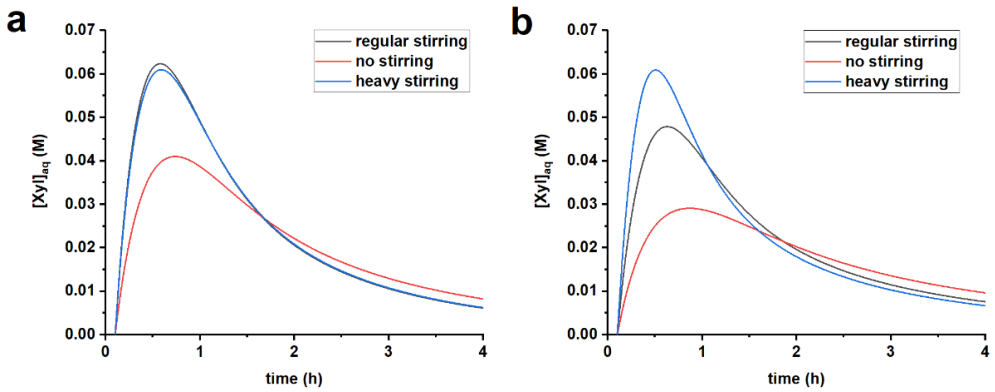

Figure 7.9 Comparison of the development of the free xylose concentration in water starting with 320 mM PBA_2X in toluene, at 3.1 M ionic strength, applying different kinds of stirring, (a) in a 1:1 toluene-water system and (b) in a 1:1 MN-water system. Curves obtained from the model equation.

Tentatively, k_{1h} is assumed to reach a maximum, of approx. 1 h^{-1}, which is not further increased by better mixing. The difference between MN and toluene in reaching optimal mixing can potentially be explained by the difference in density between the two phases in both cases. In 1:1 toluene-water (salt, acid) the difference in density between the two phases is about 0.28 g/mL, whereas that in the case of MN is about half (0.14 g/mL). So, one could expect an easier tendency for emulsification in the case of MN-water, with an improved effect of mixing. However, the opposite appears to be the case, as the values of k_{1h} are higher for toluene, and the maximum is reached at intermediate stirring speed already in this case. Potentially, the stronger interaction between MN and the diester overrules the effect of the density difference, and potentially other effects, for example a stabilization effect by population of an intermediate (*e.g.*, the monoester) at the interface between the two solvents plays a role as well.

To take the selectivity into account, k_2 can be split into k_2' to furfural and k_2" to by-products (Scheme 7.3). As the reactions that lead to by-products seems to be first order in xylose, as indicated by the fact the xylose-to-furfural selectivity is constant over the xylose conversion, k_2 is defined as $k_2 = k_2' + k_2''$. Hence, k_2' is obtained by multiplying k_2 by the average selectivity, *Y*, in the chosen scenario. The resulting values are reported in Table 7.4.

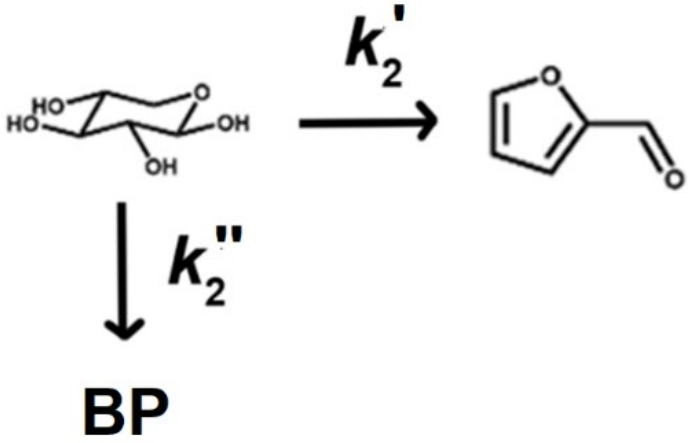

Scheme 7.3 Kinetic scheme for the dehydration of xylose to furfural, and in parallel the formation of by-products.

Table 7.4 k_2, k_2' and k_2'' values for the different scenarios.

Stirring	*I* (M)	Solvent	Source	*Y* (mol%)	k_2 (h^{-1})	k_2' (h^{-1})	k_2'' (h^{-1})
regular	0.1	Toluene	X	67.0	1.64	1.10	0.54
regular	0.1	Toluene	PBA_2X	63.4	1.64	1.04	0.60
regular	3.1	Toluene	X	75.6	2.81	2.12	0.69
no	3.1	Toluene	PBA_2X	91.1	2.81	2.56	0.25
regular	3.1	Toluene	PBA_2X	86.2	2.81	2.42	0.39
heavy	3.1	Toluene	PBA_2X	71.8	2.81	2.02	0.79
no	3.1	MN	PBA_2X	74.7	2.81	2.09	0.72
regular	3.1	MN	PBA_2X	72.7	2.81	2.04	0.77
heavy	3.1	MN	PBA_2X	73.5	2.81	2.07	0.74

This preliminary analysis shows that moving from low to high ionic strength in a toluene-water biphasic system results in an overall increase in the rate of furfural

formation. Specifically, k_2' increases by a factor 1.9 when starting from free xylose, while it increases by a factor 2.3 when starting from PBA_2X. At the same time, the changes in k_2'' look small, possibly within experimental error negligible when starting from free xylose. This change in the relative rates is related to the approx. 10 mol% xylose-to-furfural selectivity increase. However, when starting from PBA_2X, the rate of by-products formation drops almost to a half when increasing the ionic strength. This is in line with the effect of salt on the partitioning of furfural and PBA_2X (*vide supra*) causing the further enhanced selectivity. Specifically, when the sugar does not start as part of the aqueous phase, the rate of the formation of by-products is lower.

As shown in Figure 7.8, the overall rate of xylose conversion in the dehydration of xylose, using PBA_2X as a starting material, is strongly affected by the stirring speed. At the same time, the xylose-to-furfural selectivity stays high at approx. 85-90 mol% for the toluene-water biphasic system, both at no stirring and regular stirring conditions, with the highest selectivity of approx. 90 mol% obtained when not applying any stirring. At heavy stirring, a higher side reaction rate is observed. As previously discussed, additional degradation reactions of furfural are taking place in this case (*see above*). The decrease in the overall PBA_2X consumption rate in the absence of stirring, observed both when using toluene and MN, indicates that mixing affects the mass transfer within the system, affecting the equilibria of partition of free xylose/PBA_2X and the rate of PBA_2X hydrolysis, so that the absence of stirring favors the residence of PBA_2X in the organic phase. This is confirmed by the fact that applying more turbulent mixing, maximizing the mass transfer between the two phases, increases the rate of xylose consumption both in the water-toluene and in the water-MN systems. While in the case of MN changing the stirring conditions does not affect the xylose-to-furfural selectivity (which stays approx. 73-75 mol% in all cases), in the water-toluene case a marginally increased selectivity is obtained in absence of stirring (approx. 91 mol%), in comparison with regular stirring (approx. 86 mol%). This effect is also compatible with the previously mentioned hypothesis that a change in free xylose/PBA_2X partitioning, in this case triggered by a different mass transfer between the two phases, can positively affect the xylose-to-furfural selectivity.

Limiting side reactions is an important issue to boost selectivity further.[1-3] The by-products resulting from prolonged reaction times, which lead to humin formation and a decrease of the selectivity that starts to occur close to or beyond complete conversion are not discussed in this Chapter (see, for example, Chapters 3 and 4). Often, however, the xylose-to-furfural selectivity does not start at 100% when conversion commences, and there is a large part of the reaction time in which the selectivity is constant, as is also observed in the experiments described here.[8,9,21,23,24] The results presented here all seem compatible with parallel reactions (*e.g.*, xylose degradation to low molecular

weight carboxylic acids and xylose-furfural condensation) happening in water as a major influence on the selectivity.[1-3,24] A constant selectivity implies that the rate of formation of by-products is also first order in xylose and independent of the furfural concentration. Hence, relative ratios of produced furfural and by-products are neither dependent on the concentration of xylose, nor on that of furfural. Hence, traditional arguments, like the partitioning of the diester into the organic phase that lowers the xylose concentration in water, and the protection of the produced furfural, also by partitioning into the organic phase, are hard to reconcile with the observation of a constant selectivity for individual reaction runs and seem only good arguments for suppression of the later-formed humins.[1,8,9,24-26] Possibly, the higher (but constant) selectivity observed for starting from the diester in comparison to starting from free xylose, hints at the ready suitability of the released xylose to form furfural, while the formation of by-products may need a subsequent configurational change of the sugar before it can occur. Further work will have to shed further light on these different types of selectivities and their mechanistic origins.

7.3 Conclusions

The conversion of PBA_2X to furfural it is shown with improved selectivity upon increasing the ionic strength of the aqueous solution that was contacted with the PBA_2X/aromatic feed. A similar increase in selectivity was found upon salt addition to a biphasic xylose operation both in absence and presence of PBA. The highest furfural selectivity, *i.e.*, 91 mol%, is obtained at 4.1 M ionic strength, when performing the reaction in a water-toluene biphasic system, starting from PBA_2X. The increased selectivity can be rationalized by the effect of high ionic strengths on the partitioning of PBA_2X. Moreover, at similar reaction conditions (1:1 water-toluene biphasic system, I = 3.1 M) , performing the reaction starting from PBA_2X instead of free xylose resulted in a 10 mol% xylose-to-furfural selectivity improvement. This hints at the possibility that the diester hydrolysis results in a xylose conformer which is more readily suitable for dehydration to furfural, compared with starting from free xylose in water. However, additional analyses are required to confirm this hypothesis. Based on these data, a process concept for furfural manufacture from xylose-rich hydrolysates is developed. This concept follows the whole process from industrial feed to product isolation, by means of distillation. All possible losses (*i.e.*, solvents, salts, catalyst, and product) were independently determined, validating the viability of the process concept. Additional analysis and studies are necessary to further explore the application of this concept. A comprehensive kinetic model is also developed to describe the mechanistic aspects of xylose dehydration in a highly salted biphasic system, starting from PBA_2X, encompassing all the steps from PBA_2X hydrolysis to xylose dehydration. The fitting of the experimental data provided various sets of rate constants, each one describing a

specific part of the mechanism, which allow to isolate the effect of changing the solvent system on each mechanistic step, deepening the understanding of the observed xylose conversion and xylose-to-furfural selectivity.

Overall, the results presented in this Chapter deepen the understanding of biphasic dehydration of xylose at high ionic strengths, providing insight into the effect of using an organic soluble species as starting material. Granted that further studies are needed to ensure the potential industrial application of these findings, the combination of liquid-liquid xylose extraction and high ionic strength biphasic operation appears a promising path for highly selective and environmentally friendly furfural production.

7.4 Experimental Section

7.4.1 Chemicals

D-(+)-Xylose (>99%), D_2O (99.9% atom D), toluene-d_8 (99% atom D), 3-(trimethylsilyl)propionic-2,2,3,3-d_4 acid sodium salt (TMSP, 98% atom D), 1-methylnaphthalene (98%), sodium sulfate (99%), magnesium sulfate (99%) and magnesium chloride (99%) were purchased from Sigma-Aldrich, while phenylboronic acid (PBA, 99%), sodium chloride (99%) and tetramethylsilane were obtained from Alfa Aesar.

7.4.2 Methods and Equipment

All chemicals were used without further purification. PBA_2X was obtained by extraction of xylose from water using PBA in toluene in a 2:1 PBA:xylose ratio, as described in Chapter 5. ^{1}H-NMR spectra were recorded as described in Chapter 4. In all cases the reactions were performed using a heating mantle and hard-glass reaction vessels.

7.4.3 Xylose Conversion to Furfural

A 1:1 v/v biphasic system (each solvent 2 mL) of an aromatic solvent (toluene or 1-methylnaphthalene), and water (pH = 1 from added H_2SO_4 or HCl), containing an overall concentration of xylose of 160 mM (either 320 mM in its free form in water or 320 mM as PBA diester in the organic phase), and different sulfate of chloride salts at an ionic strength ranging from 0.1 M (no salt) to approx. 6 M (obtained using concentrations of Cl^- and SO_4^{2-} of Na^+ and Mg^{2+} ranging from 0.5 M to 6 M), was heated at 200 °C for reacting times varying between 0.1 and 4 h. In the case of the experiments performed with free xylose as the starting material, PBA was also added to the mixture, in a 2:1 molar ratio to xylose. Prior the analysis with ^{1}H-NMR spectroscopy, all the reactions were stopped and cooled to room temperature. Stirring was either avoided or applied at 1000 rpm, either with a stirring rod of 6 mm or with an oval stirring bar of 1.6 cm.

The latter fits the vessel but it is position diagonally on its bottom so, when the magnetic rotation starts, its rotation ensures turbulent mixing.

7.4.4 Model Fitting and Parameters

The model is implemented in Excel and solves all equations numerically and in an iterative way. For example, the calculation of the xylose concentration in the aqueous phase is evaluated, from time 0, over a time window (0-4 h) divided into intervals of 0.01 h (Δt), with the concentration of xylose at time t+1 being related to the concentration at time t of xylose, PBA and PBA_2X, following Equation 7.7.

$$[X]_{t+1} = [X]_t + (k_{1h}[PBA_2X]_t - k_{1b}[X]_t[PBA]_t^2 - k_2[X]_t) \cdot \Delta t \quad \textbf{Equation 7.7}$$

The changes in the concentration of PBA_2X are calculated in a similar manner. The fitting of the data is also performed in Excel. An initial value is given to all the model parameters to be fitted, namely K, k_2 and k_{1h} (k_{1f} is derived from K and k_{1h} and not fitted independently). Conversion values at each time for which an experimental value is available, are obtained from the simulation and compared to the experimental ones. A standard least-squares minimization routine is used to minimize the sum of errors over all conversion time points by varying the model parameters. A cumulative error is used, when applicable, to fit multiple experimental series simultaneously with one set of parameters.

7.4.5 Elemental Analysis

Elemental analysis was performed at the MikroLab Kolbe (Mikroanalytisches Laboratorium Kolbe) in Mülheim an der Ruhr on a 2 mL sample of the organic phase of the PBA_2X dehydration reaction, performed in a 1:1 v/v biphasic system of MN and water, in which full PBA_2X formation is reached. C, H, B, S and Na were quantified in duplicate.

7.5 References

1. J.-P. Lange, E. Van der Heide, J. Van Buijtenen, R. Price, *ChemSusChem* **2012**, *5*, 150-166.
2. R. Mariscal, P. Maireles-Torres, M. Ojeda, I. Sádaba, M. López Granadosa, *Energy Environ. Sci.* **2016**, *9*, 1144– 1189.
3. P. Gallezot, *Chem. Soc. Rev.* **2012**, *41*, 1538-1558.
4. J. E. Romo, N. V. Bollar, C. J. Zimmermann, S. G. Wettstein, *ChemCatChem* **2018**, *10*, 4805–4816.
5. B. Song, R. Lin, C. H. Lam, H. Wu, T.-H.Tsui, Y. Yu, *Renew. Sust. Energ. Rev.* **2021**, *135*, 1-19.

6. C. B. T. L. Lee, T. Y. Wu, *Renew. Sust. Energ. Rev.* **2021**, *137*, 1-19.
7. O. Yemiş, G. Mazza, *Waste Biomass Valori.* **2019**, *10*, 1343−1353.
8. K. R. Enslow, A. T. Bell, *ChemCatChem* **2015**, *7*, 479–489.
9. O. Ershova, K. Nieminen, H. Sixta, *ChemCatChem* **2017**, *9*, 3031−3040.
10. C. Liu, L. Wei, X. Yin, M. Wei, J. Xu, J. Jiang, K. Wang, *Ind. Crop. Prod*. **2020**, *147*, 1-10.
11. Y. Zhao, K. Lu, H. Xu, L. Zhu, S. Wang, *Renew. Sust. Energ. Rev.* **2021**, *139*, 1-27.
12. G. Marcotullio, W. De Jong, *Green Chem.* **2010**, *12*, 1739–1746.
13. G. Marcotullio, W. de Jong, *Carbohyd. Res.* **2011**, *346*, 1291–1293.
14. C. Rasrendra, I. Makertihartha, S. Adisasmito, H. Heeres, *Top. Catal.* **2010**, *53*, 1241–1247.
15. J. Teychené, H. Roux-De Balmann, S. Galier, *Carbohyd. Res.* **2017**, *448*, 118–127.
16. P. K. Banipal, A. K. C. N. Hundal, T. S. Banipal, *Carbohyd. Res.* **2010**, *345,* 2262–2271.
17. E. Combs, B. Cinlar, Y. Pagan-Torres, J. Dumesic, B. Shanks, *Catal. Commun.* **2013**, *30*, 1–4.
18. I. Dávila, J. Labidi, *Curr. Opin. Green Sustain. Chem.* **2021**, *28*, 100435-100443.
19. N. Kunthakudee, U. Pancharoen, K. Fulajtárová, T. Soták, M. Hronec, P. Ramakul *Korean J. Chem. Eng.* **2017**, *34*, 2293–2300.
20. F. Gao, R. Bai, F. Ferlin, L. Vaccaro, M. Li, Y. Gu, *Green Chem.* **2020**, *22*, 6240-6257.
21. Z. Mor, S. Assouline, J. Tanny, I. M. Lensky, N. G. Lensky, *Water Resour. Res.* **2018**, *54*, 1460-1475.
22. A. M. Salhotra, E. E. Adams, D. R. F. Harleman, *Water Resour. Res.* **1987**, *23*, 1769–1774.
23. C. Xiouras, N. Radacsi, G. Sturm, G. D. Stefanidis, *ChemSusChem* **2016**, *9*, 2159-2166.
24. I. Agirrezabal-Telleria, I. Gandarias, P. L. Arias, *Bioresour. Technol.* **2013**, *143*, 258–264.
25. R. Weingarten, J. Cho , W. C. Conner Jr., G. W. Huber*, Green Chem.* **2010**, *12*, 1423-1429.
26. S. Le Guenic, F. Delbecq, C. Ceballos, C. Lena, *J. Mol. Catal. A Chem.* **2015**, *410*, 1–7.

Chapter 8

Future Perspectives

This chapter provides a series of perspectives on alternative approaches for furfural synthesis and corresponding industrial concept processes. Directions that go beyond the research described in the previous chapters will be explored. Possible applications, as well as their societal and economic impacts, are discussed without attempting to be exhaustive.

The research described in this thesis provides new concepts to produce furfural, as well as xylose isolation and purification, from xylose-rich hydrolysate feeds. These concepts have addressed how to operate the reactions and under what conditions, and these have led to a variety of process concepts. The implementation of an extraction step opens the path to avoid rather cost-inefficient, yet relevant, operations, like solvent and pH control.[1-4] However, the potential application at large scale remains yet to be proven.

8.1 Application to Different Sugars and Feedstocks

The extension of the here described conceptual processes to other biorefinery processes and the production of different target chemicals from the same feed are still unexplored research routes. Xylose is not the only sugar that can be extracted into an apolar aromatic phase through the formation of a boronate ester (Chapter 5). While xylose remains the sugar with the highest extraction efficiency, glucose and fructose are also extracted in relevant percentages (approx. 40-50 mol%) under similar conditions. This opens the possibility of extending the process also to these economically relevant sugars. Even more so, when an organic stream of fructose and/or glucose boronate diester is obtained, the same processes of valorization, described in Chapters 6 and 7, could potentially be applied to glucose and fructose as well. In these cases, the final product would be hydroxymethylfurfural (HMF). As mentioned in Chapter 2, HMF is more complicated to obtain in comparison to furfural, mainly for its higher water solubility and its reactivity towards undesired humins.

Chapter 5 shows that other economically relevant sugars (*e.g.*, sucrose) are not extracted well using this method. However, the formation of organic-soluble glycosides or sugar esters could potentially be an extraction concept alternative to the boronate-mediated one described in this thesis. Capping most of the hydroxyl groups of the saccharides with monodentate aromatic or aliphatic primary alcohols or carboxylic acids may influence the solubility in water and potentially result in the extraction of other valuable sugars such as sucrose.

Feeds with compositions similar to hemicellulose hydrolysate can be obtained from a wide range of sources, from forestry (*e.g.*, maple wood, pinewood, eucalyptus), agriculture (*e.g.*, sugarcane bagasse, corncob, corn stover, wheat straw, barley husk) as

well as food waste (*e.g.*, cooked rice, bread waste, vegetable waste, and fruit waste).[5-8] Chemical valorization of different kinds of waste, which are currently either composted in landfills or incinerated, can potentially be upgraded using the methods explored in this thesis. Additionally, the large pool of sources for bio-based processes allows for potential development of local economies, reducing the transportation of materials, with an additional beneficial environmental impact of the overall concept.

8.2 Using the Xylose Boronate Diester to Make Chemicals

In Chapters 6 and 7, the reactivity of PBA_2X has been explored in water-rich environment, which allow the hydrolysis of the ester bonds. Working at similar conditions (acid-catalyzed, high temperature), but in a dry solvent system, would negate the hydrolysis of the ester, possibly opening alternative pathways of degradation and new reaction mechanisms, which could still include the elimination of PBA and the formation of a double bond on the sugar ring.

8.3 Process Development, Validation and Upscaling

Chapters 5, 6 and 7 have introduced three different process concepts for the isolation and valorization of xylose from an aqueous stream, with a focus on the production of furfural. In all cases, solvent recovery, and recyclability, combined with limited contamination of the aqueous waste stream, are essential points for possible applications.

The process concept presented in Chapter 7, which operates at biphasic conditions and high salt concentrations, is likely to have the fewest problems regarding recovery and recyclability. The absence of a polar organic solvent in the system and the high salinity, which improves the aqueous-organic partition, allow for good phase separation and limited cross-contamination of streams . However, a complete validation of the economics of this concept needs more data, for example on the thermodynamic parameters of the components. In the case of the process described in Chapter 6, which operates in a three-solvent system, the presence of a polar organic solvent is a potential environmental hazard due to solvent spillage, so detailed studies are needed to validate the successful separation, shown in Chapter 6. The complexity of the solvent system may pay off in the final xylose-to-furfural selectivity (approx. 10-15 mol% higher than the system presented in Chapter 7), which reduces the amount of humic waste produced. Also in this case, a full economic analysis requires additional data on the components of the system.

In all cases, ensuring a closed system for the recycling of the solvents could result in a progressive build-up of by-products in the medium, the production of which is reduced

but not fully eliminated by the high selectivity. This build-up would need purge of the medium and would lead to solvent losses. Furthermore, it could, in principle, impair the selectivity of the system after a certain number of cycles. For this reason, studies in well-integrated units that include all necessary recycles are of top importance.

8.4 The Role of Biomass and Furans in Circular Economy

As described in Chapter 1, the way we currently approach the economy of products is largely linear. Examples are single-use, non-biodegradable plastics and the use of fossil fuels as the primary energy source. Our society takes a resource, converts it to products, uses them and consequently disposes of them. Even if most countries have, and are currently trying to expand, legislation on minimizing littering and improving the waste collection the pollution of the environment that it generates, *e.g.*, CO_2 in the atmosphere or plastics in the oceans, is a real problem, yet to be solved.

Major efforts are therefore underway toward a circular economy. In contrast to current linear practice, a circular economy relies on the closing of cycles of resources and products, thus ensuring that virtually no unrecoverable waste occurs. In this scenario, biomass and the products of biorefinery are highly significant. For example, when these bio-based chemicals are used as fuels, the CO_2 produced in their combustion is part of the natural cycle of photosynthesis.[13] Moreover, the use of biomass allows for large cuts in costs and is therefore an often locally available and valuable starting material.[13] McDonough and Braungart refer to this approach as 'cradle to cradle', ensuring that all the waste produced will be eventually feedstock for other processes.[14]

Among the chemicals that can be derived from biomass, furans and their derivatives are promising and industrially applicable alternatives to petroleum-derived chemicals, specifically, in energy, polymers, textiles, and pharmacy.[15-17] Thus, these chemicals may provide alternatives in applications currently dominated by petrochemicals and fossil-derived materials, *e.g.*, furfural-based diesel alkanes or furfural-based THF and pentanediol.[18-21]

8.5 What Biomass Cannot Do

The phenomena that are at the base of the currently unfolding climate crisis are rooted in the industrial revolution that has taken place from the 18th century to today. It is unreasonable to think that banning single-use plastic and switching from fossil to renewable and/or green energy sources will instantly eliminate three hundred years of energy and chemistry developments**.** Therefore, while respecting the developments that have been and will be made, ways to solve the problems we do and will experience are to be found.

A transition to renewable energy sources and feedstocks for chemicals is imperative, but it is not the only measure necessary because their growth rates are currently too low. Carbon capture and storage is currently considered to be technically feasible at a commercial scale and may contribute to lowering CO_2 levels in the near future.[22,23] Also CO_2-to-chemicals processes are a widely recognized possibility. Likewise, regulations on single-use non-biodegradable plastics, as much as collection, recovery, and recycling (when possible) of that already dispersed in the environment, are necessary for reducing the input of fresh fossil resources and avoiding further pollution of our planet.[23]

As much as it sounds cliché, there is no "single solution" for this multifaceted problem. Biomass and bio-based chemical industry offer a viable solution to some of the aspects of the energy and climatic crisis. It is unrealistic, however, to expect a final solution through this route only.

8.6 References

1. K. Sakai, R. Sakurai, A. Yuzawa, N. Hirayama, *Tetrahedron Asymmetry* **2003**, *14*, 3713-3718.
2. H. G. J. Mol, R. C. J. van Dam, O. M. Steijger, *J. Chromatogr. A* **2003**, *1015*, 119-127.
3. K. Stebel, M. Metzger, *Comput. Chem. Eng.* **2012**, *38*, 82-93.
4. C. Zenga, S. Tanaka, Y. Suzuki, S. Fujii, *Chemosphere* **2017**, *183*, 599-604.
5. I. K. M. Yu, D. C. W. Tsang *Bioresour. Technol.* **2017**, *238*, 716-732.
6. B. Ward, *Bacterial Energy Metabolism in Molecular Medical Microbiology, 2nd Edition*, Academic Press, Cambridge (Massachusetts) **2014**, pp. 201-233.
7. J. Cai, Y. He, X. Yu, S. W. Banks, Y. Yang, X. Zhang, Y. Yu, R. Liu, A. V. Bridgwater, *Renew. Sust. Energ. Rev.* **2017**, *76*, 309-322.
8. A. Zoghlami, G. Paës, *Front. Chem.* **2019**, *7*, 1-11.
9. C. E. Brewer, Y.-Y. Hu, K. Schmidt-Rohr, T. E. Loynachan, D. A. Laird, R. C. Brown, *J. Environ. Qual.* **2012**, *41*, 1115-1122.
10. B. Hu, Q. Lu, Z.-X. Zhang, Y.-T. Wu, K. Li, C.-Q. Dong, Y.-P. Yang, *Combust. Flame* **2019**, *206*, 177-188.
11. J.-P. Lange, *ChemSusChem* **2017**, *10*, 245–252.
12. N. Sánchez-Bastardo, I. Delidovich, E. Alonso, *ACS Sustainable Chem. Eng.* **2018**, *6*, 11930–11938
13. J. Sherwood, *Bioresour. Technol.* **2020**, *300*, 1-8.
14. W. A. McDonough, M. Braungart, *Cradle to Cradle: Remaking the Way We Make Things*, North Point Press, New York (USA) **2010**.

15. R. Ghafari, K. D. Hosseini, A. Abdulkhani, S. A. Mirshokraie, *Eur. J. Wood Wood Prod.* **2016**, *74*, 609–616.
16. Z.-W. Wang, C.-J. Gong, Y.-C. He, *Bioresour. Technol.* **2020**, *303*, 1-6.A.
17. O. Iroegbu, E. R. Sadiku, S. S. Ray, Y. Hamam, *Chemistry Africa* **2020**, *3*, 481–496.
18. P. L. Arias, J. A. Cecilia, I. Gandarias, J. Iglesias, M. López Granados, R. Mariscal, G. Morales, R. Moreno-Tost, P. Maireles-Torres, *Catal. Sci. Technol.* **2020**, *10*, 2721-2757.
19. Y. Luo, Z. Li, X. Li, X. Liu, J. Fan, J. H. Clark, C. Hu, *Catal. Today* **2019**, *319*, 14-24.
20. H. Wang, C. Zhu, D. Li, Q. Liu, J. Tan, C. Wang, C. Cai, L. Ma, *Renew. Sust. Energ. Rev.* **2019**, *103*, 227–247.
21. A. A. Rosatella, S. P. Simeonov, R. F. M. Frade, C. A. M. Afonso, *Green Chem.* **2011**, *13*, 754-793.
22. J. Gibbins, H. Chalmers, *Energy Policy* **2008**, *36*, 4317-4322.
23. J.-P. Lange, *Energy Environ. Sci.* **2021**, *14*, 1-19.

Summary

Humankind is facing a climate and an energy crisis, both of which are connected to a rise in energy demand and an excessive use of fossil energy sources (*i.e.*, coal, natural gas and oil). To revert the consequences of this crisis, it is mandatory to compensate the growing energy demand and, concomitantly, to reduce the contributions of fossil fuels to the total energy balance, by the development of renewable sources of energy and chemicals. Biomass, and more specifically lignocellulosic biomass, is a promising renewable resource composed of various biopolymers (*i.e.*, lignin, cellulose and hemicellulose). Different chemicals can be obtained from lignocellulosic biomass, which opens the possibility not only for the production of biofuels (*e.g.*, bioethanol and biobased diesel), but also for redesigning chemical industry.

Among these bio-based chemicals, furfural is considered a valuable resource, both for its promising performance as a biofuel and for its commercially relevant derivatives. Furfural can be produced from the acid-catalyzed dehydration of xylose, which is obtained from hemicellulose, a component of lignocellulosic feedstock. Industrially, furfural is produced using mineral acids (*e.g.*, H_2SO_4) as catalysts both under aqueous monophasic conditions (with xylose-to-furfural selectivities of approx. 45-50 mol%) and aqueous-organic biphasic conditions (with xylose-to-furfural selectivities of approx. 65-70 mol%). The non-ideal selectivities are due to several parallel and subsequent reactions, *e.g.*, the degradation of xylose and furfural and the formation of insoluble by-products (humins). This thesis deals with the development of alternative approaches to the synthesis of furfural, with the aim of reaching high xylose-to-furfural selectivity in industrially relevant process concepts.

This thesis is divided into three parts. The first part is an introduction, comprising the first two chapters. **Chapter 1** gives a general introduction to the topic of this thesis, outlining the environmental problems that justify the urge to switch to a green and sustainable economy and pointing out the potential of biomass-derived chemicals. **Chapter 2** serves as a review of fundamental aspects of biorefinery and, more specifically, of strategies that employ polar organic solvents for the production of furans. This chapter also includes an outlook to potential industrial applicability, discussing the variables according to which a process concept needs to be designed.

The second part of this thesis, which includes **Chapters 3** and **4**, presents an analysis of the application of microwaves in organic chemistry, using xylose dehydration to furfural as a case study. **Chapter 3** deals with the combination of microwave-assisted organic synthesis (MAOS) and reactive extraction. The parameters of the reaction of xylose dehydration to furfural (*i.e.*, xylose conversion and xylose-to-furfural selectivity) are

used to probe the asymmetric response of the two phases in an aqueous-organic biphasic system to microwave heating. Synergistically combining microwave heating and reactive extraction resulted in a selectivity improvement of approx. 10-15 mol%. This selectivity improvement is obtained only under biphasic conditions, by varying the dielectric properties of the two phases. **Chapter 4** examines the effect of microwave heating on aqueous monophasic solvent systems, using xylose as a case study, and offering a kinetic model to explain the rate enhancement observed in MAOS. Traditional and microwave heating are compared to show that the rate enhancement of the chemical reaction is connected to localized overheating. The kinetic model assumes two reaction regimes, a minor overheated zone and a bulk zone at the target temperature. These two zones are defined by two interlinked parameters, α (the volume fraction that is overheated) and f (the overheating factor). Good fits were achieved with various combinations of α and f, between 0.05−0.30 and 1.2− 2.0, respectively.

The third part of this thesis, which includes Chapters 5, 6 and 7, describes the process of liquid-liquid extraction of xylose coupled with its valorization. **Chapter 5** describes and rationalizes the liquid-liquid extraction of xylose from acidic hydrolysate as a neutral boronate diester (PBA_2X). The procedure described in the chapter simplifies the extraction process, as no pH switch and no additional phase transfer agents are necessary. Moreover, the extraction is selective for xylose, allowing the separation of xylose from other C_5 and C_6 sugars from a complex biomass hydrolysate. Preliminary experiments on back-extraction efficiencies provide a good prospect for industrial application for the purification of xylose from complex feeds. **Chapter 6** deals with the use of a solvent system composed of equal volumes of acidic water, an apolar aromatic solvent, and a polar aprotic solvent, to perform xylose dehydration to furfural, in the presence of phenylboronic acid (PBA). This three-solvent system, with PBA present, transitions from biphasic to monophasic at the reaction temperature, resulting into a xylose-to-furfural selectivity > 90 mol%. The selectivity is equally high when using the PBA diester of xylose as the starting compound. Based on these results and a further analysis of solvent losses, a process concept has been presented. This conceptual process design minimizes waste and maximizes recyclability. **Chapter 7** describes the combination of the liquid-liquid extraction described in Chapter 5 and biphasic operation at high salt concentration. The selectivity to furfural in the conversion of PBA_2X improves upon increasing the ionic strength of the aqueous phase. This increased selectivity is rationalized by the effect of salt concentration on the partitioning of PBA_2X and with the possibility of the formation of a readily suitable xylose conformer for dehydration to furfural upon PBA_2X hydrolysis. Based on these data and additional analysis of the possible losses, a process concept for furfural

manufacture from xylose-rich hydrolysates is developed. Due to the high selectivity, the concept designed in Chapter 6 may still be preferred.

Chapter 8 provides a wider outlook onto the further exploration of the results achieved in this thesis. In summary, the results presented in this thesis show that a deeper understanding of fundamental aspects of the behavior of different solvent systems can be developed into alternatives for the valorization of xylose-rich hydrolysates. As the xylose-to-furfural selectivity is limited by parallel and subsequent reactions, the choice of reaction conditions (*i.e.*, solvent system, heating method, catalyst, temperature) has to be made with the aim of suppressing the side reactions and maximizing the selectivity. This can be achieved by stabilizing the product, avoiding subsequent degradation of furfural, and by minimizing the degradation of xylose. Previous studies have achieved very high xylose-to-furfural selectivities by performing the reaction of xylose dehydration in solvent systems containing polar organic solvents (*e.g.*, DMSO) or in aqueous-organic biphasic systems at high salt concentration. This, however, impairs the industrial application, as the separation of polar organic solvents and salts from the aqueous waste stream is costly and inefficient. As shown in this thesis, combining these approaches with a prior liquid-liquid extraction step allows for a viable industrial application.

Samenvatting

De mensheid wordt met een klimaat- en een energiecrisis geconfronteerd. Beide houden verband met een stijging van de energievraag en een overmatig gebruik van fossiele energiebronnen (kolen, aardgas en olie). Aan de groeiende vraag naar energie moet voldaan worden, maar tegelijkertijd moet de bijdrage van fossiele brandstoffen aan de totale energiebalans omlaag. Lignocellulose biomassa is een veelbelovende hernieuwbare hulpbron die bestaat uit verschillende biopolymeren (lignine, cellulose en hemicellulose). Uit lignocellulose kunnen verschillende verbindingen worden gewonnen, waarvan sommige gebruikt worden voor de productie van biobrandstoffen (bijv., bio-ethanol en biodiesel) en andere toegepast kunnen worden als grondstof in de chemische industrie.

Als één van deze 'biogebaseerde' chemicaliën wordt furfural als erg waardevol beschouwd, zowel vanwege de veelbelovende toepassing als biobrandstof als vanwege zijn verschillende commercieel interessante derivaten. Furfural wordt bereid door zuur gekatalyseerde dehydratatie van xylose, dat wordt verkregen uit hemicellulose, een bestanddeel van lignocellulose. In de industrie wordt furfural geproduceerd gebruikmakend van minerale zuren (bijv. H_2SO_4) als katalysatoren, zowel bij waterige monofasische omstandigheden (xylose-naar-furfural selectiviteit ca. 45-50 mol%) als bij waterig-organische bifasische omstandigheden (xylose-naar-furfural selectiviteit ca. 65-70 mol%). Het selectiviteitsverlies is te wijten aan verschillende parallelle- en vervolgreacties van xylose en furfural en de vorming van onoplosbare bijproducten (humins).

Dit proefschrift behandelt de ontwikkeling van alternatieve reactieomstandigheden voor de bereiding van furfural uit xylose met een zo hoog mogelijke selectiviteit, met als uiteindelijk doel de mogelijke toepassing in een industrieel relevant proces. De resultaten laten zien dat een dieper begrip van fundamentele aspecten van het gedrag van verschillende oplosmiddelsystemen tot alternatieven voor de valorisatie van xylose-rijke hydrolysaten kan leiden. Voor het verkrijgen van een hoge furfuralselectiviteit spelen ook de reactietemperatuur en de wijze van verwarmen (reguliere verwarming, microwave) een essentiële rol.

Hoge xylose-naar-furfural selectiviteiten kunnen verkregen worden door de xylose-dehydratatie uit te voeren in oplosmiddelsystemen die polaire organische oplosmiddelen bevatten (bijv. DMSO) of in waterig-organische bifasische systemen bij hoge zoutconcentraties. Dit belemmert echter de industriële toepassing, aangezien de scheiding van polaire organische oplosmiddelen en zouten uit de waterige afvalstroom kostbaar en inefficiënt is. In dit proefschrift wordt aangetoond dat het combineren van

deze benaderingen met een eerdere vloeistof-vloeistofextractiestap wel kan leiden tot industriële toepassing.

Meer informatie is verstrekt in de Engelstalige samenvatting van dit proefschrift.

Acknowledgements

These last 4 years of my life have been dedicated to furfural manufacture. This small molecule allowed me to grow as a scientist and as a person.

In the life of a buddhist, being grateful is one of the most important things, and there are so many people that deserve my gratitude.

I thank my supervisors**, Jurriaan Huskens**, **Wim Verboom and Jean-Paul Lange**. **Jurriaan**, you really were my guide. You are an exceptional supervisor, able to be professional and warmhearted at the same time. Thank you for sharing your knowledge and determination with me. You really were my mentor during these four years. Thank you. **Wim**, not a single word in this thesis would have been possible without you. I admire your directness and attention to details. Your dedication to chemistry and science is an inspiration. Ik ga onze gratis Nederlandse oefening missen. Dankjewel. **Jean-Paul**, during these 4 years you really pushed me out of my comfort zone (occasionally, quite overwhelmingly so). I thank you for that. You offered me points of view distant from my background and my mentality. It was challenging, I am not gonna lie, but it helped me to put things into perspective, not only in the context of my PhD.

Special thanks go to my paranymphs, **Jacopo** (Movilli), **Alice** and **Nicola**. **Movilli**, I think that without you I would be still looking for an *OV-chipkaart*. You are a wonderful flatmate and a friend. **Lucia**, thank you for all the *aperitivi* and the Just Dance nights in which I got reminded that I can't dance, and it does not really matter. **Alice**, thank you for all the dinners, the beers, and the memories about the explosive salty home-made cider. I would probably be even less mentally sane without them. **Nicola**, thanks for being there for me, you are a really important person, possibly more than you think. By the way, no, I still did not install the Google home (neither I will). **Mizar**, I want to specifically thank you for giving me the privilege of playing the '*Esselunga* Trivial Pursuit'. Yes, it was worth mentioning in the acknowledgements.

Richard, the guardian angel of Lab. 2. Without the discussions we had in the lab I am not sure there would even be a thesis to defend. Thank you for casually introducing me to microwave chemistry, an interaction that finally resulted in Chapters 3 and 4 of this thesis. Thank you for all the anecdotes, the knowledge shared and the practical help, both in and outside the lab.

I extend my gratitude also to the other members of the technical staff and the secretaries. **Regine** and **Bianca**, thanks for the helping me in the characterization of the species described in Chapter 5. **Marcel**, thank you for single-handedly designing the heating mantle used for the experiments of both Chapters 6 and 7. **Izabel** and **Nicole**,

thank you very much for all the help with bureaucracy and organization. You are the very first people I met from the MnF-BNT cluster, from the first day you have all been very welcoming (and that can do a lot for an expat). Thank you.

I also want to thank the academic staff **Jeroen**, **Pascal**, **Christian**, **Jos**, **Albert** and **Saskia**. Thank you for the fruitful discussions we had during the colloquia and the other (formal and informal) group meetings. **Albert**, thank you for keeping my brain active during all the conversations in the coffee corner. I know (or maybe I just hope) you will miss me. **Saskia**, during a PhD bootcamp, at the beginning of my PhD, you shared your experience of balancing work and personal life. It was a crucial moment in my PhD life for which I thank you to this day. **Jos**, thank you for inspiring me in adding propositions to my thesis.

The work described in this thesis also contains the help and support of very talented researchers, **Surika Van Wijk**, **Thimo te Molder**, **Thomas Brouwer**, and **Juben Chheda**. **Surika**, **Thimo**, **Thomas**, thank you very much for helping me in the thermodynamical description of the solvent system used in Chapter 6. **Juben**, thank you for the fruitful discussions that resulted in the development of the project described in Chapter 7.

During these years I had the opportunity to supervise some people in their bachelor and master projects. **Matthijs**, thanks for the experimental work that resulted in part of Chapter 3. **Fuad**, your project was very far away from my expertise, and this gave the opportunity to forget about furfural for a couple of hours every now and then. Thank you for that. Also, it is '*city center*', not '*downtown*'.

A really loud and 'Mediterranean' thanks goes to the 'Italian Wall'. **Daniele**, my friend, thank you for all the help and support throughout these four years, I will always feel very privileged of being allowed to visit your house in Deurningenstraat and your house with **Simon** in Osnabrück. **Federico**, thank you for inspiring me and for having shared with me the beauty of starting a family. Best of luck for your new *USA adventure*, with **Bea**, **Leo** and the lil' newcomer. **Francesco**, you have been the first person I hanged out with in Enschede, outside of the MnF group. We share many beautiful memories, both in the Netherlands and in Italy. Thank you so much *Professore*. **Anna**, thank you for all the culinary inspirations and the nice times spent together in Enschede. **Elio**, **Zuzanna**, thank you for the welcoming spirit you always showed every time we shared time in Enschede. **Andrea**, **Effie**, thank you for teaching me what is the real goal of a PhD, my experience here in the Netherlands wouldn't have been the same without you. I really hope to see you soon. **Giulia**, thank you for the bright and positive energy you bring always with you. Very happy to have met a person who shares the joy of cleaning a house from top to bottom. **Alessandro**, thank you for teaching me the real meaning of '*vecchio*'. I am also very thankful you will 'equilibrate' the Italian balance in the MolMat.

Jessica, you are, and you will always be, an amazing flatmate. Thank you for all the milkshakes, the make-up, the unmotivated laughter, and the motivated tears. And that's the way the news goes.

Many fully endowed thanks to my buddhies: **Dayna**, **Takako**, **Patrick**, **Cynthia**, **Casper**, **Prarthana**, **Sjoukje**, **Emmie**, **Giulia**, **Camilla**, **Sonali**, **Fransis**, **Anke**, **Ly**, **Kemily**, **Federico**, **Sara** (Saraglia) and **Chiara** (Chiarasca). You are family to me, and you will always have a special place in my heart and in my Daimoku. **Chiarasca** and **Saraglia**, you are my sisters from other misters. Whatever I will try to write will sounds cheesy and incomplete. So, I'll just say *pignegne*. **Dayna**, thank you for reminding me I am the best at being me. **Fransis**, you are the reason I kept chanting in the Netherlands. Thank you for being there for me since the very beginning. You are a powerful soul, and your faith continues to inspire me every day. I love you dearly.

So many other people contributed to my development and happiness here in the Netherlands. **Kun**, **Yao**, **Shuqin**, **Fangyuan**, **Qin**, **Min**, thank you for 'adopting' me and for all the things you taught me. **Min**, I will always remember our conversations on how boring it is to curse in English. English is a very boring language. **Yao**, you are a bright, lovely and incredibly talented scientist, as much as it was sad to say goodbye, I am sure we will see each other again. **Fangyuan**, thanks for all the laughter and for helping me in the process of finalizing the date for my defense. **Shuqin**, thanks for trying (rather unsuccessfully so) to teach me how to make dumplings. I love you very much and I will always be one skype call away. Hopefully, we can see each other soon. **Sandra**, thank you for sharing with me your excessive collection of boardgames. The equilibrium you have in your life shows how determined and powerful you are, and it is incredibly inspiring. I know that you, **Mathieu**, **Nathan** and **Raphaël** will make lovely memories in your new house(s). **Dhanya**, thank you for the conversations in the city center of Enschede in the last moths of my PhD. Sharing our experiences helped me to get perspective, and for that I am very grateful. I wish to you and **Deepak** best of luck for the new chapter of your life in Utrecht. **Naomi**, thank you for all our honest conversation about life and science. You are a determined soul and I really cherish our friendship. **Gigi**, the summer school in Gargnano really is among the highlights of my PhD, I am very grateful I could share that with you. You are strong and an amazing scientist, never forget that. **Anamarija**, thank you for the support in the lab and for all the discussions about future and work-life balance. You really are an inspiration. I wish you and **Tiho** good luck in Croatia. **Remi**, fellow Lab 2 inhabitant and the most organized organic chemist I have ever met, thank you for the fruitful discussion and for the honest feedback on my not-sweet-enough cakes. **Manuela**, thank you for all the support during the quarantine and the beautiful pictures of **Arthur** (the cutest baby I ever seen). I wish all of you best of luck in Helsinki. **Melissa**, **Robin**, **Erik** and **Nico**, thank you for

our Runelords adventures, I really hope we can keep on playing every now and then, wherever we will all end up. **Melissa**, you are an amazing DM and I really enjoyed our time in the chicken farm. **Robin**, thanks for all the f***ing amazing dinners and all the deep conversations about politics and society. **Nico**, thank you and **Bea** for the hospitality in Deventer. **Eric**, thank you for helping me with the Samenvatting and for the help in the data processing for Chapter 4. I was very happy and honored to be present at your wedding with **Elvera**. **Nicole**, thank you for all the nice time we spent in the coffee corner, drinking tea and talking about cats. **Julien**, you are one of a kind. I really enjoyed our time together in Enschede. **Ruben**, thank you for the laughter and the smiles in the corridors between Lab 2 and Lab 1. **Cande**, my friend, thank you for all the fun time and the support. I really cannot wait to see you again (either in Argentina, or in Italy where, you know, you are always welcome). **Pramod**, **Isa**, thank you for all the walks in the natural parks and the amazing ice creams. **Pramod**, you really are an inspiration and an amazing friend. **Nicolas**, we started our PhD the very same day. Even if it was a bit sad to see you go to Groningen, I am happy for your success and I wish you and **Sophie** best of luck for your future. **Hasnaa**, it is impossible not to be happy around you, thank you for the smiles you brought in lab. 2, your creativity and all your beautifully colored azobenzenes. **Jan-Willem**, I will miss our discussions about Dutch weather, science, and society. Thank you so much for bearing with my blabbing.

Without **you all** there would be nothing to celebrate, and I wish to the totality of y'all good look for all your endeavors.

I also want to thank my family, as they managed to always love and support me during these four years. **Matteo**, I am very proud of you, and I will always be there for you to tell you (possibly, in a very passive-aggressive way) . **Madre**, **Padre**, the work in this thesis is your accomplishment as much as it is mine. I am the luckiest man on the planet for having you. Thank you.

Davide, thank you for making me feel home whenever and wherever we are. You are the one. These last years have been the happiest years of my life, and I look forward for many more. *Ti amo*.

Luca,
Enschede, July 2021